# Hard Scattering Cross Sections and Parton Distribution Functions at the LHC

D I S S E R T A T I O N

zur Erlangung des akademischen Grades

d o c t o r  r e r u m  n a t u r a l i u m
(Dr. rer. nat.)
im Fach Physik

eingereicht an der
Mathematisch-Naturwissenschaftlichen Fakultät I
Humboldt-Universität zu Berlin

von
**Frau M.Sc. Petra Kovačíková**

Präsident der Humboldt-Universität zu Berlin:
Prof. Dr. Jan-Hendrik Olbertz

Dekan der Mathematisch-Naturwissenschaftlichen Fakultät I:
Prof. Dr. Stefan Hecht

Gutachter:
1. Prof. Dr. Jan Plefka
2. Dr. Sven-Olaf Moch
3. Prof. Dr. Peter Uwer
4. Prof. Dr. Matteo Cacciari

**eingereicht am:** 02.05.2012
**Tag der mündlichen Prüfung:** 20.06.2013

**Abstract**

In this thesis we will explore a Mellin space approach to the evaluation of precision cross-sections at hadron colliders. We consider three processes with known analytic results for perturbative QCD corrections up to the next-to-next-to-leading order, namely: the production of vector bosons $Z^0$, $W^{\pm}$ via the Drell-Yan mechanism in the narrow width approximation; the production of the standard model Higgs boson via gluon-gluon fusion using the large top quark mass limit and the neutral and charged current deep inelastic lepton-hadron scattering.

We develop a `c++` package `sbp` that implements the Mellin space technique. The resulting program provides an elegant, fast and accurate solution for the evaluation of inclusive cross sections. We compare our program with available results that use standard momentum space techniques. We present studies of asymptotic convergence and scale dependence of the perturbative series. We use the package to study different treatments of factorisation and renormalisation scales in cross sections.

## Zusammenfassung

Über einen Mellinraumzugang werden Methoden zur Auswertung von Wirkunsquerschnitten für verschiedene Prozesse mit Hadronen im Anfangszustand entwickelt. Die Arbeit geschieht im Hinblick auf drei Prozesse, für die die analyischen Ergebnisse für perturbative QCD Korrekturen zu "next-to-next-to-leading order" bekannt sind; diese sind: die Produktion der Vektorbosonen $Z^0$ und $W^{\pm}$ über einen Drell-Yan-Prozess in der "narrow width"-Näherung, die Produktion eines Standardmodell-Higgs-Bosons über die Fusion zweier Gluonen im Grenzfall schwerer Top-Quark-Massen und die tiefinelastische Lepton-Hadron-Streuung über neutrale und geladene Ströme.

Die Implementierung der Mellinraumtechniken erfolgt in dem `c++` Paket `sbp`. Das Programm ermöglicht auf elegante Weise eine schnelle und präzise Auswertung von inklusiven Wirkungsquerschnitten. Wir vergleichen `sbp` mit den herkömmlichen Impulsraumtechniken, und präsentieren Studien der asymptotischen Konvergenz den perturbativen Reihen und von Skalenabhängigkeiten. Als Anwendung untersuchen wir welchen Einfluss die Behandlung der Faktorisierungs- und Renormierungsskala auf den Wirkungsquerschnitt hat.

**Acknowledgements**

I would like to thank my advisor Sven-Olaf Moch for continuous support throughout the course of this work, for careful reading of the thesis and useful comments. I am grateful to the members of the theory group and the NIC group in DESY Zeuthen. I am grateful to Prof. Johannes Blümlein for useful discussions and constructive criticism and Dr. Tord Riemann for discussions on electroweak physics and complex analysis.

I am indebted to the Humboldt University in Berlin and in particular Prof. Jan Plefka for providing me the opportunity to complete my degree in physics under his official supervision. I enjoyed being an associated member of the HU Graduiertenkolleg 1504 "Masse, Spektrum, Symmetrie" and participating in the schools.

I am thankful for the opportunity of becoming a member of the HEPTOOLS network which has allowed me to travel across the Europe and attend physics schools and workshops, present my work and meet new colleagues. I would like to thank Dr. Costas Papadopoulos and Prof. Ronald Kleiss who have supported me at the very last stage of my studies and offered me to visit the institutions in Athens and in Nijmegen. I would also like to express thanks to Prof. Andreas Vogt for hosting me at the University of Liverpool.

I would like to thank Alex Hasselhuhn for his help with the German translation, to Valery Yundin for his help with programming issues and Simon Badger for proof reading the whole thesis and for his repetitive encouragement. I would like to say thanks to all my colleagues, my dear friends and my parents as they all contributed to the successful completion of this work.

# Contents

# 1. Introduction

The present day description of high energy physics is given by a quantum field theory called the Standard Model of elementary particles. It is an effective theory that encompasses all known elementary particles – six quarks and six leptons along with three of four fundamental interactions: electromagnetic, weak and strong and four corresponding gauge bosons. The Standard Model of particle physics (SM) has been developed during the twentieth century. The theory of electroweak interactions of Glashow, Weinberg and Salam [1–3] provides a unified description of the electromagnetic and weak interactions[1]. The strong interaction on the other hand, is described by Quantum Chromodynamics (QCD), which possesses the unique property of asymptotic freedom [2]. The Standard Model has predicted the existence of many new particles which have been later confirmed by experiments. These include the gauge bosons of QCD, gluons, observed in 1979 in the experiment PETRA at DESY followed by discoveries of electroweak gauge bosons $W$ and $Z$ in experiments UA1 and UA2 in CERN (1983). The most recent observations involve the top quark (1995) and the tau neutrino (2000). The last prediction of the Standard Model concerns the existence of the Higgs boson, a particle that plays a central role in the consistency of the SM. The Higgs boson has not yet been observed and has driven efforts for construction of the Large Hadron Collider (LHC), an experimental device accelerating protons. LHC, located in the laboratory CERN near Geneva has started its operation in March 2010 at the centre of mass energy of 7 TeV and up to now has collected large amount of data equivalent to the luminosity over 5 $\text{fb}^{-1}$, but so far not given an ultimate word on the existence of the Higgs boson.

Despite the great success of the Standard Model it is a general opinion that one should question its domain of validity. Apart from the Higgs boson there are issues connected to the violation of a guiding physics principle – the naturalness and related problems of hierarchy and fine tuning. And last but not least, phenomena that the model does not explain at all: The origin of dark matter and gravitational interactions. All this seems to point towards the fact that the Standard Model is not the ultimate theory of elementary particles. It is a hope that the LHC will give us more insight into the physics of elementary particles by looking at an energy region so far not explored. Looking deeper and more precisely at the predictions of the Standard Model will allow us to probe signals of theories beyond the Standard Model (BSM) such as supersymmetry or theories involving extra dimensions.

[1] Nobel Prize for the contributions to the theory of the unified weak and electromagnetic interaction has been awarded in 1979

[2] Nobel Prize for the discovery of asymptotic freedom has been awarded to Gross, Wilczek and Politzer in 2004 see [4, 5] for a historical review

At hadron colliders, the Higgs boson and possible "new physics" particles are mainly produced via short distance interactions of quarks and gluons. The probability amplitude $M_{fi}$ for the transition between initial state $i$ and final state $f$ is given in terms of series in the strong coupling constant $g_s$,

$$M_{fi} = M_{fi}^{(0)} + g_s M_{fi}^{(1)} + g_s^2 M_{fi}^{(2)} + \mathcal{O}(g_s^3), \tag{1.1}$$

where $g_s$ is smaller than one. The transition probability can then be directly translated into the cross section. Since the colour charged quarks and gluons (collectively called partons) are confined in colourless bound states known as hadrons, we are forced to deal with composite particles in the initial state. Perturbation theory is no longer applicable and a hadron collision becomes rather a complex problem, involving different short and long-distance phases of the collision. Fig. (1.1) shows a simplified picture of such a hadronic collision. The two colliding protons denoted by $p$ move towards each other and the short distance scattering of a quark and a gluon is indicated by the square box. Besides the hard interaction many soft parton level interactions take place including final and initial state radiation, interaction of hadron fragments, and multiple parton interactions. Partons subsequently cascade down and until they eventually recombine to colourless hadrons which are observed in detectors.

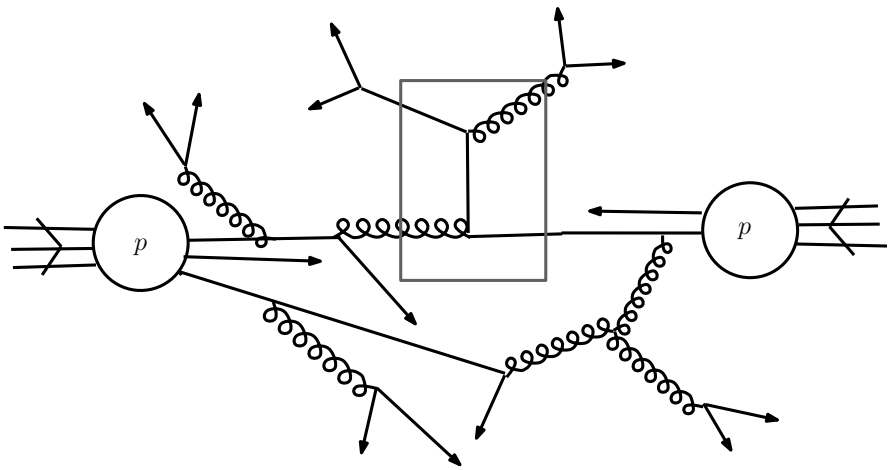


Figure 1.1.: General structure of a hadronic collision

The approach that allows to get a handle on calculations with initial state hadrons is based on the idea of factorisation [6–8]. One introduces a factorisation scale $\mu$ which separates the independent phases of a hadronic collision into long range effects, concerned with the hadron structure and short range effects that can be calculated perturbatively. The factorisation formula for a cross section for a collision of two initial state hadrons

$h_1$ and $h_2$ and some final state $X$ reads

$$\sigma_{h_1h_2\to X}(s) = \sum_{a,b=q,\bar{q},g} \int_{x_{1,\min}}^{1} \mathrm{d}x_1 \int_{x_{2,\min}}^{1} \mathrm{d}x_2 f_{a/h_1}(x_1,\mu^2) f_{b/h_2}(x_2,\mu^2) \hat{\sigma}_{ab\to X}(x_3,Q^2,\mu^2). \tag{1.2}$$

The short distance interaction among quarks and/or gluons $a$ and $b$ at a scale $Q$ is described by the hard scattering cross section $\hat{\sigma}_{ab\to X}(x_3,Q^2,\mu^2)$, which corresponds to the amplitude defined in eq. (1.1) integrated over the final particle phase space. The parton distribution functions (PDFs) $f_{a/h_1}(x_1,\mu^2)$ and $f_{b/h_2}(x_2,\mu^2)$, on the other hand, account for the long-distance effects that concern the hadron structure. In particular, $f_{a/h}(x,\mu^2)$ is the distribution of the momentum fraction $x$ of parton $a$ in hadron $h$ at some hard scale $\mu^2$. The calculation of the PDFs is beyond the scope of perturbation theory and for the non-perturbative methods as lattice gauge theory this remains still an open challenge, see for example [9]. Their values are instead determined from global fits to data on cross sections for lepton-hadron or hadron-hadron scattering experiments. The scale dependence of PDFs can be calculated perturbatively using the evolution equations [10–13],

$$\frac{\partial f_{a/h}(x,\mu^2)}{\partial \ln \mu^2} = \sum_b \int_x^1 \frac{\mathrm{d}y}{y} P_{ab}(x/y,\mu^2) f_{b/h}(y,\mu^2), \tag{1.3}$$

where the splitting functions $P_{ab}(x,\mu^2)$ have expansion in the strong coupling constant $g_s$.

Although new particles can manifest themselves as clear signals, large classes of new physics models show up as small discrepancies between data and theory [14]. It is therefore essential to have a precise understanding of background processes and those processes that are used for various calibrations (benchmark processes). Precise analyses of benchmark and background processes can be time consuming as they require repeated evaluations of cross sections. The standard way involves numerical evaluation of the two dimensional integrals in eq. (1.2) and one dimensional integrals as in eq. (1.3).

During this work we investigate the possibility that such a problem can be successfully addressed in Mellin space. The Mellin transform [3] is an integral transform between function from $x$-space, $f(x)$, and function from moment or $N$-space, $f(N)$,

$$f(N) = \int_0^1 \mathrm{d}x\, x^{N-1} f(x). \tag{1.4}$$

Such a transformation when applied to each of the components of the integrand in eq. (1.2) turns the integrals into ordinary products,

$$\sigma_{h_1h_2\to X}(N) = \sum_{a,b=q,\bar{q},g} f_{a/h_1}(N+1,\mu^2) f_{b/h_2}(N+1,\mu^2) \hat{\sigma}_{ab\to X}(N,Q^2,\mu^2). \tag{1.5}$$

[3] Named after Finnish mathematician H. Mellin (1854–1933)

In a similar way, the Mellin transform works in the case of eq. (1.3) as well as formulae for lepton-hadron cross sections. The original $x$-space is recovered by application of the inverse Mellin transform,

$$f(x) = \frac{1}{2\pi i} \oint \mathrm{d}N \, x^{-N} f(N). \tag{1.6}$$

The complex integral in eq. (1.6) is simple to evaluate as it only concerns the summation over residues. With this approach, repeated cross section evaluations become much faster.

The accuracy of the theoretical prediction depends on the experimental input and the precision of the hard-scattering cross section. The uncertainty on the latter enters due to the truncation of the perturbative series in eq. (1.1) to a finite order. Such a truncation introduces the dependence on unphysical factorisation and renormalisation scales, which can only be reduced by calculation of additional orders. The leading order (LO) is rarely sufficient for the purpose of precision physics. For the background estimates the next-to-leading order (NLO) predictions are usually good enough. Due to efforts of recent years, the NLO corrections are known for many of the most important LHC processes [15]. Large next-to-leading order corrections however require calculation of an extra order (NNLO), in particular for benchmark processes and measurements of particle properties like masses and decay widths. Though obviously beneficial to have NNLO corrections to any process, the theoretical complexity of such predictions make this task unfeasible with current techniques. However such corrections are known for the Drell-Yan process and the production of the Higgs boson via gluon-gluon fusion at hadron-hadron colliders and deep inelastic scattering at lepton hadron colliders.

In this thesis we develop a `c++` program for fast and accurate evaluation of cross sections for a set of processes for which the perturbative QCD corrections are known analytically up to the NNLO: the production of $W^{\pm}$ and $Z^0$ bosons in the narrow width approximation via the Drell-Yan mechanism, the deep inelastic lepton-hadron scattering and the production of the Standard Model Higgs boson via gluon-gluon fusion in the heavy top quark mass limit. To achieve this goal we use the Mellin space approach, which requires that all input functions, i.e. coefficient functions, splitting functions and parton distribution functions are in such a form that the analytic continuations to the complex plane of their Mellin transforms exist. The $N$-space coefficient functions are obtained from the $x$-space results [16–24] with the use of `FORM` [25] package `harmpol` [26]. The parton distribution functions are provided by linking the dedicated $N$ space `FORTRAN` package `QCD-PEGASUS` [27]. We also provide a model PDFs input with no evolution as a default input.

Our approach offers an alternative to the growing number of momentum space programs, where a lot of progress has been made in past years. In the case of Drell-Yan process it is `DYNNLO` [28, 29] and `FEWZ 2.1` [30], both fully exclusive with leptonic decays including all spin correlations. For the Higgs production via gluon-gluon fusion there are both inclusive and fully exclusive codes iHixs [31] and `FEHiP` [32].

The thesis is organised as follows. The second chapter introduces the basic concepts of perturbative QCD as a non-Abelian gauge theory. We review the parton distribution functions and their evolution and provide details on the Mellin transform. The last part of the chapter introduces concepts of the electroweak symmetry breaking and the Higgs mechanism.

Chapters 3 and 4 develop the necessary formalism for the Drell-Yan process, Higgs boson production via gluon-gluon fusion and deep inelastic scattering. More detailed attention is payed to the structure function approach. The concept of the large top mass limit, $m_t \to \infty$ is summarised.

In the chapter 5 we present the `c++` program `sbp`. After the description of the basic top level routines we discuss the numerical implementation, in particular the relationship between harmonic polylogarithms and harmonic sums in the context of Mellin transforms of hard scattering coefficient functions and details of the numerical inversion. We also discuss the limitations of this method.

Chapter 6 presents comparisons and cross-checks with results of the standard $x$-space codes `ZWPROD` [16] and `higgs.f` [23], studies on convergence of perturbative series and general scale dependence of cross sections. We present several studies focused on the effects of different treatments factorisation and renormalisation scale dependence of the cross sections. The end of the chapter is devoted to the discussion of possible applications and extensions of the program.

# 2. Theoretical background

In the following sections we cover basic elements of the Standard Model with a particular focus on the perturbative expansion in QCD, running of the strong coupling constant, evolution equations of the parton distribution functions and the electroweak symmetry breaking mechanism. For this we mostly follow the textbook of Ellis, Stirling and Webber [33, 34] and several review papers [35–44]

## 2.1. Basics of perturbative QCD

Quantum Chromodynamics (QCD) is the quantum field theory of strongly interacting relativistic elementary particles, quarks with a half integer spin and spin one massless gluons. The dynamics of strong interactions is controlled by the QCD Lagrangian density[1]

$$\mathcal{L}_{\mathrm{QCD}} = \sum_{j=1}^{n_f} \bar{\psi}_{j,a} i \not{D}_{ab} \psi_{j,b} - \frac{1}{4} \sum_{A=1}^{8} F^A_{\mu\nu} F^{A,\mu\nu} + \mathcal{L}_{\mathrm{gauge}}, \tag{2.1}$$

which is invariant under the $SU(3)$ colour gauge transformations. The upper case indices $A = 1, \ldots, 8$ denote adjoint and lower case ones $a = 1, 2, 3$ the fundamental indices of the $SU(3)$ group. We suppress the spinor indices. The spinors $\psi_{j,a}$ and $\bar{\psi}_{j,a}$ denote quark and antiquark fields, $n_f$ stands for the number of flavours. We do not include the quark mass terms. The Feynman slash is $\not{D} = \gamma_\alpha D^\alpha$ and the covariant derivative acting on the triplet fields reads

$$D_{\mu,ab} = \partial_\mu \delta_{ab} + i g_s \sum_C (t^C \mathcal{A}^C_\mu)_{ab}, \tag{2.2}$$

where $t^A$ are the fundamental generators of $SU(3)$ represented by the Gell-Mann matrices $\lambda^A$, $t^A = \lambda^A/2$. These are eight traceless hermitian matrices and their exact form can be found for instance in [33, Chapter 1]. Commutation relations and normalisations of colour matrices are given in the section A.3.1. The symbol $g_s$ denotes the strong gauge coupling. The strong coupling constant $\alpha_s$ is defined as

$$\alpha_s = \frac{g_s^2}{4\pi}. \tag{2.3}$$

[1] The terms Lagrangian and Lagrangian density are often used interchangeably, the former one being an integral over the spatial coordinates $\mathrm{d}^3x$ of the latter.

The field strength tensor reads

$$F^A_{\mu\nu} = \partial_\mu \mathcal{A}^A_\nu - \partial_\nu \mathcal{A}^A_\mu - g f^{ABC} \mathcal{A}^B_\mu \mathcal{A}^C_\nu, \tag{2.4}$$

where $\mathcal{A}^A_\mu$ represents the gluon field and the last term in eq. (2.4) reflects the non-Abelian nature of QCD. This term gives rise to triple and quartic gluon self-interactions which then as we will see relates to the asymptotic freedom. $f^{ABC}$ is the structure constant of $SU(3)$.

The last term in the Lagrangian in eq. (2.1) above $\mathcal{L}_{\text{gauge}}$ is characteristic for non-Abelian field theories and emerges due to the existence of extra unconstrained degrees of freedom in the gauge fields. The gauge fixing term usually (unless it is a physical gauge) comes together with an additional (ghost) field,

$$\mathcal{L}_{\text{gauge}} = -\frac{1}{2\lambda}(\partial^\alpha \mathcal{A}^A_\alpha)^2 + \partial_\alpha \eta^{A\dagger}(D^\alpha_{AB}\eta^B), \tag{2.5}$$

where $\lambda$ represents a gauge parameter of the ghost fields and $\eta^A$ are complex scalar fields that obey Fermi statistics. They only couple to gluons and will appear in internal closed loops or will be pair-produced in final states. The QCD Feynman rules also for the corresponding ghost fields can be found elsewhere in the literature, e.g. in [33, 35].

Amplitudes in quantum field theories will in general contain both infra-red (IR) and ultra-violet (UV) divergences. Such divergences will cancel when computing any physical observable as long as all relevant contributions are taken into account. UV singularities must be collected into re-definitions of the parameters of the bare Lagrangian by the procedure of renormalisation. IR singularities appear in both the loop corrections to the perturbative cross-section and in the real emission of additional unresolved particles. In hadron collisions IR finite observables are constructed after summing over all possible final state real emission processes and absorbing initial state radiation into the soft interaction modelled by the PDFs. The coefficient functions we will use in chapters 3 and 4 are defined to contain only the finite contributions necessary to compute the cross sections with the singular parts removed.

### 2.1.1. The running of QCD coupling

The running of the QCD coupling $\alpha_s$ is a direct consequence of the renormalisation and regularisation procedures. These are introduced in order to deal with ultra-violet divergences appearing in the loop diagrams that are part of any calculation of higher order QCD corrections.

The most commonly used regularisation is the dimensional regularisation. The principle relies in shift of the spacetime dimension $d = 4 \to d = 4 - 2\varepsilon$ where $\varepsilon$ is a small parameter, regulator. The introduction of $d \neq 4$ makes the Lagrangian and therefore also fields and couplings $d$ dependent. Since the action has to be a dimensionless quantity,

see [35],

$$\dim[S] = \dim\Big[\int \mathrm{d}^d x \mathcal{L}(x)\Big] = 0 \Rightarrow \quad \dim[\mathcal{L}] = d \tag{2.6}$$

and therefore

$$\dim[\partial_\mu \phi \partial^\mu \phi] = d \Rightarrow \quad \dim[\phi] = 1 - \varepsilon \tag{2.7}$$

$$\dim[\bar{\psi} \not{\partial} \psi] = d \Rightarrow \quad \dim[\psi] = 3/2 - \varepsilon \tag{2.8}$$

$$\dim[\bar{\psi} \not{A} \psi g] = d \Rightarrow \quad \dim[g] = \varepsilon \tag{2.9}$$

as $\dim(\partial_\mu) = 1$ and the coupling $g$ acquires a dimension. This dependence on a dimension can be extracted by introducing a dimensional parameter $\mu$ (renormalisation scale) and redefine the gauge coupling as

$$g_{\text{bare}} = Z_g^{1/2} \mu^\varepsilon g_R, \tag{2.10}$$

where the subscript "bare" refers to the original parameters of the Lagrangian, eq. 2.1, whereas the subscript "$R$" refers to the renormalised – four dimensional ones – and $Z_i$ are the renormalisation constants. The renormalisation scale $\mu$ is arbitrary and any physical quantity should not depend on a choice of this scale. This can be expressed in terms of the renormalisation group equation,

$$\frac{\mathrm{d}g_{\text{bare}}}{\mathrm{d}\mu} = 0. \tag{2.11}$$

If we now relabel $g_R \equiv g$ and use eq. (2.10) the eq. (2.11) reads,

$$\Big[\varepsilon \mu^{2\varepsilon} Z_g^2 \alpha_s + \mu^{2\varepsilon} \alpha_s 2 Z_g \frac{\mathrm{d}Z_g}{\mathrm{d}t} + \mu^{2\varepsilon} Z_g^2 \frac{\mathrm{d}\alpha_s}{\mathrm{d}t}\Big] = 0 \tag{2.12}$$

with $\mathrm{d}t = \mathrm{d}(\ln \mu^2)$. Defining the QCD beta function $\beta(\alpha_s)$

$$\beta(\alpha_s) = \frac{\mathrm{d}\alpha_s}{\mathrm{d}t} \tag{2.13}$$

allows us to rewrite the eq. (2.12) as

$$\beta(\alpha_s) + 2\frac{\alpha_s}{Z_g}\frac{\mathrm{d}Z_g}{\mathrm{d}\alpha_s}\beta(\alpha_s) = -\varepsilon \alpha_s. \tag{2.14}$$

From the above equation the QCD beta function can be determined by evaluating the renormalisation constant $Z_g$. The explicit calculation is carried out perturbatively and the details for $\mathcal{O}(\alpha_s)$ result can be found for instance in [34]. The QCD beta function is

known by now up to four loops [45–51] and its expansion reads

$$\beta(\alpha_s) = -\alpha_s \sum_{n=0}^{\infty} \beta_n \Big(\frac{\alpha_s}{4\pi}\Big)^{n+1} \tag{2.15}$$

with the first two terms

$$\beta_0 = 11 - \frac{2}{3} n_f \qquad \text{and} \qquad \beta_1 = 102 - \frac{38}{3} n_f, \tag{2.16}$$

where $n_f$ is the number of active flavours. The eq. (2.13) can be solved implicitly

$$t = \int_{\alpha_s(\mu^2)}^{\alpha_s(Q^2)} \frac{1}{\beta(\alpha'_s)} \mathrm{d}\alpha'_s. \tag{2.17}$$

The leading order solution for the running coupling $\alpha_s(Q^2)$

$$\alpha_s(Q^2) = \frac{\alpha_s(\mu^2)}{1 + \beta_0 \frac{\alpha_s(\mu^2)}{4\pi}} \tag{2.18}$$

gives the relationship for the strong coupling at some scale $Q^2$ at one loop. The $\alpha_s(\mu^2)$ is an input value obtained from experimental measurements at the reference scale $\mu^2$, usually chosen at the mass of the $Z$ boson, $\alpha_s(M_Z^2)$ [52]. It follows from the eq. (2.18) that for values $n_f \leq 16$ the sign of $\beta_0$ is positive and hence at larger values of $Q^2$ the coupling $\alpha_s(Q^2)$ decreases and the interaction among coloured particles becomes weaker. This phenomenon called asymptotic freedom is a very specific property of a non-Abelian field theories as QCD [2]. With the decreasing momentum $Q^2$ on the other hand, this interaction becomes stronger and as a consequence quarks and gluons do not appear as free particles but only exist as bound states in the form of colourless hadrons. The fig. 2.1 shows the summary of measurements of the strong coupling constant as a function of the scale $Q^2$ together with the theory prediction which is marked with full lines. The energy dependence of the coupling given by measurements follows the expectations from the theory prediction very well. The region below $Q \simeq 1\,\mathrm{GeV}$ corresponds to the case where the strong coupling exceeds unity and perturbative expansion cannot be applied. A more detailed discussions on the running of strong coupling can be found for instance in [33, Chapter 1],[44] and [41].

## 2.2. The parton distribution functions

The parton distribution functions are non-perturbative objects that provide us with the information about the hadron structure. Let us recall, that a parton distribution function $f_{a/h}(x, Q^2)$ is the distribution of the momentum fraction $x$ of the parton $a$ in the hadron $h$ at some hard scale $Q^2$.

[2] The Nobel Prize in 2004 has been awarded to Gross, Wilczek, Politzer for the discovery of asymptotic freedom in QCD in 1972

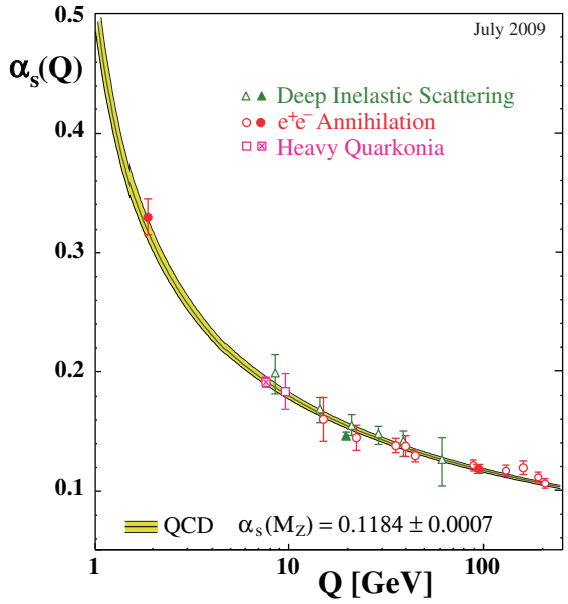


Figure 2.1.: Summary of measurements of $\alpha_s$ as a function of the respective energy scale $Q$ as given in a 2009 summary by S. Bethke [41]. The curves are QCD predictions for the combined world average value of $\alpha_s(M_Z)$, in 4-loop approximation and using 3-loop threshold matching at the heavy quark pole masses $m_c = 1.5\,\text{GeV}$ and $m_b = 4.7\,\text{GeV}$. Full symbols are results based on N$^3$LO QCD, open circles are based on NNLO, open triangles and squares on NLO QCD. The cross-filled square is based on lattice QCD. The filled triangle at $Q = 20\,\text{GeV}$ (from DIS structure functions) is calculated from the original result which includes data in the energy range from $Q = 2$ to 170 GeV

The major amount of the data on PDFs comes from the the deep inelastic lepton-hadron scattering experiments, mostly from the era of HERA $ep$ collider (experiments H1 and ZEUS) and various fixed-target experiments in $lp$ and $ld$ scattering (BCDMS, NMC, E665, experiments at SLAC), $\nu N$ scattering (CCFR, NuTeV). Further data come from Drell-Yan or jet production, namely $pp$ and $pd$ scattering at (E866/NuSea) [42] and $p\bar{p}$ data at the Tevatron (CDF, DØ) and soon at the LHC, see c.f. [53]. The kinematical range of data on PDFs measured at various experiments is shown in fig. 2.2 in pink.

### 2.2.1. The evolution equations

Once the parton distributions are measured for a given range of kinematical variable $x$ at some scale $Q_0^2$, the prediction for the value of a distribution at some other scale $Q^2$ can be calculated using the evolution equations [10–13]. They represent the renormalisation group equations for the PDFs and consist of $2n_f+1$ coupled integro-differential equations

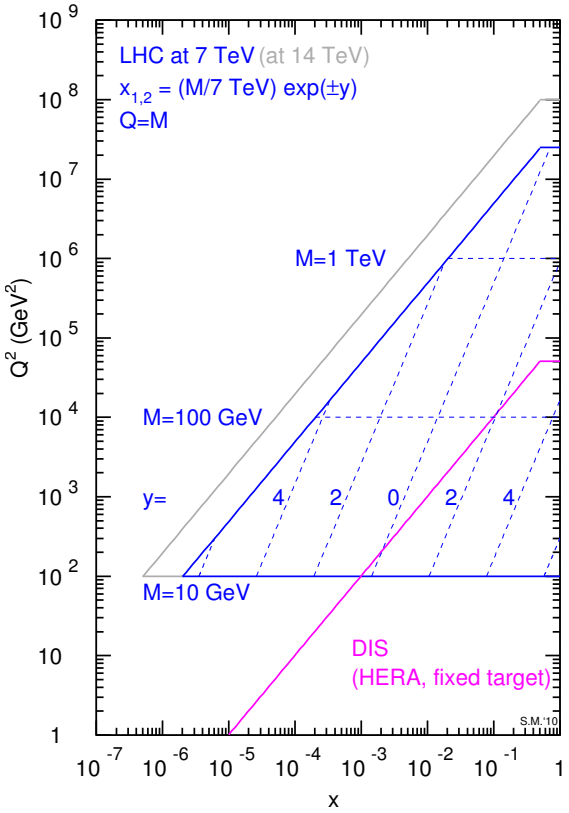


Figure 2.2.: The kinematic range of DIS and fixed target experiments shown in pink. The kinematic range for LHC at 7 TeV (14 TeV) is shown in blue (grey). Plot by S. Moch

where $n_f$ stands for the number of active flavours. These equations can be written as

$$\frac{\partial}{\partial \ln Q^2}\begin{pmatrix} f_i(x,Q^2) \\ g(x,Q^2) \end{pmatrix} = \sum_{j,\bar{j}} \begin{pmatrix} P_{ij}(x,Q^2) & P_{ig}(x,Q^2) \\ P_{gj}(x,Q^2) & P_{gg}(x,Q^2) \end{pmatrix} \otimes \begin{pmatrix} f_j(x,Q^2) \\ g(x,Q^2) \end{pmatrix}, \tag{2.19}$$

where the symbol $\otimes$ denotes convolution, see eq. (2.55) for definition and indices $i, j$ run over all quark flavours $i, j = u, d, s, \ldots, n_f$. The splitting functions $P_{ab}(x, Q^2)$, often called the evolution kernels, have a perturbative expansion in the strong coupling

$$P_{ab}^{\mathrm{N^kLO}}(x,Q^2) = \sum_{n=0}^{k} \frac{\alpha_s^{k+1}(Q^2)}{4\pi} P_{ab}^{(k)}(x) \tag{2.20}$$

and they have been calculated up to NNLO [12, 54–62]. The splitting function $P_{ab}(x)$ describes the probability of a parton $b$ with momentum $p$ radiating a soft or collinear parton $a$ with momentum $xp$. Because of flavour symmetry and charge conjugation [33,

Chapter 4][3]

$$\begin{aligned} P_{ij} &= P_{\bar{i}\bar{j}} \\ P_{i\bar{j}} &= P_{\bar{i}j} \\ P_{ig} &= P_{\bar{i}g} \equiv n_f P_{qg} \\ P_{gi} &= P_{g\bar{i}} \equiv n_f P_{gq}. \end{aligned} \tag{2.21}$$

The combination of type $q_i - q_j$ decouples from the gluon density and evolves independently. Such combinations are collectively denoted as non-singlet ones. A singlet combination

$$q_{\mathrm{s}} = \sum_{i=1}^{n_f} f_i(x, Q^2) + \bar{f}_i(x, Q^2) \tag{2.22}$$

with $\bar{f}_i = f_{\bar{i}}$ on the other hand couples maximally to the gluon density. The system in eq. (2.19) is then usually written in the term of singlet and non-singlet equations:

$$\frac{\mathrm{d}q_{\mathrm{ns}}(x, Q^2)}{\mathrm{d}\ln Q^2} = P_{\mathrm{ns}}(x, Q^2) \otimes q_{\mathrm{ns}}(x, Q^2) \tag{2.23}$$

and

$$\frac{\mathrm{d}\mathbf{q}(x, Q^2)}{\mathrm{d}\ln Q^2} = \mathbf{P}(x, Q^2) \otimes \mathbf{q}(x, Q^2) \tag{2.24}$$

with

$$\mathbf{P} = \begin{pmatrix} P_{qq} & P_{qg} \\ P_{gq} & P_{gg} \end{pmatrix} \qquad \text{and} \qquad \mathbf{q}(x, Q^2) = \begin{pmatrix} q_{\mathrm{s}}(x, Q^2) \\ g(x, Q^2) \end{pmatrix}, \tag{2.25}$$

where the perturbative expansion of the splitting functions $P_{ij} = P_{ij}(x, Q^2)$ is given in eq. (2.20). The blue and grey triangles on fig. 2.2 show the kinematical range of $x$ and $Q^2$ that is used as an input at the LHC collider. The latter are obtained with the evolution equations, eqs. (2.23) and (2.24) with the input given by the experimental data (in pink).[4] The fig. 2.3 shows the behaviour of parton distribution functions for all quarks and gluon at two different scales. At the low scales, the valence distributions peak roughly at $x = 1/3$. With increasing $Q^2$, all PDFs increase in the small $x$ region and decrease in the large $x$ region. The large number of gluons in the small $x$ region refers to the fact that the quarks inside proton are held together by a constant exchange of soft gluons [36]. In sufficiently small $x$ region and for high $Q^2$ all PDFs have roughly the same shape which is driven by the shape of gluon distribution [37].

[3] The last two definitions of eq. (2.21) sometimes differ by the multiplicative factor $n_f$ in the literature.
[4] It is not possible to obtain the full $x$ range necessary for the LHC input, as the small $x$ data are not available.

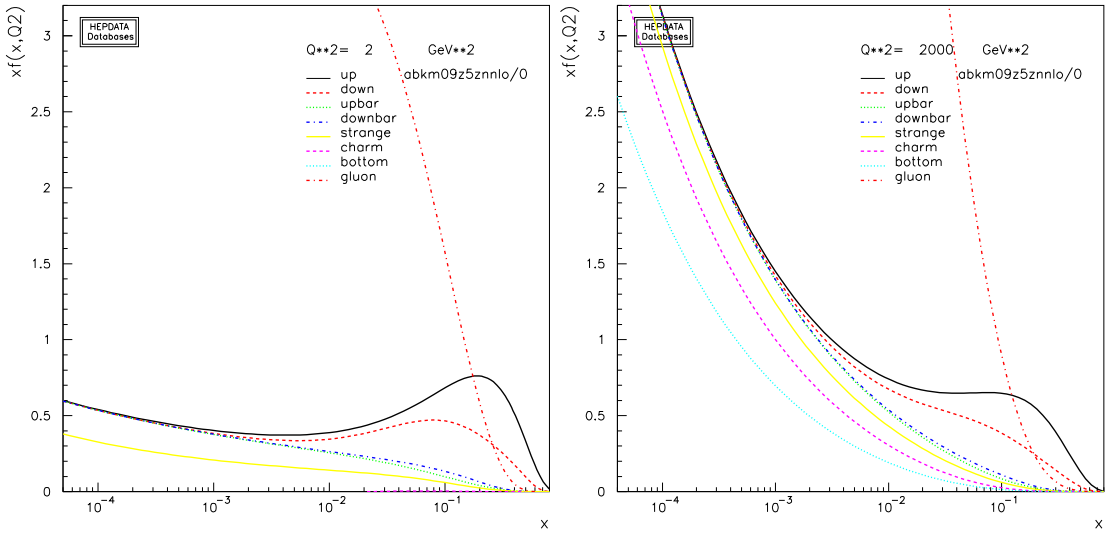


Figure 2.3.: Parton distribution functions of a proton at two different values of $Q^2$ using ABKM [63] PDF set. The gluon distribution represents the dominant part of a proton. With increasing $Q^2$ the number of quarks carrying small momentum fraction grows. Source: HEPDATA [64]

### 2.2.2. Parameterisation and fitting

Once the data is available a PDF analysis and a global fit can be performed at leading, next-to-leading or next-to-next-to leading order in the strong coupling $\alpha_s$. A first step of a global fit is a parameterisation of the $x$ dependence of all flavours. This is done at some rather low (but perturbative) scale $Q_0^2$ ~1–2 GeV$^2$. Such a distribution can then be evolved to higher scales using the evolution equations. The evolved PDFs are then convoluted with the hard cross sections and the theoretical predictions are matched to the data. The input parameters are then varied to minimise a global goodness-of-fit measure ($\chi^2$) [42]. A typical parameterisation has the following form [43]

$$f(x, Q_0) = A_0 x^{A_1} (1 - x)^{A_2} P(x; A_3, \dots). \tag{2.26}$$

The parameter $A_1$ relates to the small $x$ behaviour whereas the parameter $A_2$ models the large $x$ behaviour. The third term $P(x; A_3, \dots)$ is a suitably smooth function that contains one or more parameters and adds flexibility to the PDF parameterisation. The parameterisations are further constrained by a couple of sum rules. The sum rule for baryon number conservation reads

$$\int_0^1 \mathrm{d}x [f_{u/p}(x, Q^2) - f_{\bar{u}/p}(x, Q^2)] = 2 \tag{2.27}$$

$$\int_0^1 \mathrm{d}x [f_{d/p}(x, Q^2) - f_{\bar{d}/p}(x, Q^2)] = 1, \tag{2.28}$$

where subscript $p$ refers to proton and the difference can be identified with the valence distribution

$$f_a(x,Q^2) - \bar{f}_a(x,Q^2) = f_{a,\text{valence}}(x,Q^2). \tag{2.29}$$

The second momentum sum rule represents total energy-momentum conservation

$$\int_0^1 \mathrm{d}x \sum_{i=1}^{n_f} x[f_i(x,Q^2) + f_{\bar{i}}(x,Q^2) + g(x,Q^2)] = 1. \tag{2.30}$$

PDFs represent the largest source of theoretical uncertainties in cross section predictions. There are many groups which determine the PDFs from global fits and each of them produces its own PDF sets. The most up-to date sets are ABM11 [65], MSTW08 [66], CT10 [67], HERAPDF1.5, JR09 [68] and NNPDF2.1 [69]. The sets differ in various respects as the choice of data set, the form of initial parameterisation, and method used for the error analysis. There are also theoretical uncertainties coming along with PDF fitting which come from different values of the parameters entering the analysis treatment of heavy quark thresholds, uncertainties coming from scale variations, treatment of electroweak effects and various approximations, see for instance [70]. The data coming from the LHC experiments will soon provide more constraints on PDFs and give us more insight into this field [53].

## 2.3. Electroweak interactions and the Higgs mechanism

The Electroweak sector of the Standard Model is concerned with the interaction of the charged leptons and neutrinos via both electromagnetic and weak forces. The model was originally proposed by Glashow, Weinberg and Salam [1–3] and introduces the Higgs mechanism for Electroweak symmetry breaking responsible for the masses of the gauge bosons. The model is based on the $SU(2) \otimes U(1)$ symmetry group that corresponds to conservation of weak hypercharge and weak isospin. The gauge fields are one massless field $B_\mu$ and three massless fields $W^a_\mu$ with $a = 1, 2, 3$. The Lagrangian reads

$$\mathcal{L}_{\text{EW}} = -\frac{1}{4} B_{\mu\nu} B^{\mu\nu} - \frac{1}{4} W^a_{\mu\nu} W^{a\,\mu\nu} + i\bar{\psi}_f \not{D} \psi_f, \tag{2.31}$$

where $\psi_f$ stands for the left and right handed fermion fields $\psi_{L,i}$ and $\psi_{R,i}$, that form doublets and singlets under $SU(2)$, respectively and the index $i = 1, \ldots, 3$ refers to generation. The lepton fields read

$$\begin{aligned} &\psi_{L,1} = \gamma_L \begin{pmatrix} \nu_e \\ e^- \end{pmatrix}, \quad \psi_{L,2} = \gamma_L \begin{pmatrix} \nu_\mu \\ \mu^- \end{pmatrix}, \quad \psi_{L,3} = \gamma_L \begin{pmatrix} \nu_\tau \\ \tau^- \end{pmatrix} \\ &e_{R,1} = \gamma_R e^-, \quad \mu_{R,2} = \gamma_R \mu^-, \quad \tau_{R,3} = \gamma_R \tau^-. \end{aligned} \tag{2.32}$$

The quark fields read

$$\begin{aligned}
&\psi_{L,1} = \gamma_L \begin{pmatrix} u \\ d' \end{pmatrix}, \quad \psi_{L,2} = \gamma_L \begin{pmatrix} c \\ s' \end{pmatrix}, \quad \psi_{L,3} = \gamma_L \begin{pmatrix} t \\ b' \end{pmatrix} \\
&u_{R,1} = \gamma_R u, \quad c_{R,2} = \gamma_R c, \quad t_{R,3} = \gamma_R t \\
&d'_{R,1} = \gamma_R d', \quad s'_{R,2} = \gamma_R s', \quad b'_{R,3} = \gamma_R b'
\end{aligned} \tag{2.33}$$

and the relationship between left and right handed fields is given in terms of Dirac matrices is

$$\gamma_R = \frac{1}{2}(1+\gamma_5) \qquad \text{and} \qquad \gamma_L = \frac{1}{2}(1-\gamma_5). \tag{2.34}$$

In the eq. (2.31) we have ignored the fermion masses. $\not{D} = \gamma_\mu D^\mu$ and the covariant derivative is defined as

$$D^\mu = \delta_{ab}\partial^\mu + i g_w (T \cdot W^\mu)_{ab} + iY\delta_{ab} g'_w B^\mu, \tag{2.35}$$

where $Y$ is the weak hypercharge, generator of $U(1)$ and $T^a$ are the $SU(2)$ weak isospin generators that are proportional to Pauli matrices. The $g_w$ and $g'_w$ are $SU(2)$ and $U(1)$ gauge couplings. The field strengths read

$$\begin{aligned}
B_{\mu\nu} &= \partial_\mu B_\nu - \partial_\nu B_\mu \\
W^a_{\mu\nu} &= \partial_\mu W^a_\nu - \partial_\nu W^a_\mu - g_w \epsilon^{abc} W^b_\mu W^c_\nu.
\end{aligned} \tag{2.36}$$

As in QCD, we can see the non-Abelian nature of the $SU(2)$ group which gives rise to the self coupling of gauge bosons.

The Lagrangian in eq. (2.31) does not describe observations of one massless gauge boson (the photon) and the three massive ones. In particular the mass of the $Z^0$ boson is $M_Z = 91.1876 \pm 0.0021\,\text{GeV}$ and the $W^\pm$ bosons are little lighter, with masses $M_W = 80.399 \pm 0.023\,\text{GeV}$ [52]. Direct inclusion of mass terms for gauge bosons is not possible as it violates the local $SU(2) \otimes U(1)$ gauge invariance. The fermion masses cannot be written down in a naive way either, as this violates the isospin symmetry.

In order to describe the observed gauge boson and fermion masses, the mechanism of electroweak symmetry breaking, also know as the Higgs mechanism has been proposed [71–75]. The idea resides in introduction of a complex doublet of scalar field $\phi$

$$\phi = \begin{pmatrix} \phi^+ \\ \phi^0 \end{pmatrix}, \tag{2.37}$$

which has the potential

$$V = \lambda(\phi^\dagger\phi)^2 - \mu^2\phi^\dagger\phi, \qquad \lambda, \mu^2 > 0 \tag{2.38}$$

with a minimum that is different from zero. In particular, the potential has a circle of degenerate minima which are different from zero. In one dimension, the potential

has the shape as in fig. 2.4. The choice of a particular direction for the minimum that

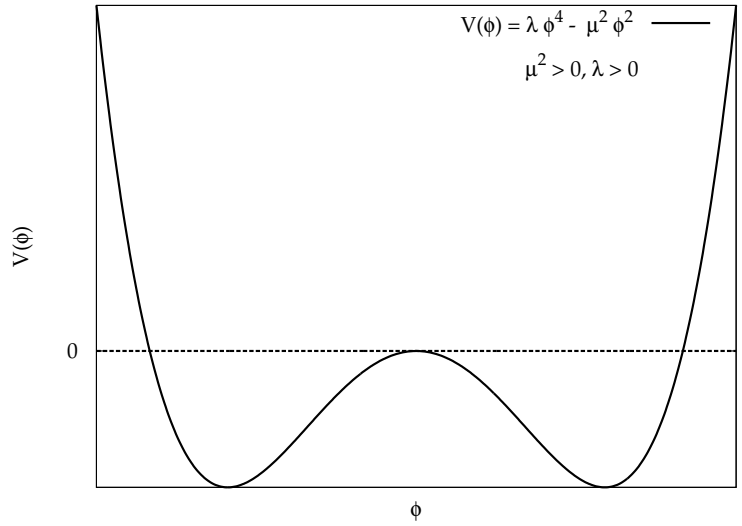


Figure 2.4.: The shape of the Higgs potential $V(\phi)$ in one dimension

corresponds to the choice of the vacuum expectation value

$$\langle\phi\rangle = \frac{1}{\sqrt{2}}\begin{pmatrix} 0 \\ v \end{pmatrix} \qquad \text{with} \qquad v = \sqrt{\frac{\mu^2}{\lambda}}, \tag{2.39}$$

which breaks the $SU(2) \otimes U(1)$ symmetry. The gauge boson mass terms come from coupling the Higgs field to the vector bosons using the covariant derivative

$$(D_\mu\phi)^\dagger D^\mu\phi \tag{2.40}$$

and expanding it around the ground state. As a result of the symmetry breaking, three of four scalar field components of the Higgs field get absorbed by the gauge particles to form the massive vector bosons $W^\pm_\mu$ and $Z^0_\mu$ and the remaining single neutral scalar particle gives rise to the Higgs boson. The masses that the gauge bosons have acquired are

$$M_W = \frac{1}{2}g_w v \qquad M_Z = \frac{1}{2}v\sqrt{g_w^2 + g_w'^2} = \frac{M_W}{\cos\theta_w}. \tag{2.41}$$

The $W^\pm$ are new fields introduced as

$$W^\pm_\mu = \frac{1}{\sqrt{2}}(W^1_\mu \mp iW^2_\mu) \tag{2.42}$$

and the weak mixing angle $\theta_w$ is the angle that appears in the change of the basis from

$(W_\mu^3, B_\mu) \to (Z_\mu, A_\mu)$

$$\begin{pmatrix} W_\mu^3 \\ B_\mu \end{pmatrix} = \begin{pmatrix} \cos\theta_w & \sin\theta_w \\ -\sin\theta_w & \cos\theta_w \end{pmatrix} \begin{pmatrix} Z_\mu \\ A_\mu \end{pmatrix}, \tag{2.43}$$

where $A_\mu$ is the massless photon field and $\theta_w$ is fixed by the relative strengths of coupling constants

$$\sin^2\theta_w = \frac{g_w'^2}{g_w'^2 + g_w^2} \sim 0.23. \tag{2.44}$$

The Higgs mass $m_H$ is then extracted from the self-coupling terms of the Higgs boson

$$(\partial^\mu \phi^\dagger \partial_\mu \phi) - V(\phi^\dagger \phi) \tag{2.45}$$

and reads

$$m_H = \sqrt{2}\mu. \tag{2.46}$$

It is possible to make an identification based on low energy weak interactions

$$\frac{G_F}{\sqrt{2}} = \frac{1}{2v^2}, \tag{2.47}$$

where $G_F = 1.166 \times 10^{-5}\,\mathrm{GeV}^2$ is the Fermi constant. This gives us the value of the vacuum expectation value of the Higgs field, $v = 246\,\mathrm{GeV}$.

The fermion masses are included via Yukawa interactions of the Higgs field with fermion fields,

$$g_f \bar{\psi}_f \phi \psi_f, \tag{2.48}$$

which results to a rather broad range of Yukawa couplings $g_f$ which are required to match the observed fermion masses. The fermion masses acquire a form

$$m_f = \frac{g_f v}{\sqrt{2}} \tag{2.49}$$

and their values are plotted on fig. 2.5 The full Lagrangian, together with the Higgs field reads

$$\mathcal{L} = D_\mu \phi^\dagger D^\mu \phi + V(\phi^\dagger \phi) + g_f \bar{\psi}_f \phi \psi_f + \bar{\psi}_f \not{D} \psi_f \tag{2.50}$$

from which one can extract the part describing electroweak interactions of fermions

$$\begin{aligned} \mathcal{L} = & \sum_f \bar{\psi}_f (i\not{\partial} - m_f - g_w \frac{m_f H}{2M_W}) \psi_f \\ & - \frac{g_w}{2} \sum_f \bar{\psi}_f (\gamma^\mu (v_{W,f} - a_{W,f}\gamma_5) T^+ W_\mu^+ + \gamma^\mu (v_{W,f} - a_{W,f}\gamma_5) T^- W_\mu^-) \psi_f \\ & - e \sum_f Q_f \bar{\psi}_f \not{A} \psi_f - \frac{g_w}{2\cos\theta_w} \sum_f \bar{\psi}_f \gamma^\mu (v_{Z,f} - a_{Z,f}\gamma_5) \psi_f Z_\mu, \end{aligned} \tag{2.51}$$

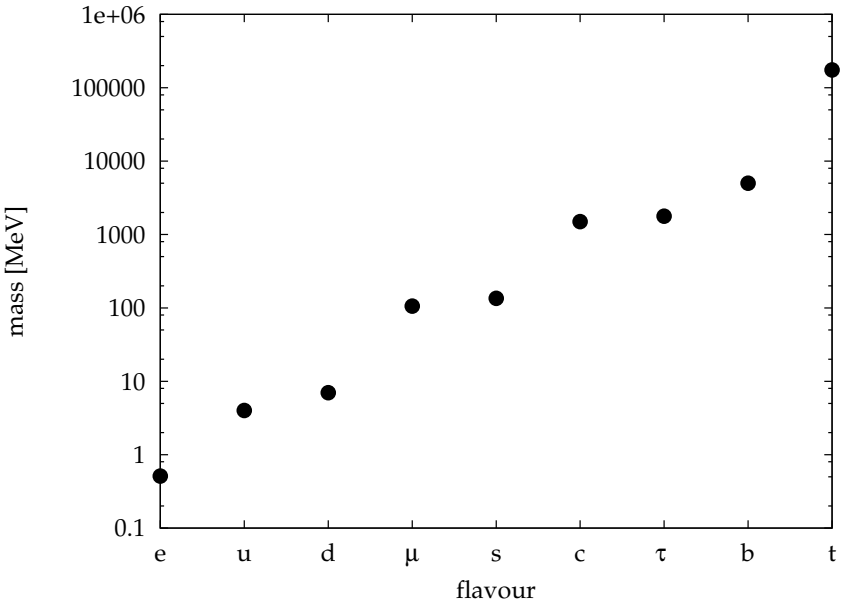


Figure 2.5.: Masses of charged fermions.

where $Q_f$ summarised in tab. 2.2 is the fermion fractional charge and the couplings to bosons $v_{V,f}$ and $a_{V,f}$ are given in the tab. 4.1. The full details of the Higgs mechanism can be found for instance in the recent reviews [38–40] or standard textbooks [33, 34].

### 2.3.1. The electroweak vertex

The general form of the vertex with a gauge boson $V$ and two fermions $f_1$ and $\bar{f}_2$ reads

$$-ie\gamma^{\mu}c_{V,f}(v_{V,f} - a_{V,f}\gamma_5), \tag{2.52}$$

where the label $f$ denotes the combination of fermions $f_i$ and $\bar{f}_j$ and $c_{V,f}$, $v_{V,f}$ and $a_{V,f}$ are an overall factor, vector and axial couplings, respectively. The exact values are given in the tab. 2.1. The tab. 2.2 gives complementary information concerning the labelling and notation. The elements of CKM (Cabibbo-Kobayashi-Maskawa) mixing matrix $V_{q_u q_d}$ in the tab. 2.1 express the relationship between primed down-type quarks in eq. (2.31) and their mass eigenstate combinations. The CKM matrix is a unitary matrix which reads

$$V = \begin{pmatrix} V_{ud} & V_{us} & V_{ub} \\ V_{cd} & V_{cs} & V_{cb} \\ V_{td} & V_{ts} & V_{tb} \end{pmatrix} \tag{2.53}$$

| $V$ | $\gamma$ | $W$ | | | | $Z$ | | | |
|---|---|---|---|---|---|---|---|---|---|
| $f_1\bar{f}_2$ | $f\bar{f}$ | $l\bar{\nu}_{l'}$ | $\bar{l}\nu_{l'}$ | $q_u\bar{q}_d$ | $q_d\bar{q}_u$ | $l\bar{l}$ | $\nu\bar{\nu}$ | $q_u\bar{q}_u$ | $q_d\bar{q}_d$ |
| $c_{V,f}$ | 1 | $\frac{1}{2\sin\theta_W}\delta_{ll'}$ | | $\frac{1}{2\sin\theta_W}V_{q_uq_d}$ | | $\frac{1}{2\cos\theta_W\sin\theta_W}$ | | | |
| $v_{V,f}$ | $Q_f$ | $\frac{1}{\sqrt{2}}$ | | | | $a_f - 2Q_f\sin^2\theta_W$ | | | |
| $a_{V,f}$ | 0 | $\frac{1}{\sqrt{2}}$ | | | | $-\frac{1}{2}$ | $\frac{1}{2}$ | $\frac{1}{2}$ | $-\frac{1}{2}$ |

Table 2.1.: Feynman rules for fermion electroweak interactions

| | up-type quarks | down-type quarks | neutrinos | charged leptons |
|---|---|---|---|---|
| | $q_u = u, c, t$ | $q_d = d, s, b$ | $\nu_l = \nu_e, \nu_\mu, \nu_\tau$ | $l = e, \mu, \tau$ |
| $Q_f$ | $\frac{2}{3}$ | $-\frac{1}{3}$ | 0 | -1 |

Table 2.2.: Summary of fermion fractional charges. The charges of antifermions are opposite, $\bar{q}_f = -Q_f$.

and has four independent parameters, three mixing angles and one phase. The unitarity constraint imposes nine conditions,

$$\sum_{j=1}^{3}|V_{ij}|^2 = \sum_{i=1}^{3}|V_{ij}|^2 = 1, \qquad \sum_{k=1}^{3}V_{ki}^*V_{kj} = 0, \quad i \neq j. \tag{2.54}$$

The measurement of the values of entries are important for determination provides an important information about the CP violation [52].

## 2.4. Cross sections via Mellin space

In chapter 1 we already sketched the basic idea of Mellin transform and its use in cross section evaluations. The cross section formula represents a particular case of the convolution integral

$$(f_1 \otimes f_2 \otimes \cdots \otimes f_k)(x) = \\ \int_0^1 \mathrm{d}x_1 \int_0^1 \mathrm{d}x_2 \ldots \int_0^1 \mathrm{d}x_k\, \delta(x - x_1x_2\ldots x_k) f_1(x_1)f_2(x_2)\ldots f(x_k). \tag{2.55}$$

The number of convolution signs $\otimes$ in eq. (2.55) represents the number of integrations. Convolution of two functions appears in the case of deep inelastic scattering cross section

and evolution equations for parton distribution functions. The explicit expression reads

$$\begin{aligned}(f_1 \otimes f_2)(x) &= \int_0^1 \mathrm{d}x_1 \int_0^1 \mathrm{d}x_2\, \delta(x_1 x_2 - x) f_1(x_1) f_2(x_2) \\ &= \int_x^1 \frac{\mathrm{d}x_1}{x_1} f_1(x_1) f_2(x/x_1),\end{aligned} \tag{2.56}$$

where in the second step we applied the property of the delta function, see eq. (A.17). The limit on the integral over $x_1$ is set by the delta function

$$x_2 = \frac{x}{x_1} \leq 1 \qquad \Rightarrow x_1 \geq x. \tag{2.57}$$

The Drell-Yan and Higgs cross sections involve the convolution of two PDFs and a hard scattering cross section. In particular,

$$\begin{aligned}(f_1 \otimes f_2 \otimes f_3)(x) &= \int_0^1 \mathrm{d}x_1 \int_0^1 \mathrm{d}x_2 \int_0^1 \mathrm{d}x_3\, \delta(x_1 x_2 x_3 - x) f_1(x_1) f_2(x_2) f_3(x_3) \\ &= \int_{x_{1,\min}}^1 \mathrm{d}x_1 \int_{x_{2,\min}}^1 \mathrm{d}x_2 f_1(x_1) f_2(x_2) f_3\Big(\frac{x}{x_1 x_2}\Big) \frac{1}{x_1 x_2} \\ &= \int_x^1 \frac{\mathrm{d}x_1}{x_1} \int_{x/x_1}^1 \frac{\mathrm{d}x_2}{x_2} f_1(x_1) f_2(x_2) f_3\Big(\frac{x}{x_1 x_2}\Big),\end{aligned} \tag{2.58}$$

where in the last step we set the limits for $x_{1,\min}$ and $x_{2,\min}$ after the application of the delta function using

$$x_3 = \frac{x}{x_1 x_2} \leq 1 \qquad \Rightarrow x_2 > \frac{x}{x_1} \tag{2.59}$$

$$\text{and since} \quad x_2 \leq 1 \quad \Rightarrow x_1 > x. \tag{2.60}$$

Mellin transform is an integral transform between a function from momentum fraction space, referred to as $x$-space $f(x)$ and a function from moment space $f(N)$ denoted commonly $N$-space. It is common not to make any distinctions between the functions in the two representations and denote them both by the same symbol. We will adopt this notation. The Mellin transform of a function $f(x)$

$$f(N) = \int_0^1 \mathrm{d}x\, x^{N-1} f(x), \tag{2.61}$$

turns the integrals in eq. (2.55) into ordinary products,

$$(f_1 \otimes f_2 \otimes \cdots \otimes f_k(x))(x) \to f_1(N) f_2(N) \ldots f_k(N) \equiv f(N). \tag{2.62}$$

The inverse Mellin transform is then used to recover the original momentum space,

$$f(x) = \frac{1}{2\pi i} \int_{c-i\infty}^{c+i\infty} \mathrm{d}N\, x^{-N} f(N), \tag{2.63}$$

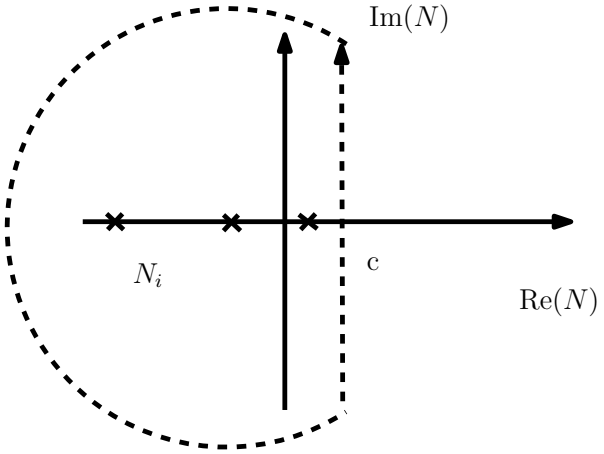


Figure 2.6.: The inverse Mellin transform.

where $c$ represents a point on the real axis such that all poles $N_i$ in the function $f(N)$ lie to the left from $c$, see fig. 2.6.

# 3. Hadron-hadron scattering

The chapter presents the formalism that concerns fully inclusive cross sections for the production of vector bosons $W^{\pm}$ and $Z^0$ and the SM Higgs boson $H$ via gluon-gluon fusion in a collision of two hadrons up to next-to-next-to-leading in perturbative QCD. The cross sections are expressed in terms of structure functions. The $W^{\pm}$ and $Z^0$ production supplemented with leptonic decays represents the Drell-Yan process. The Higgs boson production is treated with the effective Lagrangian approach that emerges from the Standard Model by taking the top quark mass limit $m_t \to \infty$. We introduce harmonic polylogarithms that appear in the hard scattering Wilson coefficients and discuss the connection between the Drell-Yan structure function and hadronic cross section.

## 3.1. The Drell-Yan process

The Drell-Yan process, originally described in the context of the parton model [76], concerns the production of a lepton pair of large invariant mass in hadron-hadron collisions with an intermediate state virtual photon. Historically, it was the first process at hadron-hadron colliders where the parton model ideas, developed earlier in the deep inelastic scattering, were applied. The non-existence of final state QCD radiation makes this process sufficiently simple such that higher order perturbative corrections are theoretically feasible. The parton model result has been supplied by the next-to-leading order QCD result in the end of the 70's[77–93]. With the increase of the centre of mass energy at particle accelerators, the Drell-Yan process led to the discovery of $W^{\pm}$ and $Z^0$ particles at UA1 and UA2 experiments [94, 95][1]. The study of properties of electroweak bosons (masses, decay widths and asymmetries) at LEP and Tevatron followed and together with the next-to-next-to-leading prediction in 1990 [16, 17] the values of the Standard Model parameters have been determined to very high precision. At the Tevatron the vector boson rapidity distributions and charge asymmetry gave more information on particular combinations of the parton distribution functions, see c.f. [96]. At present, the Drell-Yan process serves as a standard candle for the Large Hadron Collider detector calibration and luminosity measure and provides a test of the Standard Model at new range of centre of mass energies. It will provide us with more insight into the proton structure. The need of electroweak corrections to the Drell-Yan process turned out to be non-negligible, in particular with increasing centre of mass energy of hadron colliders. These have been calculated up to NLO [97–100] and supplemented with the

[1] In 1984 Carlo Rubbia and Simon van der Meer were awarded the Nobel Prize for the contribution to the project which led to the discovery of particles mediating weak interactions

combined EW+QCD results, see for instance [101] and references therein. The fully exclusive results are also known up to NNLO [102].

### 3.1.1. The formalism

We consider the inclusive production of a single vector boson $V = W^+, W^-$ or $Z^0$ via the Drell-Yan mechanism. This corresponds to a production of a lepton pair $l\bar{l}$ of an invariant mass close to the vector boson peak. The word inclusive refers to the fact that except for the required lepton pair also anything else in the final state (denoted by $X$) is allowed [103], see fig. 3.1. The lepton pair is in the case of neutral current represented by the combination $l^+l^-$ whereas in the case of charged current by $\bar{l}\nu_l$ or $l\bar{\nu}_l$ with $l = e, \mu, \tau$ in both cases. We treat all external particles contributing to the hard subprocess as massless. Applying the factorisation formula, the cross section can

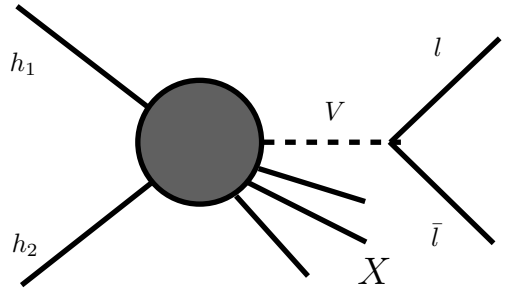


Figure 3.1.: The production of a massive lepton pair $l$ and $\bar{l}$ via vector boson in a collision of two hadrons $h_1$,$h_2$. $X$ denotes any inclusive final hadronic state allowed by conservation of quantum numbers.

be expressed in terms of two parton distribution functions $f_a(x_1, Q^2)$ and $f_b(x_2, Q^2)$ and a hard scattering cross section $\hat{\sigma}^V_{ab}(\hat{s}, Q^2)$ [2]

$$\frac{\mathrm{d}\sigma^V(s, Q^2)}{\mathrm{d}Q^2} = \sum_{a,b \in q,\bar{q},g} \int_{x_{1,\min}}^{1} \mathrm{d}x_1 \int_{x_{2,\min}}^{1} \mathrm{d}x_2 f_a(x_1, Q^2) f_b(x_2, Q^2) \frac{\mathrm{d}\hat{\sigma}^V_{ab}(\hat{s}, Q^2)}{\mathrm{d}Q^2}. \tag{3.1}$$

For the moment we do not make the distinction among the various hard scales and set $\mu_f = \mu_r = Q$. The sum represents a summation over appropriate channels that contribute to the hard subprocess with partons $a$ and $b$ in the initial state. For initial hadrons with momenta $P_1$ and $P_2$ the centre of mass energy $s$ is given by

$$s = (P_1 + P_2)^2 \tag{3.2}$$

[2] The superscript $V$ denoting a vector boson will further on appear on several quantities and there is no distinction of $V$ being subscript or superscript.

and the invariant mass of the final state lepton pair $M_{l\bar{l}}$ with momenta $p_3$ and $p_4$ is equal to the momentum of the intermediate vector boson

$$Q^2 = (p_3 + p_4)^2 = M_{l\bar{l}}^2. \tag{3.3}$$

The eq. (3.1) also contains kinematical variables $x_1$ and $x_2$ which represent the momentum fraction carried by partons $a$ and $b$ and $x_1, x_2 \in (0, 1)$. We define a variable $\tau$ in terms of $s$ and $Q^2$ as

$$\tau = \frac{Q^2}{s}, \qquad \tau \in (0, 1) \tag{3.4}$$

and $\hat{s}$ is the centre of mass energy of colliding partons with momenta $p_1$ and $p_2$,

$$\hat{s} = (p_1 + p_2)^2 = s x_1 x_2. \tag{3.5}$$

The condition

$$Q^2 \leq \hat{s} \quad \Rightarrow \quad x_1 x_2 \geq \tau \tag{3.6}$$

with the equality corresponding to no initial state radiation, sets the values of $x_{1,\min}$ and $x_{2,\min}$

$$x_2 \leq \tau / x_1 \quad \text{and} \quad x_1 \leq \tau \tag{3.7}$$

or vice versa. Substituting the limits in eq. (3.1) the cross section can be expressed in terms of the hadronic structure function $W_V(x, Q^2)$ and point-like cross section $\sigma_0^V(Q^2, M_V^2)$,

$$\frac{\mathrm{d}\sigma^V(s, Q^2)}{\mathrm{d}Q^2} = \tau \sigma_0^V(Q^2, M_V^2) W_V(\tau, Q^2). \tag{3.8}$$

The expression for $\sigma_0^V(Q^2, M_V^2)$ is given in eqs. (3.45) and (3.46) and the structure function is given in terms of convolution of two parton functions and perturbative coefficient functions $\Delta_{ab}(x, Q^2)$

$$\begin{aligned} W_V(\tau, Q^2) &= \sum_{a,b \in q,\bar{q},g} \int_\tau^1 \frac{\mathrm{d}x_1}{x_1} \int_{\tau/x_1}^1 \frac{\mathrm{d}x_2}{x_2} C_{ab}^V f_a(x_1, \mu_f^2) f_b(x_2, \mu_f^2) \Delta_{ab}(\tau/(x_1 x_2), Q^2, \mu_f^2) \\ &= \sum_{a,b \in q,\bar{q},g} \int_\tau^1 \frac{\mathrm{d}x_1}{x_1} \int_{\tau/x_1}^1 \frac{\mathrm{d}x_2}{x_2} PD_{ab}^V(x_1, x_2, \mu_f^2) \Delta_{ab}(\tau/(x_1 x_2), Q^2, \mu_f^2), \end{aligned} \tag{3.9}$$

where the factor $C_{ab}^V$ represents a generic factor that describes the coupling of partons to the vector boson. The exact $N$ space equivalent of the Drell-Yan structure function formula up to NNLO as given in equation (A.20) of [16] reads

$$W_V(N, Q^2) = \sum_{i,j \in \mathrm{Q}, \bar{\mathrm{Q}}} C^{\mathrm{ii}}(i, \bar{j})(v_i^2 + a_i^2) \Delta_{q\bar{q}}(N) f_{i,\bar{j}}(N)$$

$$
\begin{aligned}
&+\Big\{\sum_{\substack{i\in\mathrm{Q},\bar{\mathrm{Q}}\\ j,k\in\mathrm{Q}}} C^{\mathrm{ff}}(j,\bar{k})(v_j^2+a_j^2)\Delta^{(2)}_{q\bar{q},\mathrm{B}^2}(N)\\
&+\sum_{i,j\in\mathrm{Q},\bar{\mathrm{Q}}} \{C^{\mathrm{if}}(i,\bar{j})+C^{\mathrm{if}}(\bar{i},j)\}(v_i^2+a_i^2)\Delta^{(2)}_{q\bar{q},\mathrm{BC}}(N)\\
&+\sum_{\substack{i\in\mathrm{Q},\bar{\mathrm{Q}}\\ j\in\mathrm{Q}}} C^{\mathrm{ff}}(j,\bar{j})\{v_iv_j\Delta^{(2),\mathrm{V}}_{q\bar{q},\mathrm{AB}}(N)+a_ia_j\Delta^{(2),\mathrm{A}}_{q\bar{q},\mathrm{AB}}(N)\}\\
&\Big\}f_{i,\bar{i}}(N)\\
&+\sum_{i,j\in\mathrm{Q}\bar{\mathrm{Q}}} C^{\mathrm{if}}(i,j)(v_i^2+a_i^2)\Delta_{qg}(N)(f_{i,g}+f_{g,i})\\
&+\Big\{\sum_{i,j,k\in\mathrm{Q},\bar{Q}} \{C^{\mathrm{if}}(i,k)(v_i^2+a_i^2)+C^{\mathrm{if}}(j,k)(v_j^2+a_j^2)\}\Delta^{(2)}_{qq,\mathrm{C}^2}(N)\\
&+\sum_{i,j\in\mathrm{Q},\bar{Q}} C^{\mathrm{if}}(i,i)\{v_iv_j\Delta^{(2),\mathrm{V}}_{q_iq_j,\mathrm{CD}}(N)+a_ia_j\Delta^{(2),\mathrm{A}}_{qq,\mathrm{CD}}(N)\}\\
&+\sum_{i,j\in\mathrm{Q},\bar{Q}} \{C^{\mathrm{if}}(i,j)(v_i^2+a_i^2)+C^{\mathrm{if}}(j,i)(v_j^2+a_j^2)\}\Delta^{(2)}_{qq,\mathrm{CE}^2}(N)\\
&+\sum_{i,j,k\in\mathrm{Q},\bar{Q}} C^{\mathrm{if}}(i,k)(v_i^2+a_i^2)\Delta^{(2)}_{qq,\mathrm{CF}^2}(N)\\
&\Big\}f_{i,j}(N)\\
&+\sum_{i,j\in\mathrm{Q}} C^{\mathrm{ff}}(i,\bar{j})(v_i^2+a_i^2)\Delta^{(2)}_{gg}(N)f_{g,g}(N),
\end{aligned}
\tag{3.10}
$$

where $v_i$, $a_i$ and $C^{\mathrm{ii/if/ff}}$ refer to vector coupling, axial coupling and a factor selecting the non-zero quark combinations, respectively. An extra label $V$ in couplings and selection factor that refers to the type of vector boson is omitted in eq. (3.10) for simplicity reasons and in order to keep analogy with eq. (A.20) of [16]. The vector and axial couplings are smaller by a factor of two from those defined in eq. (A.13) of [16] for the $Z^0$ boson which is then compensated by in the overall point-like cross section, see eqs. (3.45) and (3.53). The vector and axial couplings are given in tab. 2.1 and

$$
C^{\mathrm{ii},Z}(i,j)=C^{\mathrm{ff},Z}(i,j)=\begin{cases}1 & \text{if } i=\bar{j}\\ 0 & \text{otherwise}\end{cases}
\tag{3.11}
$$

$$
C^{\mathrm{ii},W^\pm}(i,j)=C^{\mathrm{ff},W^\mp}(i,j)=\begin{cases}1 & \text{if } Q_i+Q_j=\pm 1\\ 0 & \text{otherwise}\end{cases}
\tag{3.12}
$$

$$
C^{\mathrm{if},Z}(i,j)=\begin{cases}1 & \text{if } i=j\\ 0 & \text{otherwise}\end{cases}
\tag{3.13}
$$

$$C^{\text{if},W^\pm}(i,j) = \begin{cases} 1 & \text{if } Q_i - Q_j = \pm 1 \\ 0 & \text{otherwise,} \end{cases} \tag{3.14}$$

where $Q_i$ refers to the quark fractional charge, see tab. 2.2.

$$\Delta_{q\bar{q}}(N) = 1 + \Delta^{(1)}_{q\bar{q}}(N) + \Delta^{(2),\text{NS}}_{q\bar{q}}(N), \tag{3.15}$$

$$\begin{aligned} \Delta^{(2),\text{NS}}_{q\bar{q}}(N) &= \Delta^{(2),\text{S+V}}_{q\bar{q}}(N) + \Delta^{(2),C_A}_{q\bar{q}}(N) + \Delta^{(2),C_F}_{q\bar{q}}(N) + \Delta^{(2)}_{q\bar{q},\text{AC}}(N) \\ &+ \frac{\alpha_s}{4\pi}\beta_0 \Delta^{(1)}_{q\bar{q}}(N) \ln\Big(\frac{\mu_r^2}{\mu_f^2}\Big), \end{aligned} \tag{3.16}$$

$$\Delta_{qg}(N) = \Delta^{(1)}_{qg}(N) + \Delta^{(2)}_{qg}(N), \tag{3.17}$$

$$\Delta^{(2)}_{qg}(N) = \Delta^{(2),C_A}_{qg}(N) + \Delta^{(2),C_F}_{qg}(N) + \frac{\alpha_s}{4\pi}\beta_0 \Delta^{(1)}_{qg}(N) \ln\Big(\frac{\mu_r^2}{\mu_f^2}\Big). \tag{3.18}$$

The summation sets in eq. (3.10) run over all active quark flavours

$$Q = \{d, u, s, c, b\}, \qquad \bar{Q} = \{\bar{d}, \bar{u}, \bar{s}, \bar{c}, \bar{b}\}. \tag{3.19}$$

The functions $f_{i,j}(N)$ correspond to the combination of PDFs,

$$f_{i,j}(N) = f_{i/h_1}(N) f_{j/h_2}(N) \tag{3.20}$$

with hadrons $h_1$ and $h_2$ and note that the order of indices matters. We also use

$$f_{i/p}(N) = f_{\bar{i}/\bar{p}}(N), \qquad f_{\bar{i}/p}(N) = f_{i/\bar{p}}(N), \tag{3.21}$$

where $p$ and $\bar{p}$ denotes proton and anti-proton.

We obtained the $N$ space expressions for coefficient functions $\Delta_{ab}(N)$ using the `FORM` [25] package `harmpol` [26], that allowed us to do the Mellin transforms of $x$ space expressions in an automated way. The final result is expressed in terms of harmonic sums up to the depth four to which we applied additional identities in order to reduce them to sums of lower depth. We used Taylor expansion for some particular sums which do not have direct Mellin transforms. More details on the numerical implementation are given in the Section 5.2.

For the $x$ space input we used the results of V. Ravindran, who provided us with his private file [104]. These expressions follow (also in terms of notation) the original publication by Hamberg et. al. [16]. The file includes the corrections of Harlander and Kilgore [105] and most of the corrections pointed out by Anastasiou et. al. [102], namely the prefactor $T_f$ in the eq. (B.13) of [16] and a factor of $x$ multiplying the last term of eq. (B.11) of [16]. We further corrected the input file of[104] for the factor $T_f$ multiplying

the term corresponding to eq. (B.16) of of [16] and an overall factor of 2 in the term that corresponds to eq. (B.25) of [16] [3].

The $N$ space results for coefficient functions were also presented by J. Blümlein earlier and can be found in [106].

### 3.1.2. The Drell-Yan structure function

In this section we derive the cross section in terms of structure function as given in eq. (3.9). The derivation follows the Appendix A of the PhD thesis of Tsuyoshi Matsuura [107] with more focus on some particular details.

Let us consider the $2 \to n$ scattering process with massless external particles. The initial state partons $a$ and $b$ have momenta $p_1$ and $p_2$ and there are $n-2$ final state partons $m_i$ with momenta $k_i$ and leptons $l$ and $\bar{l}$ with momenta $p_3$ and $p_4$ produced via decay of an intermediate vector boson $V$

$$a(p_1) + b(p_2) \to \sum_{i=1}^{n-2} m_i(k_i) + V(q) \to l(p_3) + \bar{l}(p_4). \tag{3.22}$$

We define the total momentum of incoming and outgoing particles as follows

$$P_{\text{in}} = p_1 + p_2, \qquad P_{\text{out}} = \sum_{i=1}^{n-2} k_i + \sum_{j=3}^{4} p_j. \tag{3.23}$$

Working in $d = 4 - 2\varepsilon$ dimensions the differential cross section for this process reads

$$\mathrm{d}\hat{\sigma}^V_{ab} = \frac{(2\pi)^d}{4I}\Big\{\prod_{j=3}^{4}\frac{\mathrm{d}^d p_j}{(2\pi)^{d-1}}\delta^+(p_j^2)\Big\}\Big\{\prod_{i=1}^{n-2}\frac{\mathrm{d}^d k_i}{(2\pi)^{d-1}}\delta^+(k_i^2)\Big\}\delta^{(d)}(P_{\text{in}} - P_{\text{out}})|\mathcal{M}^V_{ab}|^2, \tag{3.24}$$

where $\delta^{(d)}(P_{\text{in}} - P_{\text{out}})|\mathcal{M}^V_{ab}|^2$ represents the amplitude squared and $I$ stands for the flux factor. In CM system of incoming particles

$$\frac{1}{4I} = \frac{1}{2\hat{s}}, \tag{3.25}$$

where $\hat{s}$ is the CM energy of incoming particles. The function $\delta^+(p^2) = \delta(p^2)\theta(p_0)$ selects the positive energy solutions. The amplitude $|\mathcal{M}^V_{ab}|^2$ can be written in terms of leptonic and partonic tensors and $L^V_{\mu\nu}$ and $T^{V,\mu\nu}_{ab}$ a (dressed) vector boson propagator

$$|\mathcal{M}^V_{ab}|^2 = \frac{L^V_{\mu\nu}T^{V,\mu\nu}_{ab}}{(Q^2 - M_V^2)^2 + M_V^2\Gamma_V^2}, \tag{3.26}$$

where $M_V$ (not to be confused with $\mathcal{M}^V$) and $\Gamma_V$ are mass and decay width of the

[3] There is a further correction in an overall factor for $W$ boson of [16], namely eqs. (A.3) and (A.11) should be factor 2 larger [102].

vector boson $V$, respectively. We rewrite the momentum conserving delta function in the eq. (3.24)

$$\delta^{(d)}(P_{\rm in} - P_{\rm out}) = \int \mathrm{d}^d q \, \mathrm{d}Q^2 \delta^+(q^2 - Q^2)\delta(q - \sum_{j=3}^{4} p_j)\delta^{(d)}(P_{\rm in} - q - \sum_{i=1}^{n-2} k_i) \tag{3.27}$$

and after some rearrangement of factors of $2\pi$ the eq. (3.24) reads

$$\begin{aligned}\frac{\mathrm{d}\hat{\sigma}^V_{ab}}{\mathrm{d}Q^2} = &\frac{1}{2\hat{s}(2\pi)^{d-1}} \frac{1}{(Q^2 - M_V^2)^2 + M_V^2\Gamma_V^2} \\ &(2\pi)^d \int \frac{\mathrm{d}^d q}{(2\pi)^{d-1}} \Big\{ \prod_{i=1}^{n-2} \int \frac{\mathrm{d}^d k_i}{(2\pi)^{d-1}} \delta^+(k_i^2) \Big\} \delta^+(q^2 - Q^2)\delta^{(d)}(P_{\rm in} - q - \sum_{i=1}^{n-2} k_i) T^{V,\mu\nu}_{ab} \\ &\Big\{ \prod_{j=3}^{4} \int \mathrm{d}^d p_j \delta^+(p_j^2) \Big\} \delta^{(d)}(q - \sum_{j=3}^{4} p_j) L^V_{\mu\nu}. \end{aligned} \tag{3.28}$$

The above expression is in the form which separates the leptonic and partonic parts of the cross section. In addition, since we are not interested in the QED corrections the phase space integral over the lepton tensor can be evaluated directly. The lepton tensor can be written as

$$\begin{aligned} L^V_{\mu\nu} = \langle B_\mu B^\dagger_\nu \rangle &= e^2 c^2_{V,l}(v^2_{V,l} + a^2_{V,l}) \langle \tilde{B}_\mu \tilde{B}^\dagger_\nu \rangle \\ &= 2e^2 c^2_{V,l}(v^2_{V,l} + a^2_{V,l})(p_{3\mu}p_{4\nu} + p_{4\mu}p_{3\nu} - g_{\mu\nu} p_3.p_4), \end{aligned} \tag{3.29}$$

where the label $l$ denotes lepton flavour, the angular brackets refer to averaging over initial state boson polarisation and sum over final spin states of the leptons. Factors $c_{V,l}$, $v_{V,l}$ and $a_{V,l}$ are given in the table 2.1 As there is no longitudinal polarisation at the tree level the average over initial boson polarisation gives a factor of $\frac{1}{2}$. $\tilde{B}_\mu$ is the amplitude for the process under consideration with a vertex replacement

$$ie\gamma^\mu c_{V,f}(v_{V,f} + a_{V,f}\gamma^5) \to i\gamma^\mu. \tag{3.30}$$

This replacement can be done in the case of massless fermions, as the squared amplitude will be proportional to

$$e^2 c^2_{V,l}(v^2_{V,f} + a^2_{V,f}) \tag{3.31}$$

and the overall factor that contains information about coupling of fermions to the vector boson can be pulled out from the squared amplitude. Since the most general structure of the leptonic tensor can be written as

$$L^V_{\mu\nu} = \lambda_1 q_\mu q_\nu - \lambda_2 q^2 g_{\mu\nu}, \tag{3.32}$$

where $\lambda_1$ and $\lambda_2$ are unknown constants, the phase space integral can be written in a

similar way,

$$\int \mathrm{d}^d p_3 \int \mathrm{d}^d p_4 \delta^+(p_3^2)\delta^+(p_4^2)\delta^{(d)}(q-p_3-p_4)L^V_{\mu\nu} = \tilde{\lambda}_1 q_\mu q_\nu - \tilde{\lambda}_2 q^2 g_{\mu\nu}. \tag{3.33}$$

To determine the unknown constants $\tilde{\lambda}_1$ and $\tilde{\lambda}_2$ we multiply eq. (3.33) separately by $g^{\mu\nu}$ and $q^\mu q^\nu$ [108]. Multiplication by $q^\mu$ will give zero due to the momentum conservation, $q^\mu L^V_{\mu\nu} = 0$ and therefore the first equation is

$$\tilde{\lambda}_1 = \tilde{\lambda}_2 \equiv \lambda. \tag{3.34}$$

The second equation reads

$$\int \mathrm{d}^d p_3 \int \mathrm{d}^d p_4 \delta^+(p_3^2)\delta^+(p_4^2)\delta^{(d)}(q-p_3-p_4)L^V_{\mu\nu} g^{\mu\nu} = \lambda q^2 (1-d), \tag{3.35}$$

where $d = 4 - 2\varepsilon$. It turns out that the solution for $\lambda$ reads

$$\lambda = \frac{2\pi}{(d-1)} e^2 c^2_{V,l}(v^2_{V,l} + a^2_{V,l}) \tag{3.36}$$

and

$$\Big\{ \prod_{j=3}^{4} \int \mathrm{d}^d p_j \delta^+(p_j^2) \Big\} \delta^{(d)}(q - \sum_{j=3}^{4} p_j) L^V_{\mu\nu} \overset{d=4}{=} (q_\mu q_\nu - q^2 g_{\mu\nu}) \frac{2\pi}{3} e^2 c^2_{V,l}(v^2_{V,l} + a^2_{V,l}). \tag{3.37}$$

More details on the phase space evaluation of the lepton tensor are given in the section A.2.

In the formula for the cross section, eq. (3.28) the term proportional to $q_\mu T^{V,\mu\nu}_{ab}$ is zero due to the Ward identity and only the term proportional to $g_{\mu\nu} T^{V,\mu\nu}_{ab}$ will survive. Each squared parton amplitude will contain exactly one electroweak vertex of the type $V q_i \bar{q}_j$. We can therefore further simplify the term $g_{\mu\nu} T^{V,\mu\nu}_{ab}$ and pull out the overall vertex prefactor in a similar manner as for the lepton tensor. At the leading order QCD we can write

$$g_{\mu\nu} T^{V,\mu\nu}_{ab} = \langle A^\mu_{ab} A^{\dagger,\nu}_{ab} \rangle = e^2 c^2_{V,t}(v^2_{V,t} + a^2_{V,t}) g_{\mu\nu} \langle \tilde{A}^\mu_{ab} \tilde{A}^{\dagger,\nu}_{ab} \rangle. \tag{3.38}$$

The angular brackets refer to averaging over initial state quantum numbers (colour and spin) and sum over final state ones and $\tilde{A}^\mu_{ab}$ is the amplitude for the process under consideration with the replacement defined in eq. (3.30) and label $t$ corresponds to the combination $ab$. Since

$$c^2_{V,t} = c^2_{V,l} |V_{ab}|^2, \tag{3.39}$$

then the eq. (3.28) reads

$$\begin{aligned}\frac{\mathrm{d}\hat{\sigma}^V_{ab}}{\mathrm{d}Q^2} &= -\frac{Q^2}{\hat{s}}\frac{e^4 c^4_{V,l}(v^2_{V,l}+a^2_{V,l})(v^2_{V,t}+a^2_{V,t})|V_{ab}|^2}{24\pi^2(Q^2-M_V^2)^2+M_V^2\Gamma_V^2}(2\pi)^d\int\frac{\mathrm{d}^d q}{(2\pi)^{d-1}}\\ &\times\Big\{\prod_{i=1}^{n-2}\int\frac{\mathrm{d}^d k_i}{(2\pi)^{d-1}}\delta^+(k_i^2)\Big\}\delta^+(q^2-Q^2)\delta(P_{\mathrm{in}}-q-\sum_{i=1}^{n-2}k_i)g_{\mu\nu}\langle\tilde{A}^\mu_{ab}\tilde{A}^{\dagger,\nu}_{ab}\rangle\\ &= \frac{\tau}{x_1x_2}\sigma_0^V(Q^2,M_V^2)(v^2_{V,t}+a^2_{V,t})|V_{ab}|^2\hat{W}_{ab}(\frac{\tau}{x_1x_2},Q^2,\varepsilon),\end{aligned}\tag{3.40}$$

where the parton structure function

$$\begin{aligned}\hat{W}_{ab}(x,Q^2,\varepsilon) = -\frac{N_c}{2\pi(1-\varepsilon)}(2\pi)^d\int\frac{\mathrm{d}^d q}{(2\pi)^{d-1}}\Big\{\prod_{i=1}^{n-2}\int\frac{\mathrm{d}^d k_i}{(2\pi)^{d-1}}\delta^+(k_i^2)\Big\}\delta^+(q^2-Q^2)\\ \delta(P_{\mathrm{in}}-q-\sum_{i=1}^{n-2}k_i)g_{\mu\nu}\langle\tilde{A}^\mu_{ab}\tilde{A}^{\dagger,\nu}_{ab}\rangle\end{aligned}\tag{3.41}$$

with $\varepsilon=(4-d)/2$ is normalised such that at leading order in QCD

$$\hat{W}_{ab}(x,Q^2,\varepsilon)=\delta(1-x).\tag{3.42}$$

$N_c$ stands for number of colours,

$$x=\frac{\tau}{x_1x_2}\tag{3.43}$$

and the point-like cross section is defined as

$$\sigma_0^V(Q^2,M_V^2)=\frac{e^4c^4_{V,l}(v^2_{V,l}+a^2_{V,l})}{12\pi N_c}\frac{1}{(Q^2-M_V^2)^2+M_V^2\Gamma_V^2}.\tag{3.44}$$

The exact expressions for point-like cross sections $\sigma_0^V(Q^2,M_V^2)$ read

$$\sigma_0^Z(Q^2,M_Z^2)=\frac{\pi\alpha^2}{48\sin^4\theta_W\cos^4\theta_W}\frac{1}{N_c}\frac{1+(1-4\sin^2\theta_W)^2}{(Q^2-M_Z^2)^2+M_Z^2\Gamma_Z^2},\tag{3.45}$$

$$\sigma_0^W(Q^2,M_W^2)=\frac{\pi\alpha^2}{12\sin^4\theta_W}\frac{1}{N_c}\frac{1}{(Q^2-M_W^2)^2+M_W^2\Gamma_W^2}.\tag{3.46}$$

After we plug the result in eq. (3.40) into the eq. (3.1) and substitute for the limits from eq. (3.7)

$$\frac{\mathrm{d}\sigma^V(s,Q^2)}{\mathrm{d}Q^2}=\tau\sigma_0^V(Q^2,M_V^2)\sum_{a,b}\int_\tau^1\frac{\mathrm{d}x_1}{x_1}\int_{\tau/x_1}^1\frac{\mathrm{d}x_2}{x_2}PD^V_{ab}(x_1,x_2)\hat{W}_{ab}(\frac{\tau}{x_1x_2},Q^2,\varepsilon)\tag{3.47}$$

with

$$PD^V_{ab}(x_1,x_2)=C_{V,ab}f_a(x_1)f_b(x_2),\tag{3.48}$$

where the factor $C_{V,ab}$ is a generic factor that selects the appropriate combinations of PDFs and couplings of vector boson to quarks. In this representation, the overall prefactor $\sigma_0^V(Q^2, M_V^2)$ has been extracted and the dependence on the type of vector boson has been moved out of the matrix element. The calculation of the higher order $\alpha_s$ corrections therefore reduces to calculation of QCD corrections of the partonic structure function $\hat{W}_{ab}(x, Q^2, \varepsilon)$.

### 3.1.3. The narrow width approximation

Sometimes called also the zero width approximation, it can be applied to the region of invariant lepton mass around the peak of $W$ or $Z$ boson. This approximation acts on the propagators in the point like cross sections in eqs. (3.46) and (3.45) which are replaced with a delta function,

$$\frac{1}{(Q^2 - M_V^2)^2 + M_V^2\Gamma_V^2} \to \frac{\pi}{M_V\Gamma_V}\delta(Q^2 - M_V^2). \tag{3.49}$$

Additionally, the point-like cross sections contain partial decay widths $\Gamma_{V\to l\bar{l}}$ [33, Chapter 8]

$$\Gamma_{Z\to l\bar{l}} = \frac{\alpha M_Z[1 + (1 - 4\sin^2\theta_W)^2]}{48\sin^2\theta_W\cos^2\theta_W} \tag{3.50}$$

$$\Gamma_{W\to l\bar{l}} = \frac{\alpha M_W}{12\sin^2\theta_W}, \tag{3.51}$$

which can be expressed in terms of a branching ratio $\mathrm{Br}_{V\to l\bar{l}}$ and the sum over all decay channels – the total decay width $\Gamma_V$ as follows:

$$\Gamma_{V\to l\bar{l}} = \mathrm{Br}_{V\to l\bar{l}}\Gamma_V. \tag{3.52}$$

Then the eqs. (3.45) and (3.46) become

$$\sigma_0^Z(Q^2, M_Z^2) = \frac{\pi^2\alpha\,\mathrm{Br}_{Z\to l\bar{l}}}{\sin^2\theta_W\cos^2\theta_W N_c M_Z^2}\delta(Q^2 - M_Z^2) \tag{3.53}$$

$$\sigma_0^W(Q^2, M_W^2) = \frac{\pi^2\alpha\,\mathrm{Br}_{W\to l\bar{l}}}{\sin^2\theta_W N_c M_W^2}\delta(Q^2 - M_W^2). \tag{3.54}$$

In the narrow width approximation the integration over $Q^2$ becomes trivial and the full hadronic cross section for the vector boson production (without decays to leptons) reads

$$\begin{aligned}\sigma^Z(s) = {} & \frac{\pi^2\alpha}{\sin^2\theta_W\cos^2\theta_W N_c}\frac{1}{s}\sum_{a,b}\int_0^1 \mathrm{d}x_1\int_0^1 \mathrm{d}x_2\int_0^1 \mathrm{d}x\,\delta(x_1x_2x - \tau) \\ & C_{Z,ab}f_a(x_1)f_b(x_2)\hat{W}_{ab}(M_Z^2/s, M_Z^2, \varepsilon) \\ \equiv {} & \frac{\pi^2\alpha}{\sin^2\theta_W\cos^2\theta_W N_c}\frac{1}{s}W^Z(M_Z^2/s, M_Z^2)\end{aligned}$$

$$\sigma^W(s) = \frac{\pi^2\alpha}{\sin^2\theta_W N_c}\frac{1}{s}\sum_{a,b}\int_0^1 \mathrm{d}x_1 \int_0^1 \mathrm{d}x_2 \int_0^1 \mathrm{d}x\, \delta(x_1x_2x-\tau)$$
$$C_{W,ab} f_a(x_1) f_b(x_2) \hat{W}_{ab}(M_W^2/s, M_W^2, \varepsilon)$$
$$\equiv \frac{\pi^2\alpha}{\sin^2\theta_W N_c}\frac{1}{s} W^W(M_W^2/s, M_W^2). \tag{3.55}$$

The corresponding branching ratios $\mathrm{Br}_{V\to l\bar{l}}$ are given in the tables 3.1 and 3.2.

| $Z^0$ | |
|---|---|
| decay mode | branching fraction |
| $l^+l^-$ | $(3.3658 \pm 0.0023) \times 10^{-2}$ |
| $e^+e^-$ | $(3.363 \pm 0.004) \times 10^{-2}$ |
| $\mu^+\mu^-$ | $(3.366 \pm 0.007) \times 10^{-2}$ |
| $\tau^+\tau^-$ | $(3.367 \pm 0.008) \times 10^{-2}$ |

Table 3.1.: Branching ratios for $Z^0$ boson to leptons as given by [52].

| $W^+$ | |
|---|---|
| decay mode | branching fraction |
| $l^+\nu_l$ | $(10.80 \pm 0.09) \times 10^{-2}$ |
| $e^+\nu_e$ | $(10.75 \pm 0.13) \times 10^{-2}$ |
| $\mu^+\nu_\mu$ | $(10.57 \pm 0.15) \times 10^{-2}$ |
| $\tau^+\nu_\tau$ | $(10.25 \pm 0.20) \times 10^{-2}$ |

Table 3.2.: Branching ratios for $W^+$ boson to leptons as given by [52]. The corresponding ratios for $W^-$ modes are given by charge conjugation.

## 3.2. The Higgs boson production

The understanding of the mechanism which explains the non-zero masses of fermions and electroweak gauge bosons requires the knowledge about the existence of the Higgs particle (or particles). The search for the Higgs boson has started many years ago at LEP, followed by searches at Tevatron and at present at the LHC. These experiments have so far provided us with exclusion of Higgs mass up to several hundreds of GeV, except for a narrow window around 120 GeV[4]. The precise knowledge of theory predictions is therefore essential.

[4]The status in December 2011

We are concerned with the production of the Standard Model Higgs particle. Several processes contribute to the production of which the dominant one in the range up to about 1 TeV [109] is the gluon-gluon fusion channel. Above all this is due to the size gluon distribution functions which dominate the proton content in the corresponding kinematic range. This channel is realised via a massive quark loop, see fig. 3.2 (a) as the coupling of Higgs to fermions is proportional to the mass of a fermion.

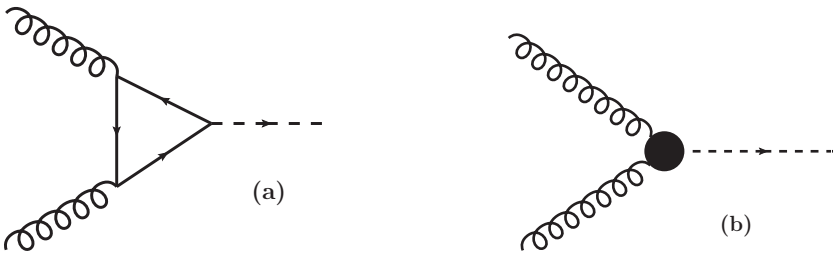


Figure 3.2.: Production of a SM Higgs boson in gluon-gluon fusion. (a): via the top quark loop (b): in the effective approximation

The lowest order contribution is proportional to $\alpha_s^2$ and possesses a strong dependence on the renormalisation scale $\mu_r$. The theoretical result of this contribution is known since the late seventies [110]. The total integrated cross section for the NLO has been calculated in [111, 112].

The calculation can be simplified by considering the limit of a large top quark mass $m_t \to \infty$ which leads to a replacement of a top quark loop by an effective vertex and thus the Higgs boson couples directly to the gluons, see fig. 3.2 (b). It has been shown that the error of this approximation compared to the full result is less then a few per cent for $m_{\mathrm{H}} \leq 2m_t$ [111–113]. The LO and NLO contributions to the total cross section in the large $m_t$ limit were calculated in [114, 115]. The NLO contribution to the total cross section improves the scale dependence however the corrections themselves are large. The NNLO result has been calculated only in the large top mass limit [23, 24, 105, 106, 116–119] The NNLO calculation has been improved by the soft-gluon resummation up to NNLL [120] and an evaluation of the leading soft contributions at the N$^3$LO [121–123].

### 3.2.1. The formalism

In this section we follow closely the notation of [23]. The Higgs boson production via gluon-gluon fusion in the approximation of large top quark mass limit is described by an effective Lagrangian density

$$\mathcal{L}_{\mathrm{eff}}^{\mathrm{H}} = -\frac{1}{4} G_{\mathrm{H}} \phi(x) F_{\mu\nu}^{A}(x) F^{A,\mu\nu}(x), \tag{3.56}$$

where the gluon field strength tensor $F^{A,\mu\nu}(x)$ is defined in eq. (2.4), $\phi(x)$ represents the scalar Higgs field and $G_{\mathrm{H}}$ is the effective coupling constant determined by the top-quark triangular loop graph, including all available QCD corrections, taken in the limit

of infinite top quark mass, $m_t \to \infty$. The effective coupling reads

$$G_{\rm H} = -2^{5/4}\sqrt{G_F}a_s(\mu_r^2)\tau_t F(\tau_t) C\left(\alpha_s, \frac{\mu_r^2}{m_t^2}\right), \tag{3.57}$$

where $G_F$ is the Fermi constant and

$$a_s(\mu_r^2) = \frac{\alpha_s(\mu_r^2)}{4\pi}. \tag{3.58}$$

The function $F(\tau_t)$ is given by

$$F(\tau_t) = 1 + (1-\tau_t) f(\tau_t), \tag{3.59}$$

where

$$f(\tau_t) = \begin{cases} \arcsin^2 \frac{1}{\sqrt{\tau_t}} & \text{if } \tau_t \geq 1 \\ -\frac{1}{4}\left(\ln \frac{1-\sqrt{1-\tau_t}}{1+\sqrt{1-\tau_t}} + i\pi\right)^2 & \text{if } \tau_t < 1 \end{cases} \tag{3.60}$$

and the variable $\tau_t$ is represented by a ratio of top quark mass and Higgs mass $m_{\rm H}$,

$$\tau_t = \frac{4m_t^2}{m_{\rm H}^2}. \tag{3.61}$$

In the limit $m_t \to \infty$ the function $F(\tau_t)$,

$$F(\tau_t) = \frac{2}{3\tau_t}. \tag{3.62}$$

The Wilson coefficient $C(\alpha_s, \mu_r^2/m_t^2)$ [133] for the general numbers of colours $N_c$ and $n_f = 5$ in the $\overline{\rm MS}$ scheme reads

$$\begin{aligned} \mathcal{C}\left(\alpha_s, \frac{\mu_r^2}{m_t^2}\right) = 1 + \frac{\alpha_s(\mu_r^2)}{4\pi}\left[5\,C_A - 3\,C_F\right] + \left(\frac{\alpha_s(\mu_r^2)}{4\pi}\right)^2 \left[\frac{27}{2}\,C_F^2\right. \\ - \frac{100}{3}\,C_A\,C_F + \frac{1063}{36}\,C_A^2 - \frac{4}{3}\,C_F\,T_f - \frac{5}{6}\,C_A\,T_f + \Big(7\,C_A^2 \\ \left. - 11\,C_A\,C_F\Big)\,\ln\frac{\mu_r^2}{m_t^2} + n_f\,T_f\,\left(-5\,C_F - \frac{47}{9}\,C_A + 8\,C_F\,\ln\frac{\mu_r^2}{m_t^2}\right)\right]. \end{aligned} \tag{3.63}$$

The expressions for colour factors are given in eq. (A.34) and $T_f = T_R$. The $x$ space formula for total cross section of the process with two hadrons $h_1 + h_2 \to H + X$ in

initial state is given by

$$\sigma^H(s) = \frac{\pi G_{\rm H}^2}{8(N_c^2-1)} \sum_{a,b\in q,\bar{q},g} \int_x^1 {\rm d}x_1 \int_{x/x_1}^1 {\rm d}x_2\, f_a(x_1,\mu^2) f_b(x_2,\mu^2) \Delta_{ab,{\rm H}}\left(\frac{x}{x_1 x_2}, \frac{m_{\rm H}^2}{\mu^2}, \alpha_s\right), \tag{3.64}$$

where $x$ is expressed in terms of Higgs mass and the centre of mass energy of hadrons $s$,

$$x = \frac{m_{\rm H}^2}{s} \tag{3.65}$$

and variable $\mu$ represents the renormalisation/factorisation scale. The expansion of the $x$ space coefficient functions $\Delta_{ab,{\rm H}}$ up to NNLO

$$\Delta_{ab,{\rm H}}\left(x, \frac{m_{\rm H}^2}{\mu^2}, \alpha_s\right) = \Delta_{ab,{\rm H}}^{(0)}(x) + a_s(\mu_r^2)\Delta_{ab,{\rm H}}^{(1)}\left(x, \frac{m_{\rm H}^2}{\mu^2}\right) + a_s^2(\mu_r^2)\Delta_{ab,{\rm H}}^{(2)}\left(x, \frac{m_{\rm H}^2}{\mu^2}\right) \tag{3.66}$$

and $\Delta_{ab}^{(k)}$ are given in the [23][5]. The $N$ space equivalent of the cross section formula reads

$$\sigma_{h_1h_2\to H}(s) = \frac{\pi G_{\rm H}^2}{8(N^2-1)} \sum_{a,b=q,\bar{q},g} f_a(N+1,\mu^2) f_b(N+1,\mu^2) \Delta_{ab}\left(N, \alpha_s, \frac{m_{\rm H}}{\mu^2}\right) \tag{3.67}$$

We obtained the $N$ space expressions for coefficient functions $\Delta_{ab}(N)$ using the `FORM` [25] package `harmpol` [26], that allowed us to do the Mellin transforms of $x$ space expressions in an automated way. The final result is expressed in terms of harmonic sums. More details on the numerical implementation of coefficient functions are given in the Section 5.2. For the $x$ space input we used the results of V. Ravindran, who provided us with his private file [104]. The $N$ space results for coefficient functions were also presented by J. Blümlein earlier and can be found in [106].

[5] The term $\Delta_{gg,H}^{(2),S+V}$ for the general number of colours is given in later publication, [121]

# 4. The deep inelastic lepton-hadron scattering

The deep inelastic scattering process represents probably the most important and most studied process for physics at hadron colliders. It has been studied since more than forty years. The original description has been given in the framework of the quark-parton model proposed by Feynman [103, 134]. It describes the nucleon at short distances as a collection of non-interacting, point-like particles, partons. This model has explained the scaling behaviour of the structure function $F_2$ observed at the SLAC-MIT experiments [135] predicted earlier by Bjorken [136]. In the context of QCD, the scaling behaviour that implied non existence of interactions between quarks when probed with highly virtual photon has been explained by introducing the idea of asymptotic freedom that manifests itself by vanishing of the effective strong coupling at small distances. Later measurements of the logarithmic scaling violations in the DIS structure function indicated the non-Abelian nature of QCD. Since many years the data on the DIS coming from fixed-target experiments and mainly from H1 an ZEUS experiments at HERA collider have been the largest source of information about the proton structure, the parton distribution functions. DIS experiments are also sensitive to the measurements of electroweak parameters as the coupling constant $\alpha_s$, weak mixing angle $\sin\theta_W$ and masses of vector bosons, see c.f. [137–139] and references therein. In 1990, the Nobel Prize has been awarded jointly to Jerome I. Friedman, Henry W. Kendall and Richard E. Taylor for their pioneering investigations concerning deep inelastic scattering of electrons on protons and bound neutrons, which have been of essential importance for the development of the quark model in particle physics. The perturbative calculations for the unpolarised DIS structure functions is known up to next-to-next-to leading order in perturbative QCD for the neutral and charged current processes and for some cases even to the third order in the strong coupling constant [18, 19, 21, 140, 141].

## 4.1. The formalism

We consider as in the case of hadron-hadron scattering an unpolarised process and massless particles. The fig. 4.1 illustrates the deep inelastic scattering process with initial/final state lepton $l/l'$, initial state hadron $h$ and inclusive hadronic final $X$

$$l(k) + h(P) \to l'(k') + X(P_X), \tag{4.1}$$

where the neutral current (NC) corresponds to $\gamma^*$ or $Z^0$ and the charged current (CC) to the $W^\pm$ intermediate states. The four momentum of the intermediate boson $q^\mu = k^\mu - k'^\mu$

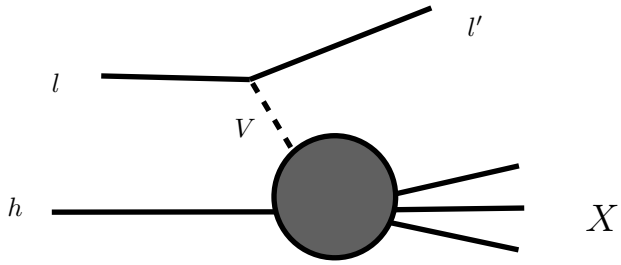


Figure 4.1.: The lepton $l$ scatters of a hadron $h$ via exchange of a boson $V = \gamma, Z^0, W^{\pm}$ producing a final hadronic state $X$ and lepton $l'$.

represents the momentum transfer between leptonic and hadronic part of the process and its square

$$Q^2 = -q^2 \tag{4.2}$$

is much larger than the invariant mass of the nucleon, $Q^2 \gg P^2$. The four momentum of the system $X$ recoiling against the scattered lepton $P_X^\mu = P^\mu + q^\mu$ with

$$P_X^2 = (P+q)^2 \tag{4.3}$$

is required to be much larger than invariant mass of the proton $P_X^2 \gg P^2$ in order for the process to be an inelastic one. The centre of mass energy $s$ is defined as

$$s = (P+k)^2. \tag{4.4}$$

Further on we define two kinematic variables. The first one introduced by Bjorken and often referred to as Bjorken $x$ (or Bjorken scaling variable) and $y$ defined in terms of scalar products of momenta,

$$x = \frac{Q^2}{2P.q} \qquad y = \frac{P.q}{P.k}. \tag{4.5}$$

Both of the kinematical variables lie in the region $x, y \in (0,1)$. Neglecting masses,

$$s = 2P.k, \qquad y = \frac{Q^2}{xs} \qquad \text{and} \qquad P_X^2 = \frac{Q^2(1-x)}{x}. \tag{4.6}$$

The cross section can be written in terms of the DIS structure functions $F_1, F_2$ and $F_3$, which are introduced to parametrise the structure of the hadronic tensor. As in the case of Drell-Yan the cross section can be written in terms of leptonic and hadronic tensors [52, Chapter 16],

$$\frac{\mathrm{d}\sigma}{\mathrm{d}x\mathrm{d}y} = \frac{2\pi y\alpha^2}{Q^4} \sum_i \eta_i L_i^{\mu\nu} W_{\mu\nu}^i \tag{4.7}$$

with $i = \gamma, Z, \gamma Z$ for NC and $i = W$ for CC, $\alpha$ is the electroweak coupling constant and

the overall prefactors read

$$\begin{aligned}\eta_\gamma &= 1\\ \eta_{\gamma Z} &= \Big(\frac{G_F M_Z^2}{2\sqrt{2}\pi\alpha}\Big)\Big(\frac{Q^2}{Q^2+M_Z^2}\Big)\\ \eta_Z &= \eta_{\gamma Z}^2\\ \eta_W &= \frac{1}{2}\Big(\frac{G_F M_W^2}{4\pi\alpha}\frac{Q^2}{Q^2+M_W^2}\Big)^2,\end{aligned} \tag{4.8}$$

where $G_F$ is the Fermi coupling constant and $M_Z$ and $M_W$ masses of vector bosons. The unpolarised hadronic tensor reads

$$W_{\mu\nu} = \Big(-g_{\mu\nu}+\frac{q_\mu q_\nu}{q^2}\Big)F_1(x,Q^2) + \frac{\hat{P}_\mu\hat{P}_\nu}{P.q}F_2(x,Q^2) - i\varepsilon_{\mu\nu\alpha\beta}\frac{\hat{q}^\alpha\hat{P}^\beta}{2P.q}F_3(x,Q^2) \tag{4.9}$$

with

$$\hat{P}_\mu = P_\mu - \frac{P.q}{q^2}q_\mu. \tag{4.10}$$

Combined together with the leptonic tensor $L_{\mu\nu}$ for which the expressions can be found for instance in [52, Chapter 16] leads to the formula for cross section in terms of the structure functions

$$\frac{\mathrm{d}^i\sigma}{\mathrm{d}x\mathrm{d}y} = \frac{2\pi\alpha^2}{xyQ^2}\eta^i[Y_+F_2^i(x,Q^2) - Y_-xF_3^i(x,Q^2) - y^2F_L^i(x,Q^2)], \tag{4.11}$$

where $i = \mathrm{NC,CC}$ corresponds to the neutral current ($e^-N \to e^-X$) or charged current ($e^-N \to \nu X$ or $\nu N \to e^-Z$) processes, respectively and

$$Y_\pm = 1 \pm (1-y)^2. \tag{4.12}$$

The longitudinal structure function is in the limit of $Q^2 \to \infty$ defined as

$$F_L^i(x,Q^2) = F_2^i(x,Q^2) - 2xF_1^i(x,Q^2) \tag{4.13}$$

and obeys in the Callan-Gross relation [142], $F_L^i = 0$. This relation is valid at tree level in perturbative QCD and it is a consequence of quarks carrying half-integer spin, which cannot absorb longitudinally polarised photons. In the Bjorken limit where $Q^2 \to \infty$ and $\nu = 2P.q \to \infty$ for fixed $x$ the structure functions obey the approximate scaling law,

$$F_i(x,Q^2) \to F_i(x). \tag{4.14}$$

## 4.2. Structure functions

The **neutral current** structure functions are given by [143]

$$F_k^{\mathrm{NC}}(x,Q^2) = F_k^{\gamma}(x,Q^2) - \Big(v_{Z,l\bar{l}} \pm \lambda a_{Z,l\bar{l}}\Big)\eta_{\gamma Z} F_k^{\gamma Z}(x,Q^2) + \Big(v_{Z,l\bar{l}}^2 + a_{Z,l\bar{l}}^2 \pm 2\lambda v_{Z,l\bar{l}} a_{Z,l\bar{l}}\Big)\eta_Z F_k^{Z}(x,Q^2); \qquad k = 1,2 \tag{4.15}$$

and

$$xF_3^{\mathrm{NC}}(x,Q^2) = -\Big(a_{Z,l\bar{l}} \pm \lambda v_{Z,l\bar{l}}\Big)\eta_{\gamma Z} xF_3^{\gamma Z}(x,Q^2) + \Big(2v_{Z,l\bar{l}} a_{Z,l\bar{l}} \pm \lambda(v_{Z,l\bar{l}}^2 + a_{Z,l\bar{l}}^2)\Big)\eta_Z xF_3^{Z}(x,Q^2), \tag{4.16}$$

where vector and axial couplings $v_{Z,l\bar{l}}$ and $a_{Z,l\bar{l}}$ are given in tab. 4.1 and helicity $\lambda = \pm 1$. The NC structure functions are given by [144]

| $V$ | $\gamma$ | $W$ | | | | $Z$ | | | |
|---|---|---|---|---|---|---|---|---|---|
| $f_1\bar{f}_2$ | $f\bar{f}$ | $l\bar{\nu}_{l'}$ | $\bar{l}\nu_{l'}$ | $q_u\bar{q}_d$ | $q_d\bar{q}_u$ | $l\bar{l}$ | $\nu\bar{\nu}$ | $q_u\bar{q}_u$ | $q_d\bar{q}_d$ |
| $v_{V,f}$ | $Q_f$ | $\frac{1}{\sqrt{2}}\delta_{ll'}$ | | $\frac{1}{\sqrt{2}}$ | | $a_f - 2Q_f \sin^2\theta_W$ | | | |
| $a_{V,f}$ | 0 | $\frac{1}{\sqrt{2}}\delta_{ll'}$ | | $\frac{1}{\sqrt{2}}$ | | $-\frac{1}{2}$ | $\frac{1}{2}$ | $\frac{1}{2}$ | $-\frac{1}{2}$ |

Table 4.1.: Vector and axial couplings of bosons to quarks and leptons. The fractional charges $Q_f$ are given in tab. 2.2.

$$F_a^V(x,Q^2) = f_a(x)\sum_{i=1}^{n_f}(v_{V,i\bar{i}}^2 + a_{V,i\bar{i}}^2)(C_{a,\mathrm{ns}}^{+} \otimes q_{i,\mathrm{ns}}^{+} + C_{a,\mathrm{q}} \otimes q_{\mathrm{s}} + C_{a,\mathrm{g}} \otimes g) \tag{4.17}$$

with $a = 1,2$, $f_1(x) = \frac{1}{2}$, $f_2(x) = x$ and

$$F_3^Z(x,Q^2) = \sum_{i=1}^{n_f}(2v_{Z,i\bar{i}} a_{Z,i\bar{i}})(C_{3,\mathrm{ns}}^{-} \otimes q_{i,\mathrm{ns}}^{-} + C_{3,\mathrm{ns}}^{\mathrm{v}} \otimes q_{\mathrm{ns}}^{\mathrm{v}}) \tag{4.18}$$

with $V = \gamma, Z^0$ (not to be confused with the upper case subscript which denotes valence) and vector and axial couplings are given in tab. 4.1. The combination of parton distributions,

$$q_{\mathrm{s}} = \sum_{i=1}^{n_f} f_i(x,Q^2) + \bar{f}_i(x,Q^2) \qquad q_{\mathrm{ns}}^{\mathrm{v}} = \sum_{i=1}^{n_f} f_i(x,Q^2) - \bar{f}_i(x,Q^2) \tag{4.19}$$

$$q_{i,\mathrm{ns}}^{+} = f_i(x,Q^2) + \bar{f}_i(x,Q^2) - q_{\mathrm{s}} \qquad q_{i,\mathrm{ns}}^{-} = f_i(x,Q^2) - \bar{f}_i(x,Q^2) - q_{\mathrm{ns}}^{\mathrm{v}}, \tag{4.20}$$

where $n_f$ is the number of active flavours, $g = f_g(x, Q^2)$ and $\bar{f}_i(x, Q^2) \equiv f_{\bar{i}}(x, Q^2)$ . The DIS coefficient functions up to third order read

$$C_{a,j} = C_{a,j}(x, a_s, L_M, L_R) = C^{(0)}_{a,j}(x) + a_s C^{(1)}_{a,j}(x, L_M) + a_s^2 C^{(2)}_{a,j}(x, L_M, L_R) + a_s^3 C^{(3)}_{a,j}(x, L_M, L_R) + \mathcal{O}(a_s^4), \tag{4.21}$$

where $a_s$ is defined in eq. (3.58), $j = \mathrm{ns}^+, \mathrm{ns}^-, \mathrm{ns}^{\mathrm{v}}, \mathrm{q}, \mathrm{g}$ and

$$L_M \equiv \ln(Q^2) - \ln(\mu_f^2), \qquad L_R \equiv \ln(\mu_f^2) - \ln(\mu_r^2). \tag{4.22}$$

The coefficient functions in eq. (4.21) for $\mu_f = \mu_r$ can be written in terms of the scale logarithms $L_M$ in the following way [145],

$$C_{a,j}(x, a_s, L_M, L_R) \overset{\mu_f=\mu_r}{=} C^{(0)}_{a,j}(x) + a_s C^{(1)}_{a,j}(x, L_M) + a_s^2 C^{(2)}_{a,j}(x, L_M, 0) + a_s^3 C^{(3)}_{a,j}(x, L_M, 0) + \mathcal{O}(a_s^4) \tag{4.23}$$

$$\equiv c^{(0)}_{a,j}(x) + \sum_{k=1}^{3} a_s^k [c^{(k)}_{a,j}(x) + \sum_{m=1}^{k} c^{(k,m)}_{a,j}(x) L_M^m] + \mathcal{O}(a_s^4). \tag{4.24}$$

The coefficients $C^{(2)}_{a,j}(x, L_M, L_R)$ and $C^{(3)}_{a,j}(x, L_M, L_R)$ are obtained from $C^{(2)}_{a,j}(x, L_M, 0)$ and $C^{(3)}_{a,j}(x, L_M, 0)$ by substituting for $a_s$ in the eq. (4.23) with the eq. (4.25) and doing the proper order matching

$$a_s(\mu_f^2) = a_s(\mu_r^2) - \beta_0 L_R a_s^2(\mu_r^2) - (\beta_1 L_R - \beta_0^2 L_R^2) a_s^3(\mu_r^2) \tag{4.25}$$

which leads to [145]

$$\begin{aligned} C^{(2)}_{a,j}(x, L_M, L_R) &= c^{(2)}_{a,j}(x) + c^{(2,1)}_{a,j}(x) L_M + c^{(2,2)}_{a,j}(x) L_M^2 - \beta_0 L_R [c^{(1)}_{a,j}(x) + c^{(1,1)}_{a,j}(x) L_M] \\ C^{(3)}_{a,j}(x, L_M, L_R) &= c^{(3)}_{a,j}(x) + c^{(3,3)}_{a,j}(x) L_M^3 + c^{(3,2)}_{a,j}(x) L_M^2 + c^{(3,1)}_{a,j}(x) L_M \\ &\quad - 2\beta_0 L_R [c^{(2)}_{a,j}(x) + c^{(2,1)}_{a,j}(x) L_M + c^{(2,2)}_{a,j}(x) L_M^2] \\ &\quad - (\beta_1 L_R - \beta_0^2 L_R^2) [c^{(1)}_{a,j}(x) + c^{(1,1)}_{a,j}(x) L_M]. \end{aligned} \tag{4.26}$$

The coefficients $c^{(k,p)}_{a,j}$ in eq. (4.24) and (4.26) are proportional to the coefficients with one argument $c^{(m)}_{a,j}, m < k$ and these are summarised in tab. 4.2. The former expressions are derived by differentiating the structure function $F_{a,j}(x, Q^2)$ with respect to $\ln Q^2$ first at $\mu_f^2 = Q^2$ and second at at $\mu_f^2 \neq Q^2$ and set $\mu_f^2 = Q^2$ after the differentiation. Solution of this equation gives us the coefficients $c^{(k,1)}_{a,j}$. For $p > 1$ the equation has to be differentiated $p$ times

$$\frac{\mathrm{d}^p F_{a,j}(x, Q^2)_{Q^2 \neq \mu_f^2}}{\mathrm{d}^p \ln Q^2}\Big|_{Q^2=\mu_f^2} = \frac{\mathrm{d}^p F_{a,j}(x, Q^2)|_{Q^2=\mu_f^2}}{\mathrm{d}^p \ln Q^2}, \tag{4.27}$$

where we dropped the superscript $V$ denoting the vector boson. It is convenient to deal with the singlet and non-singlet contributions to the structure function separately

$$F_{\mathrm{ns},j}(x,Q^2) \overset{Q^2\neq\mu_f^2}{=} C_{\mathrm{ns},j}(x,a_s(\mu_f^2),L_M)) \otimes q_{\mathrm{ns}}(x,\mu_f^2) \tag{4.28}$$

$$F_{\mathrm{s},j}(x,Q^2) \overset{Q^2\neq\mu_f^2}{=} \mathbf{C}_j(x,a_s(\mu_f^2),L_M)) \otimes \mathbf{q}(x,\mu_f^2), \tag{4.29}$$

where $\mathbf{C}_j(x,a_s(\mu_f^2),L_M))$ is a two component vector

$$\mathbf{C}_j(x,a_s(\mu_f^2),L_M)) = \Big(C_{q,j}(x,a_s(\mu_f^2),L_M), C_{g,j}(x,a_s(\mu_f^2),L_M)\Big) \tag{4.30}$$

and

$$\mathbf{q}(x,\mu_f^2) = \begin{pmatrix} q_{\mathrm{s}}(x,\mu_f^2) \\ g(x,\mu_f^2) \end{pmatrix}. \tag{4.31}$$

The differentiation operator on the left-hand side of eq. (4.27) ($\mu_f \neq Q$) will only have effect on the coefficient functions, in particular on the term proportional to $L_M$ in eq. (4.24). For the evaluation of right-hand side of eq. (4.27) ($L_M = 0$) we will need the the renormalisation group equation

$$\frac{\mathrm{d}a_s(Q^2)}{\mathrm{d}Q^2} = -\sum_{k=0}^{1} \beta^k a_s(Q^2)^{k+2}, \tag{4.32}$$

see eqs. (2.13) and (2.15) and the evolution equations for non-singlet and singlet parton distributions, eqs. (2.23) and (2.24). The results for the singlet $\mathbf{c}_a^{(k,p)}$ can be found in [145] and the non-singlet expression are analogous. The **charged current** structure functions

$$F_k^{\mathrm{CC}} = F_k^{W^\pm}, \qquad k = 1,2,3 \tag{4.33}$$

read [144]

$$F_a^{W^\pm}(x,Q^2) = \frac{f_a(x)}{n_f} \sum_{j=1}^{n_f} (v_{W,j\bar{j}}^2 + a_{W,j\bar{j}}^2)(C_{a,\mathrm{ns}}^- \otimes (\pm)\delta q_{\mathrm{ns}}^- + C_{a,\mathrm{q}} \otimes q_{\mathrm{s}} + C_{a,\mathrm{g}} \otimes g) \tag{4.34}$$

with $a = 1,2$, $f_1(x) = \frac{1}{2}$, $f_2(x) = x$ and

$$F_3^{W^\pm}(x,Q^2) = \frac{1}{n_f} \sum_{j=1}^{n_f} (2v_{W,j\bar{j}} a_{W,j\bar{j}})(C_{3,\mathrm{ns}}^+ \otimes (\pm)\delta q_{\mathrm{ns}}^+ + C_{3,\mathrm{ns}}^{\mathrm{v}} \otimes q_{\mathrm{ns}}^{\mathrm{v}}) \tag{4.35}$$

and since both vector and axial couplings are equal to $1/\sqrt{2}$, the sums in eqs. (4.34) and (4.35) can be replaced by a factor $n_f$ respectively. The $\delta q_{\mathrm{ns}}^\pm$ is given in terms of

differences between up-type and down-type quarks,

$$\delta q_{\rm ns}^{\pm} = \sum_{i=u\text{-type}} f_i(x,Q^2) \pm \bar{f}_i(x,Q^2) - \sum_{i=d\text{-type}} f_i(x,Q^2) \pm \bar{f}_i(x,Q^2) \tag{4.36}$$

and the only difference between $W^+$ and $W^-$ is the sign of the terms multiplied by $\delta q_{\rm ns}^{\pm}$.

In the tab. 4.2 we present a summary of available coefficient functions $c^{(n)}(x)$ corresponding to the given structure functions. Note that using the eqs. (4.17), (4.18), (4.34), (4.35) both pure-singlet and the gluon coefficient functions from [18] as well as the splitting functions $P_{qg}^{(0)}$, $P_{qg}^{(1)}$ and $P_{\rm ps}^{(1)}$ of [61] and [62] need to be divided by a factor $(2n_f)$ to account for the contribution of one individual quark flavour. We summarise

| | $i = 2, L$ | | | | |
|---|---|---|---|---|---|
| $\gamma,\ Z^0$ | $c_{i,\rm ns}^{(n),+}(x)$[18] | $c_{i,\rm q}^{(n)}(x)$ [18] | $c_{i,\rm g}^{(n)}(x)$[18] | $c_3^{(n),-}(x)$[19] | $c_3^{(3),\rm s}(x)$ |
| $W^{\pm}$ | $c_i^{(n),-}(x)$[20, 21][1] | $c_{i,\rm q}^{(n)}(x)$[18] | $c_{i,\rm g}^{(n)}(x)$[18] | $c_3^{(n),+}(x)$[22][2] | $c_3^{(3),\rm s}(x)$ |

Table 4.2.: The summary of DIS coefficient functions together with references to their parametrised form up to the available order.

some commonly used notation,

$$c_{i,\rm ns}^{(n),+}(x) \equiv c_{i,\rm ns}^{(n)}(x) \qquad i = 2, L \tag{4.37}$$

$$c_{3,\rm ns}^{(n),k}(x) \equiv c_3^{(n),k}(x), \qquad k = \pm, \mathrm{v}, \mathrm{s} \tag{4.38}$$

$$c_{i,\rm ns}^{(n),k}(x) \equiv c_i^{(n),k}(x) \qquad i = 2, L \qquad k = \pm \tag{4.39}$$

and some useful identities

$$c_{i,\rm q}^{(n)}(x) = c_{i,\rm ns}^{(n)}(x) + c_{i,\rm ps}^{(n)}(x) \tag{4.40}$$

$$c_3^{(n),\rm v}(x) = c_3^{(n),-}(x) + c_3^{(n),\rm s}(x) \qquad c_{3,\rm ns}^{(n),\rm s}(x) = 0 \text{ for } n < 3 \tag{4.41}$$

$$c_3^{(n),+}(x) = c_3^{(n),-}(x) + \delta c_3^{(n)}(x) \tag{4.42}$$

$$c_i^{(n),-}(x) = c_i^{(n),+}(x) + \delta c_i^{(n)}(x) \qquad i = 2, L, \tag{4.43}$$

where the contribution from valence coefficient functions appears first at the order $\alpha_s^3$

$$c_3^{(0),\rm s}(x) = c_3^{(1),\rm s}(x) = c_3^{(2),\rm s}(x) = 0 \tag{4.44}$$

[1] Exact expressions up to $n = 2$, for $i = 2$ later confirmed in[146]. Approximated results for $n = 3$ given in [21].

[2] Exact expressions up to $n = 2$, later confirmed in[146]. Approximated results for $n = 3$ given in [21].

and the contribution for CC even-odd differences starts at second order,

$$\delta C_k^{(n)}(x) = \sum_{n=2} a_s^n \delta c_k^{(n)}(x) \qquad k = 2, L, 3. \tag{4.45}$$

In our implementation we provide the expressions for neutral current structure functions for neutral and charged current up to NNLO, which corresponds to $\mathcal{O}(\alpha_s^2)$ for $F_2$ and $F_3$ and $\mathcal{O}(\alpha_s^3)$ for $F_L$. We used the parametrised expressions $\mathcal{O}(\alpha_s^3)$ given in [18] for the virtual photon exchange. The case of $Z^0$ uses the parametrised version of coefficient functions for $F_3$ given in [19]. In the case of the charged current $\mathcal{O}(\alpha_s^2)$ using the results given in [21], which includes the approximate expressions for $F_L$ using half of the sum of coefficients $\delta c_{L,A}^{(3)}$ and $\delta c_{L,B}^{(3)}$ given eq. (3.8) of [21]. We obtained the $N$ space expressions for coefficient functions $c_k^{(n)}(N)$ using the `FORM` [25] package `harmpol` [26]. The final result is expressed in terms of harmonic sums. More details on the numerical implementation of coefficient functions are given in the Section 5.2.

# 5. The program sbp

The chapter summarises main features of the c++ program sbp and the numerical implementation of the Mellin $N$-space coefficient functions and parton distributions. We discuss the details of the numerical inversion.

## 5.1. The program description

The program sbp evaluates cross sections up to NNLO in perturbative QCD using Mellin space approach for the following Standard Model processes: production of a single electroweak vector boson in the narrow width approximation, the Higgs boson production using the limit of infinite top quark mass and deep inelastic scattering structure functions. The program is written in c++. An external FORTRAN code QCD-PEGASUS [27] can be linked to provide realistic parameterisation of PDFs.

Our approach offers an alternative to the growing number of momentum space programs, where lot of progress has been made in past years. In the case of Drell-Yan process it is DYNNLO [28, 29] and FEWZ 2.1 [30], both fully exclusive with leptonic decays including all spin correlations. The inclusive Higgs cross section including electroweak and mixed electroweak-QCD corrections and several other features has been implemented in the recently published program iHixs [31]. The fully exclusive evaluation of the the Higgs production via gluon-gluon fusion including the Higgs decay into two photons is provided by FEHiP [32].

The $N$ space equivalent for calculation the Wilson coefficients for the unpolarised and polarised Drell-Yan Process and Higgs boson production at NNLO exists in the form of private code DYHIG 1.00 [106, 147] and can be downloaded from the homepage of the author [147].

### 5.1.1. Installation

The latest version of the code can be downloaded at http://www-zeuthen.desy.de/~kpetra/sbp/. The sequence of commands:

1. tar -xzf sbp<version>.tar.gz
2. cd sbp<version>
3. make

produces executables main.exe and example.exe. Running example.exe generates three benchmark tables for cross sections at NNLO with toy parton distribution functions (no evolution and fixed value of $\alpha_s$). The benchmark numbers can be found in the file

example.log which is also printed in the section A.4.1. The file main.exe contains routines for generation of data for plots in the chapter 6.

### 5.1.2. Linking the code to QCD-PEGASUS

The FORTRAN program QCD-PEGASUS by A. Vogt [27] provides realistic PDFs with running strong coupling and it can be interfaced with sbp by following these steps:

1. Download the code at http://www.liv.ac.uk/~avogt/pegasus.html
2. Place pegasus.tar.gz into the main (sbp) directory
3. tar -xzvf pegasus.tar.gz[1]
4. In the sbp makefile uncomment the two lines:
   CFL=-Dpeg
   QCD-PEGASUS_OBJECTS=
5. make clean
6. make

When linking QCD-PEGASUS we strongly recommend the user to familiarise with the basic input parameters that concern the evolution described in sections (4.1)–(4.3) of the Pegasus manual [27].
**Important note:** Every time the linking of QCD-PEGASUS is allowed/forbidden the code has to be cleaned and recompiled.

### 5.1.3. User interface

The basic usage of the code is demonstrated in the file example.cpp, which is included and commented in the Appendix. We focus on the two key features of the program, which are represented by classes Parameter and Constant.

#### Class Constant (file constant.h)

Members of this class are of the type static const and can not be changed anywhere in the program. The only way to change these is by hand directly in the file constant.cpp. There are several groups of constants:

- Generic mathematical constants (Zeta functions, Bernoulli numbers, $\pi$)
- Electroweak parameters
- Abscissas and weights for Gaussian quadratures
- Colour and flavour factors

[1] Particular routines in the folder Pegasus/Routines have to be updated, according to the instructions provided by the QCD-PEGASUS web page.

- Unit conversion factors
- Toy PDF benchmark parameterisation constants

The values of electroweak parameters and the unit conversion constant are taken from PDG 2010 [52], except for the electroweak coupling constant $\alpha$ which is set to the value of $\alpha$ at $M_Z$ and the values of the CKM matrix elements are set according to the `ZWPROD` [16]

$$V_{\mathrm{ud}} = V_{\mathrm{cs}} = \cos\theta_C, \qquad V_{\mathrm{us}} = -V_{\mathrm{cd}} = \sin\theta_C, \tag{5.1}$$

where $\theta_C$ is chosen such that $\sin^2\theta_C + \cos^2\theta_C = 1$. The values for the toy PDF parameterisation are set according to 2001/2 benchmark tables [148].

#### Class `Parameter`

Members of the class `Parameter` are of type `static`. They need to be declared before the `main()` routine. Their values can be changed anywhere in the program using the initialisation routines of type `init_<process>` and `npartoninit` that are designed for this purpose. Any of the parameters can be in principle changed by inserting the line
`Parameter::member=value`
There are three basic groups of parameters.

- Parameters entering coefficient functions and structure functions

  These should be changed only by using the corresponding routine of the type `init_dy`, `init_higgs`, `init_dis`, see the section 5.1.3 for details. Here is the a list of all parameters initialised by these type of routines:

  - `static double nf`
    Number of active flavours that enters coefficient functions and PDFs either as a multiplicative factor or via QCD beta function.
  - `static double muf`
    Factorisation scale in GeV.
  - `static double mur`
    Renormalisation scale in GeV.
  - `static double Q`
    In the case of vector boson or Higgs boson production $Q$ is set to the value of the boson mass. The case of DIS corresponds to the momentum transfer of the process defined in eq. (4.2).
  - `static double mh`
    Mass of the Higgs boson.
  - `static double alphas`
    Strong coupling constant $\alpha_s$.
  - `static int order`
    Perturbative order of the coefficient functions. Except for DIS structure function $F_L$ corresponds to the order in strong coupling constant.

  - `static int boson`
    $0 = \gamma$, $1 = Z^0$, $2 = W^+$, $3 = W^-$, $4 = H$
  - `static int collider`
    Value 1 corresponds to proton-proton, -1 to proton-anti proton collider.

- Mellin inversion parameters

  Since the speed and accuracy of the inversion can be tuned by modifying the number of points for Gaussian integration and shape of the contour we leave these as parameters. These together with the pointer to the function used for PDFs can be changed directly modifying the lines above the `main()` routine.

  - `static double contour`
    The rightmost point of the contour on real axis $c$. Hint: $c > 1.5$.
  - `static double phi`
    The angle between integration contour and positive real axis $\varphi$. Hint: $\pi/2 < \varphi < \pi$.
  - `static double z[19]`
    The array of integration intervals. For the integration each interval is divided into 32 points. If there is a need to modify the size of the array `z` it also has to be done inside `parameter.h` accordingly.
  - `static int s1, ...s4`
    The number of elements of `z` that will be used for corresponding values of $x$, summarised in the tab. 5.1
  - `static FPTR pt2pdf`
    Pointer to the parton distribution functions. Options: `toypdf, pegasuspdf`. The second option can be used only if `QCD-PEGASUS` is linked, see section 5.1.2.

- The `QCD-PEGASUS` parameters

  Four input parameters for the `QCD-PEGASUS` routine `NPARTON`. We refer to the `QCD-PEGASUS` manual [27, Chapter 4] for a detailed description. These parameters are initialised automatically in one of the `init_<process>` routines via a call of `npartoninit` when the flag `peg` is on and some of them (`evolpar` and `inppar`)can be changed by a call of `npartoninit`, see section 5.1.3.

  - `static int ipstd`
    Notation for output arrays p.19 of [27].
  - `static int ipol`
    Polarisation. 1 = polarised, 0 = unpolarised evolution.
  - `static int evolpar`
    `evolpar=1` uses `usrinit.dat` that is produced during the run of the program and placed in the main directory, `evolpar=0` uses default input. Default input sets the variables `FR2 = 1.0` and `NPORD=1`.

– `static int inppar`
`inppar=1` uses `initinp.dat`, `inppar=0` uses default input. For `inppar=1` the file `Pegasus/usrinp.dat` must be placed in working directory.

The consistency between the internal parameters of `QCD-PEGASUS` and those of `sbp` is controlled by two parameters. The first is the ratio of factorisation and renormalisation scales `FR2` and second one the perturbative order of evolution, `NPORD` (see [27]). An automatic consistency of these two is provided using `evolpar=1` which corresponds to the call of `npartoninit(1,0,0,0,1)`.

#### The functions `sigma, f2, fL, f3`

are the top level functions. `double sigma(double s)` returns the value of the full cross section for a given process with a CM energy `s` in nb and `f2(double x)`, `fL(double x)`, `f3(double x)` the DIS structure functions for the given values if $x$ and $Q^2$.

#### The initialisation routines

There are two overloaded versions of each of the initialisation function that sets values of all members of the class `Parameter` except for those which concern the contour. The difference between the two versions is that one sets $\mu_f^2 = \mu_r^2 = Q^2$ whereas the other sets these scales not equal. In the case flag `peg` is on `npartoninit(1,0,0,0,1)` is called. The initialisation routines are defined in the file `cross.cpp`.

- `void init_dy(double nf, double muf, double mur, double alphas, int order, int boson, int collider)`
sets
`Parameter::mh = 120.0` (not used)
`Parameter::Q = Constant::M_<boson>`

- `void init_dy(double nf, double alphas, int order, int boson, int collider)`
sets $\mu_f = \mu_r = M_{<boson>}$,
`Parameter::muf = Parameter::mur = Parameter::Q` ,
`Parameter::Q = Constant::M_<boson>`,
`Parameter::mh = 120.0` (not used)

- `void init_higgs(double nf, double mh, double muf, double mur, double alphas, int order, int collider)`
sets `Parameter::boson = 4` ,
`Parameter::Q = mh`

- `void init_higgs(double nf, double mh, double alphas, int order, int collider)`
sets $\mu_f = \mu_r = M_H$,
`Parameter::muf = Parameter::mur = Parameter::Q` ,

Parameter::boson = 4 ,
Parameter::Q = mh

- void init_dis(double nf, double Q, double muf, double mur, double alphas, int order, int boson)
  sets
  Parameter::collider = 1 (not used)
  Parameter::mh = 120.0 (not used)

- void init_dis(double nf, double Q, double alphas, int order, int boson)
  sets $\mu_f = \mu_r = M_H$,
  Parameter::muf = Parameter::mur = Parameter::Q
  Parameter::collider = 1 (not used)
  Parameter::mh = 120.0 (not used)

#### The function npartoninit

npartoninit(int evolpar, int inppar, int ifast, int ivfns, int imodev) initialises four of the input parameters for QCD-PEGASUS routine NPARTON:
Parameter::evolpar = evolpar,
Parameter::inppar = inppar,
Parameter::ipstd = 1,
Parameter::ipol = 0,
and in the case evolpar=1 calls routine writeusrinit(int ifast, int ivfns, int imodev) which writes a file usrinit.dat. npartoninit also sets the value of strong coupling constant $\alpha_s$ in sbp equal to the one provided by QCD-PEGASUS,
Parameter::alphas=pegasus_alphas(Parameter::mur)
(the argument alphas in init will be overwritten).
It is defined in the file pdf.cpp and is called by default by both overloaded versions of init_<*process*> if QCD-PEGASUS is linked.

## 5.2. Numerical implementation

The momentum space coefficient functions are represented by powers of $x$, plus distributions and harmonic polylogarithms [26]. Mellin transforms of harmonic polylogarithms are harmonic sums [149, 150]. The field of Mellin transforms and their analytic continuations to the complex plane has been extensively studied over the past twenty years and the results for nearly all of functions appearing in the hard scattering coefficients are known analytically [18, 19, 21, 106, 150, 151].

We use the FORM [25] package harmpol [26] to perform the Mellin transforms of $x$ space coefficient functions. The final result is expressed in terms of harmonic sums up to the depth four (depth six in case third order DIS approximation) to which we apply additional identities in order to reduce them to sums of lower depth. We use the Taylor

expansions for those sums which do not have direct Mellin transforms. We verify the correctness of the Mellin transforms by evaluation of the $N$-space results for a fixed value of moment against numerical integration of the $x$-space expression with `Maple`, (except for the plus distributions) and in some cases we work also the other way around using the package of Gehrmann and Remiddi for the numerical evaluation of harmonic polylogarithms [152].

We use model parton distribution functions with their Mellin space representations in terms of Euler Beta functions. For realistic PDF input we use the $N$ space output of `QCD-PEGASUS` [27]. The inversions are done numerically using the method of Gaussian quadratures.

### 5.2.1. The harmonic polylogarithms

The harmonic polylogarithms (hpl's) introduced by Remiddi and Vermaseren [26] are generalisation of Nielsen's polylogarithms. The coefficients of their expansions and their Mellin transforms are harmonic sums. The Nielsen generalised polylogarithm is defined as [153]

$$\mathcal{S}_{n,p}(x) = \frac{(-1)^{n+p-1}}{(n-1)!p!} \int_0^1 \frac{\ln^{n-1}(t)\ln^p(1-xt)}{t} \mathrm{d}t \tag{5.2}$$

and reduces to a polylogarithm for the case

$$\mathcal{S}_{n-1,1}(x) = \mathrm{Li}_n(x). \tag{5.3}$$

The harmonic polylogarithms of weight $w$ and argument $x$ are identified by a set of $w$ indices grouped into a $w$-dimensional vector $\vec{m}_w$ and are indicated by $\mathrm{H}(\vec{m}_w; x)$. For $w = 1$ is defined

$$\mathrm{H}(0; x) = \ln(x), \tag{5.4}$$

$$\mathrm{H}(1; x) = \int_0^x \frac{\mathrm{d}x'}{1-x'} = -\ln(1-x), \tag{5.5}$$

$$\mathrm{H}(-1; x) = \int_0^x \frac{\mathrm{d}x'}{1+x'} = \ln(1+x). \tag{5.6}$$

The derivative

$$\frac{\mathrm{d}}{\mathrm{d}x}\mathrm{H}(a; x) = f(a; x) \qquad a = 0, \pm 1, \tag{5.7}$$

where

$$f(0; x) = \frac{1}{x} \tag{5.8}$$

$$f(1; x) = \frac{1}{1-x} \tag{5.9}$$

$$f(-1; x) = \frac{1}{1+x} \tag{5.10}$$

We can quite generally write

$$\vec{m}_w = (a, \vec{m}_{w-1}), \qquad a = m_w \text{ is the leftmost component of } \vec{m}_w. \tag{5.11}$$

If we define $\vec{0}_w$ as a vector whose $w$ components are all equal to index 0, the harmonic polylogarithms of weight $w$ are defined as follows

$$\mathrm{H}(\vec{0}_w; x) = \frac{1}{w!} \ln^w x \tag{5.12}$$

and for $\vec{m}_w \neq \vec{0}_w$

$$\mathrm{H}(\vec{m}_w; x) = \int_0^x \mathrm{d}x' f(a; x') \mathrm{H}(\vec{m}_{w-1}; x'). \tag{5.13}$$

In analogy with eq. (5.12) we can write

$$\mathrm{H}(\vec{1}_w; x) = \frac{1}{w!}(-\ln(1-x))^w \tag{5.14}$$

$$\mathrm{H}(\vec{-1}_w; x) = \frac{1}{w!} \ln^w(1+x). \tag{5.15}$$

The derivatives can be written in a compact form

$$\frac{\mathrm{d}}{\mathrm{d}x}\mathrm{H}(\vec{m}_w; x) = f(a; x)\mathrm{H}(\vec{m}_{w-1}; x), \tag{5.16}$$

where again $a$ is the leftmost component of $\vec{m}_w$. The relationship between hpl's and the Nielsen polylogarithm in this notation reads

$$\mathcal{S}_{n,p}(x) = \mathrm{H}(\vec{0}_n, \vec{1}_p; x). \tag{5.17}$$

### 5.2.2. Harmonic sums

Harmonic sums of depth one are defined [149] for an integer values of $n$

$$S_m(n) = \sum_{i=1}^{n} \frac{1}{i^m} \tag{5.18}$$

and

$$S_{-m}(n) = \sum_{i=1}^{n} \frac{(-1)^i}{i^m} \tag{5.19}$$

for $m > 0$. The depth of a harmonic sum is equivalent to the number of its indices. The analytic continuation of simple harmonic sums to the complex plane is expressed in terms of digamma and polygamma functions (eqs. (A.8) and (A.9)) and a beta function [106], see eq. (5.23) (not to be confused with Euler Beta function).

$$S_k(n) = \frac{(-1)^{k+1}}{(k-1)!}\psi^{(k-1)}(n+1) + \zeta(k) \tag{5.20}$$

$$S_{-1}(n) = (-1)^n \beta(n+1) - \ln(2) \tag{5.21}$$

$$S_{-k}(n) = \frac{(-1)^{n+k-1}}{(k-1)!}\beta^{(k-1)}(n+1) - \Big(1 - \frac{1}{2^{k-1}}\Big)\zeta(k); \qquad k \geq 2, \tag{5.22}$$

where the $\beta(n)$ [106] is defined as

$$\beta(n) = \frac{1}{2}\Big[\psi\Big(\frac{1+n}{2}\Big) - \psi\Big(\frac{n}{2}\Big)\Big]. \tag{5.23}$$

Harmonic series of depth $p+1$ are defined as [149]

$$S_{m,j_1,\ldots,j_p}(n) = \sum_{i=1}^{n} \frac{1}{i^m} S_{m,j_1,\ldots,j_p}(i) \tag{5.24}$$

and

$$S_{-m,j_1,\ldots,j_p}(n) = \sum_{i=1}^{n} \frac{(-1)^i}{i^m} S_{m,j_1,\ldots,j_p}(i) \tag{5.25}$$

again for $m > 0$. The $m$ and $j_i$ are referred to as the indices of the harmonic series. The weight of a harmonic series is defined as the sum of the absolute values of its indices [149]

$$W(S_{j_1,\ldots,j_m}(n)) = \sum_{i=1}^{m} |j_i|. \tag{5.26}$$

There are three kinds of identities we used to further simplify the result of `harmpol`.

- The relationship that exchanges the order of summation for sums with two indices [149], eq. (9)

  $$S_{j,k}(n) + S_{k,j}(n) = S_j(n)S_k(n) + S_{j\&k}(n), \tag{5.27}$$

  where the operator &

  $$j\&k = \begin{cases} |j| + |k| & \text{if } \operatorname{sgn}(j) = \operatorname{sgn}(k) \\ -(|j| + |k|) & \text{if } \operatorname{sgn}(j) \neq \operatorname{sgn}(k). \end{cases}$$

  The relations between sums with three indices are given in eqs. (177-180) of [150]

- The depth of sums with repeated indices can be reduced according to eqs. (92-94) of [149]

  $$2S_{1,1}(n) = [S_1(n)]^2 + S_2(n) \tag{5.28}$$

  $$6S_{1,1,1}(n) = [S_1(n)]^3 + 3S_1(n)S_2(n) + 2S_3(n) \tag{5.29}$$

  $$\begin{aligned} 24S_{1,1,1,1}(n) = {} & [S_1(n)]^4 + 6[S_1(n)]^2(n)S_2(n) \\ & + 8S_1(n)S_3(n) + 3[S_2(n)]^2 + 6S_4(n) \\ & \vdots \end{aligned} \tag{5.30}$$

More general and compact form of the expression above can be found in eq.(158) of [150]

- Synchronisation in order to make the arguments of sums identical

$$S_k(n+p) = S_k(n) + \sum_{j=1}^{p} \frac{1}{(n+j)^k}. \tag{5.31}$$

### 5.2.3. Special harmonic sums

The Drell-Yan coefficient functions contain in total harmonic sums that need special treatment, in the sense that they cannot be analytically Mellin transformed. It concerns the four double sums, $S_{-2,1}(n), S_{-2,2}(n), S_{-3,1}(n), S_{2,1}(n)$ and two triple sums, $S_{2,1,1}(n), S_{-2,1,1}(n)$ . The expressions for these sums can be found in [106], eqs. (55) and (56). The objects

$$g_3 = \frac{\mathrm{Li}_2(x)}{1+x} \quad \Leftrightarrow \quad S_{-2,1}(n) \tag{5.32}$$

$$g_5 = \frac{\ln(x)\mathrm{Li}_2(x)}{1+x} \quad \Leftrightarrow \quad S_{-2,2}(n) \tag{5.33}$$

$$g_6 = \frac{\mathrm{Li}_3(x)}{1+x} \quad \Leftrightarrow \quad S_{-2,2}(n), S_{-3,1}(n) \tag{5.34}$$

$$g_8 = \frac{S_{1,2}(x)}{1+x} \quad \Leftrightarrow \quad S_{-2,1,1}(n) \tag{5.35}$$

$$g_{18} = \frac{\mathrm{Li}_2(x) - \zeta(2)}{x-1} \quad \Leftrightarrow \quad S_{2,1}(n) \tag{5.36}$$

$$g_{21} = \frac{S_{1,2}(x) - \zeta(3)}{x-1} \quad \Leftrightarrow \quad S_{2,1,1}(n) \tag{5.37}$$

$$g_{22} = \frac{\ln(x)\mathrm{Li}_2(x)}{x-1} \quad \Leftrightarrow \quad S_{3,1}(n) \tag{5.38}$$

are labelled according to the publication of J. Blümlein [154] where a solution to this problem has been implemented in a program `ANCONT` [154] for a larger set of objects. We adopted a similar approach.

We use `Maple` to Taylor expand the functions $g_i$ around the points 0 or/and 1, depending on their behaviour around these end points. We then subtract these expansions from the original function which results in a function that is smooth enough to be used for rational approximation. The approximation is done with the `MINIMAX` method of `Maple`. The precision of the approximation is better than $2 \times 10^{-9}$ for all of $g_i$ on the whole range of $x$. The accuracy of our approximation is shown in the figure 5.1. We then use `harmpol` [26] package to do the Mellin transforms and check the correctness via numerical evaluation of $x$ space functions for a fixed value of $N$.

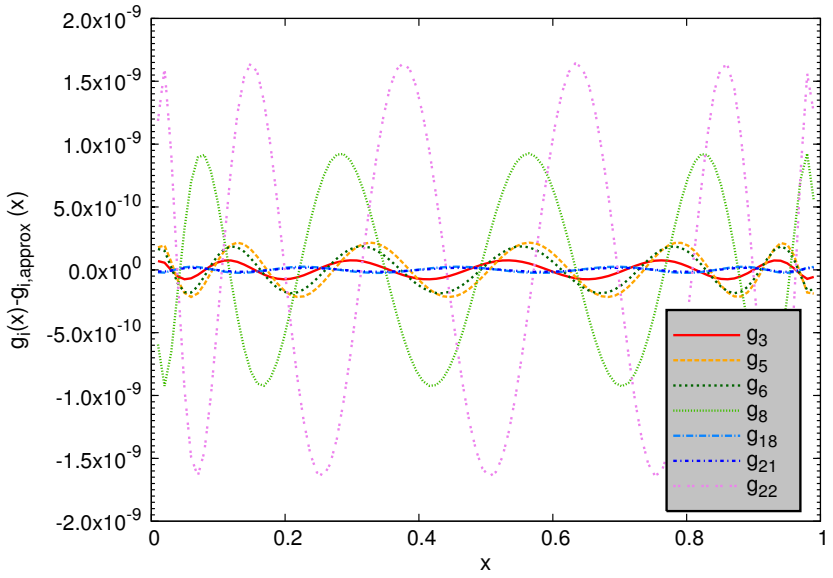


Figure 5.1.: The accuracy of the numerical approximation of the functions $g_i(x)$ defined in eq. (5.38) with a rational function $g_{i,\mathrm{approx}}(x)$ over the range of $x \in (0, 1)$. The $y$ axis denotes the difference $g_i(x) - g_{i,\mathrm{approx}}(x)$.

### 5.2.4. Stirling's series

The numerical evaluation of the complex valued Gamma function and related functions requires an asymptotic expansion. Stirling's expansion gives rapid convergence for large values of complex variable $z = a + ib$ and in particular, good enough convergence is obtained for $|z| > 10$ [155, Chapter 10]. Using the factorial representation for Gamma function

$$\Gamma(z) = (z-1)!. \tag{5.39}$$

The Stirling expansion reads

$$\ln(z!) = C_2 + \left(z + \frac{1}{2}\right)\ln(z) - z + \frac{B_2}{2z} + \cdots + \frac{B_{2n}}{2n(2n-1)z^{2n-1}} + \cdots, \tag{5.40}$$

where $B_k$ are Bernoulli numbers and the constant of integration $C_2$

$$C_2 = \frac{1}{2}\ln 2\pi. \tag{5.41}$$

For smaller values of $|z|$ Stirling formula, eq. (5.40) can be applied after shifting the argument to larger values. The shifted argument is then subtracted from the final

expression using the functional equation, eq. (A.6),

$$\Gamma(z) = \frac{\Gamma(z+1)}{z}. \tag{5.42}$$

For the implementation we used 7 terms in the Stirling expansion in eq. (5.40). In the evaluation of digamma and polygamma functions we expand the logarithm of the Gamma function before the differentiation.

### 5.2.5. The plus distribution

The plus distributions appear in the form

$$\left[\frac{\ln^k(1-x)}{(1-x)}\right]_+, \qquad k = 0, \ldots 3 \tag{5.43}$$

transform into $N$ space conveniently according to the definition eq. (A.14),

$$\Big[\frac{\ln^k(1-x)}{(1-x)}\Big]_+ \quad \longleftrightarrow \quad \int_0^1 \Big[\mathrm{d}x \frac{\ln^k(1-x)}{(1-x)}(x^{N-1}-1)\Big]. \tag{5.44}$$

### 5.2.6. The PDFs

As the default option we chose the following form of model parton distribution functions

$$xf(x) = nx^a(1-x)^b \qquad n, a, b \in \mathrm{Re}, \qquad a \in (-1, 1), b > 1, \tag{5.45}$$

where the parameter $a$ is associated with small $x$ and $b$ with large $x$. Such shape describes sufficiently the generic PDF behaviour. The Mellin transform of eq. (5.45) can be expressed in terms of Euler Beta function in eq. (A.11),

$$f(N) = n\int_0^1 x^{a+N}(1-x)^b = nB(a+N+1, b+1). \tag{5.46}$$

From the primary definition of the Euler Beta function in terms of the Gamma function defined in eq. (A.10) and taking into account the range of parameters $a$ and $b$ the position of the rightmost pole $N_{\max}$ of the PDFs is determined. It is given by the first pole in

$$\Gamma(a+N+1) \quad \Rightarrow \quad N_{\max} = -1-a, \tag{5.47}$$

which implies that the rightmost pole in PDFs is smaller than 0.

The second option is provided by `QCD-PEGASUS` [27]. This program when linked to `sbp`, see section 5.1.2 provides the PDF input in $N$ space at a given value of $Q^2$ using evolution in Mellin space. The package provides flexibility in the parameterisation of input distributions. The default option offers the choice between two functional forms. Furthermore, recent study has given results for some non-trivial input PDF parameterisation, which has extended the set of PDFs that can be used [156] and implemented into

`QCD-PEGASUS`.

### 5.2.7. Inverse Mellin transform

The inverse Mellin transform is expressed in terms of an integral over a complex plane

$$f(x) = \frac{1}{2\pi i} \int_{c-i\infty}^{c+i\infty} \mathrm{d}N\, x^{-N} f(N), \tag{5.48}$$

where $c$ represents a rightmost point of the integration contour on the positive real axis. This is well suited for numerical evaluation and for which we adopt the approach of [27]. The complex integral over variable $N$ in eq. (5.48) is rewritten in terms of an integral over a real variable $\rho$ and at the same time deform the contour in such a way that maximum accuracy and speed of the numerical integration is achieved. The contour deformation

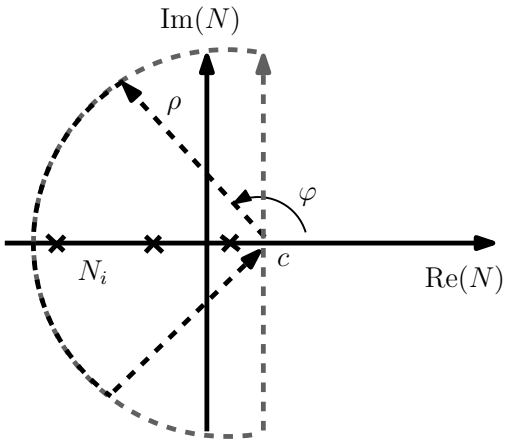


Figure 5.2.: Deformation of the contour. The grey dashed line shows the original shape of the contour and the black one the new deformed contour. This corresponds to the shift $\varphi = \pi/2 \to \varphi > \pi/2$. $c$ represents a point where the contour crosses the positive real axis and a point where the original and modified contour coincide.

is shown on the fig. 5.2. It makes use of the fact that all poles in the function $f(N)$ lie to the left from the point $c$ and are on the negative real axis. The whole procedure goes as follows. The variable $N$ can be written as

$$N = c + \rho e^{i\varphi} \qquad \text{with} \qquad \rho \in (-\infty, +\infty) \quad \text{and} \quad \varphi = \pi/2 \tag{5.49}$$

and contour deformation essentially corresponds to a shift in an angle $\varphi$ between the contour and positive real axis from $\pi/2$ to a value that lies between $\pi/2$ and $\pi$ (see fig. 5.2). Using $\mathrm{d}N = c + e^{i\varphi}\mathrm{d}\rho$ we rewrite the integral over $N \in (c + i\infty, c - i\infty)$ in

eq. (5.48) in terms of integral over $\rho$. This leads to

$$f(x) = \frac{1}{2\pi i}\int_{c-i\infty}^{c+i\infty} \mathrm{d}N\, x^{-N} f(N) = \frac{1}{2\pi i}\int_{-\infty}^{\infty} \mathrm{d}\rho\, x^{-N} f(N) e^{i\varphi} \tag{5.50}$$

$$= \frac{1}{\pi}\int_{0}^{\infty} \mathrm{d}\rho\, \mathrm{Im}[e^{i\varphi} x^{-N} f(N)], \tag{5.51}$$

where in the last step we split the integral into two and used relations

$$f(N^*) = f^*(N) \qquad \text{and} \qquad f^*(N) - f(N) = 2i\mathrm{Im}[f(N)]. \tag{5.52}$$

The numerical integration is done using 32-point Gaussian quadratures and the maximal value of the integration variable $\rho$ is set set in the dependence on the value of $x$. In our program we adopted the values in tab. 5.1. The main contribution to the integrand in eq. (5.51) comes from the region close to the rightmost singularity $N_{\max}$. This has consequences for the speed and the accuracy of the numerical evaluation. The shape of the contour around $N_{\max}$ must not be too close to this point, which implies that $c > N_{\max}$ and $\varphi < \pi$. Setting these very far from the $N_{\max}$ on the other hand, does not have too much of an effect on the accuracy. For the Drell-Yan process where $N_{\max} = 1$ a reasonable choice of the contour turns out to be $c = 1.5$ and $\varphi = 3\pi/4$. The evaluation of the full cross section at NNLO depends on the type of the process and on the value of $x$ at which the Mellin inversion is performed. The smaller the value of $x$ the less evaluations are required to recover the original $x$ space, see Table 5.1. In general, the Higgs cross section takes the longest. One point for a cross section for the Higgs production takes less than one second for the most difficult kinematics with `g++` compiler on the Intel Core i7 2.7GHz machine.

| $x$ | $< 0.01$ | $0.01 - 0.3$ | $0.3 - 0.7$ | $> 0.7$ |
|---|---|---|---|---|
| $\rho_{\max}$ | 5 | 14 | 32 | 80 |
| # of intervals | 8 | 11 | 14 | 19 |

Table 5.1.: Maximal values of the integration variable $\rho$ corresponding to different values of $x$. Last row when multiplied by 32 gives the number of points evaluated during the Gaussian integration.

# 6. Results and discussion

In this section we present comparisons of our program `sbp` with publicly available $x$-space codes. We evaluate $K$-factors and investigate the scale dependence of cross sections and structure functions. We apply our program to a study of two different treatments of renormalisation and factorisation scales. At the end of the section we discuss further applications and extensions of the program.

## 6.1. Checks

We compared the results for Drell-Yan and Higgs cross sections at NNLO with programmes `ZWPROD` [16, 17] and `higgs.f` [23]. These are $x$-space unpublished programmes written by the authors of original NNLO calculations. Comparisons for NNLO DIS structure functions were made with private $N$ space code of S. Moch. In all the cases we used a toy input as in eq. (5.46) that corresponds to the choice made in [148],

$$\begin{aligned} xu_v(x) &= 5.107200x^{0.8}(1-x)^3 \\ xd_v(x) &= 3.064320x^{0.8}(1-x)^4 \\ xg(x) &= 1.700000x^{-0.1}(1-x)^5 \\ x\bar{d}(x) &= 0.1939875x^{-0.1}(1-x)^6 \\ x\bar{u}(x) &= (1-x)x\bar{d}(x) \\ xs(x) &= x\bar{s}(x) = x(1-x) = 0.2x(\bar{u}+\bar{d})(x). \end{aligned} \tag{6.1}$$

We use no evolution and a fixed value of the strong coupling constant $\alpha_s = 0.1$. The values of the electroweak parameters correspond to the ones in PDG 2010 [52] except for the values of CKM matrix elements which were set according to eq. (5.1)

$$\begin{aligned} V_{\rm ud} &= V_{\rm cs} = 0.9736529156 \\ V_{\rm us} &= -V_{\rm cd} = 0.2280350850 \\ V_{\rm ub} &= V_{\rm cb} = V_{\rm td} = V_{\rm ts} = V_{\rm tb} = 0. \end{aligned} \tag{6.2}$$

The Drell-Yan process was first compared at the level of individual channels: $q\bar{q}$ non-singlet, $q(\bar{q})g$, $gq$ singlet and non-identical $qq$, identical $qq$ and $gg$ channel up to NNLO. The fig. (6.1) shows the comparison of the full cross section for $W^-$ production. The relative accuracy is better than $6 \times 10^{-6}$ in the kinematical range $x \in (10^{-4}, 0.8)$. The decreasing accuracy in the region of $x \to 1$ is both due to the behaviour of Mellin inversion and due to the numerical inaccuracy caused by the rapid drop of the cross

section towards large values of $x$. Similar level of accuracy is obtained in the $Z^0$ and $W^+$ case. The fig. (6.2) shows the comparison for Higgs production via gluon-gluon

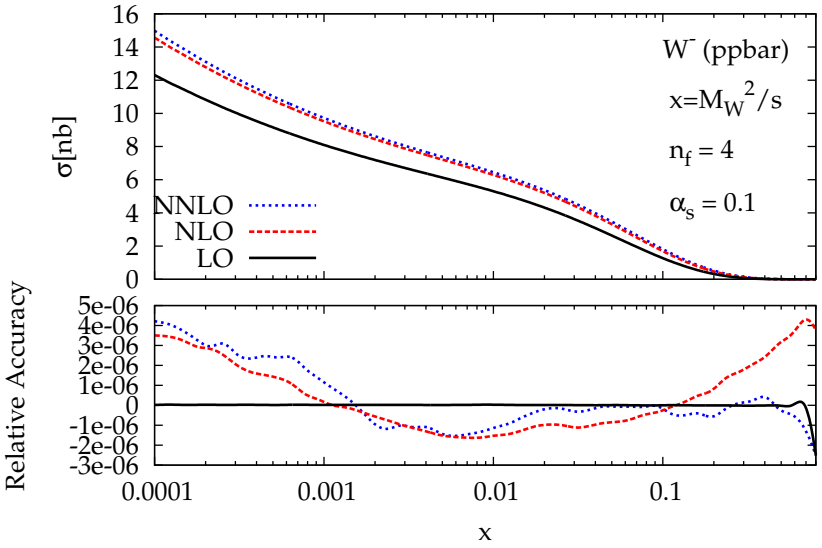


Figure 6.1.: The comparison of $W^-$ production cross section up to NNLO in the narrow width approximation with `ZWPROD` using the model parton distribution functions defined in eq. (6.1) with no evolution and a fixed value of the strong coupling constant $\alpha_s = 0.1$. Upper part: The full cross section. Lower part: Relative accuracy with respect to the `ZWPROD`.

fusion in the relevant kinematical range $x \in (10^{-4}, 0.1)$ and $n_f = 5$[1] and mass of the Higgs boson $m_{\mathrm{H}} = 120\,\mathrm{GeV}$.

We further made a detailed comparisons of the DIS structure functions $F_1$, $F_2$ and $F_3$ at the level of individual singlet and non-singlet contributions in the full domain of Bjorken $x$ and the case of $\mu_f \neq \mu_r \neq Q$. With the private $N$ space program of S. Moch we found an agreement at the level of 10 digits up to the NLO and a per-mil agreement at NNLO. These differences are caused by a different NNLO coefficient function parameterisation.

## 6.2. Applications

We applied our program to study the perturbative convergence and dependence on unphysical scales in the cross sections. We use the parton distribution functions provided

[1] $n_f = 5$ is the only allowed value for number of flavours due to the definition of the overall cross section prefactor in eq. (3.63)

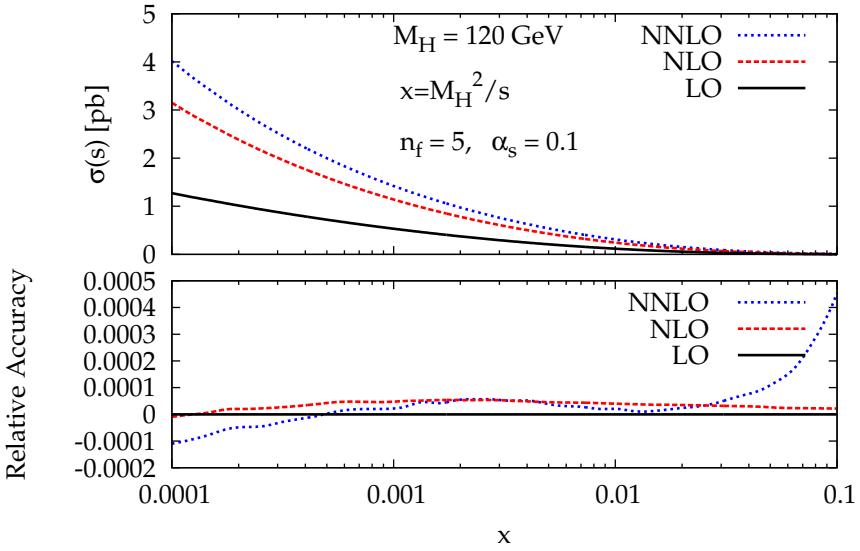


Figure 6.2.: The cross section for the Higgs production in gluon gluon fusion using the model parton distribution functions defined in eq. (6.1) with no evolution and a fixed value of the strong coupling constant $\alpha_s = 0.1$. Upper part: The full cross section. Lower part: The relative accuracy with respect to `higgs.f`.

by `QCD-PEGASUS` [27] with the default input parameterisation that is identical to the model one in eq. (6.1). The order of evolution is done accordingly to the perturbative order of coefficient functions.

The rate of convergence of perturbative series can be conveniently described in terms of $K$-factors. These are defined as follows [2]

$$K^{\mathrm{NLO}} = \frac{\sigma^{\mathrm{NLO}}}{\sigma^{\mathrm{LO}}} \quad \text{and} \quad K^{\mathrm{NNLO}} = \frac{\sigma^{\mathrm{NNLO}}}{\sigma^{\mathrm{NLO}}}. \tag{6.3}$$

The size of $K$ factor depends in general on several aspects. These include opening up of new channels at higher orders, the choice of factorisation and renormalisation scales, renormalisation and mass factorisation schemes and the choice of PDFs [16]. As a general rule, a large $K$ factor usually points to the necessity of a higher order calculation.

Figures 6.3, 6.4, 6.5, 6.6 and 6.7 show the rate of convergence of perturbative series for DY and Higgs cross sections as well as DIS structure functions. All the NLO $K$ factors are rather large and show the expected behaviour $K^{\mathrm{NNLO}} < K^{\mathrm{NLO}}$. Although the kinematics of both Drell-Yan and Higgs production are very similar, these processes

[2] Sometimes the $K$-factors are defined with respect to the Born process

differ quantitatively due to the difference in leading contributions. In the Higgs case the corrections come with a factor of $C_A = 3$, whereas in the case of Drell-Yan this factor is smaller, $C_f = 4/3$. This corresponds to the different behaviour of the $K$ factors with respect to the CM energy $s$.

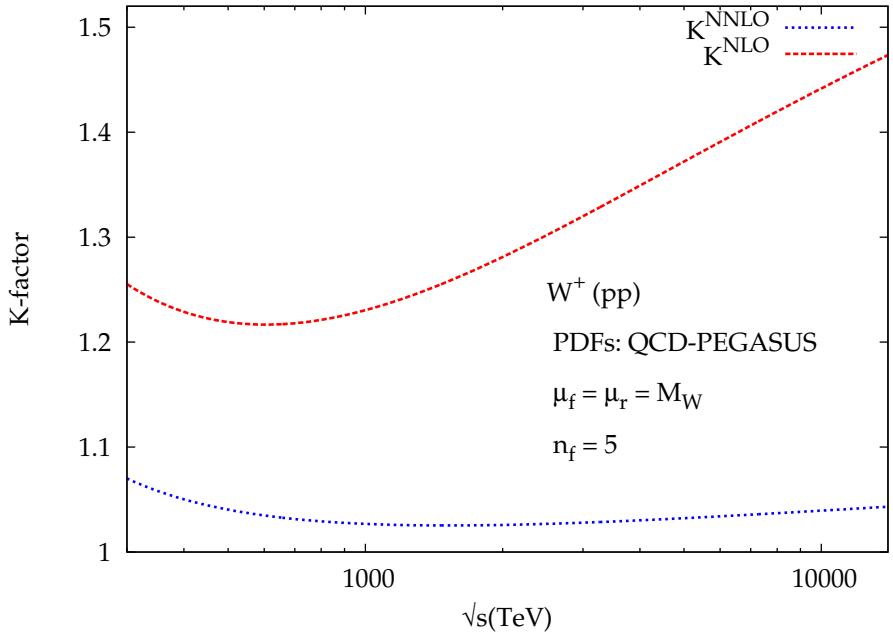


Figure 6.3.: The Drell-Yan $K$-factors at NLO and NNLO for $W^+$ production.

To get a handle on the residual uncertainty coming from uncalculated higher orders one usually varies the unphysical momentum scales (factorisation and renormalisation) around some central value $\mu_0$ that usually coincides with the energy of the underlying scattering process $Q$, typically around $(\mu_0/2, 2\mu_0)$ [14]. Figures (6.8), (6.9) and (6.10) show the variations of cross section with respect to the scale $\mu_f = \mu_r \neq Q$. This is defined according to [23] as a ratio $N$

$$N\left(\frac{\mu_f}{Q}\right) = \frac{\sigma(\mu_f)}{\sigma(Q)}. \tag{6.4}$$

For all of the processes one observes reduced dependence on the choice of factorisation scale $\mu_f$ going form the leading order to the NNLO.

We further investigated the case where all scales entering the hadronic cross section are different, $Q \neq \mu_f \neq \mu_r$. The dependence on these scales enters in the form of logarithms of the ratio of two scales

$$\ln\left(\frac{Q^2}{\mu_f^2}\right) \equiv L_M \qquad \text{and} \qquad \ln\left(\frac{\mu_f^2}{\mu_r^2}\right) \equiv L_R. \tag{6.5}$$

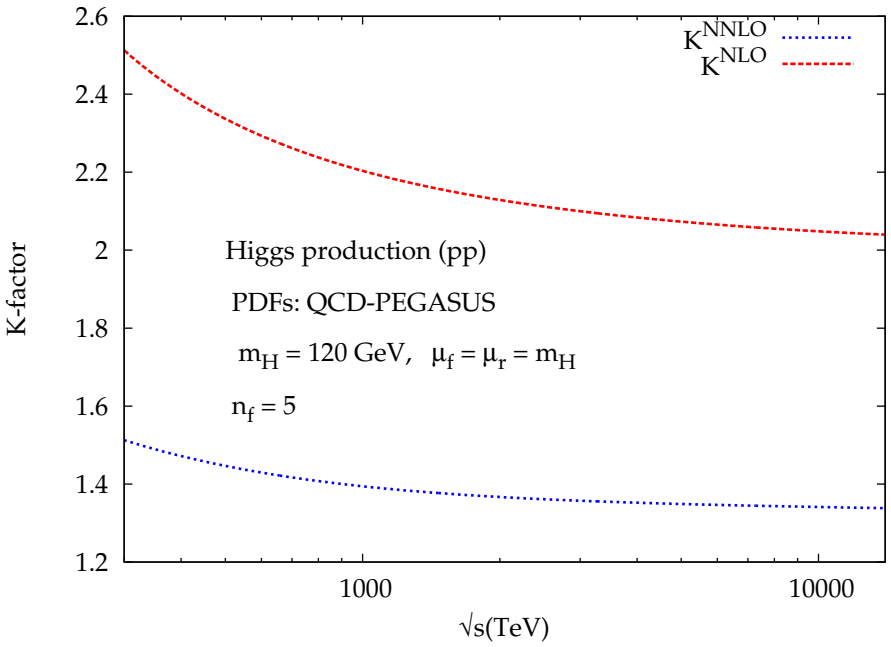


Figure 6.4.: The Higgs $K$-factors at NLO and NNLO.

The cross section with the explicit scale dependence then reads

$$\sigma \sim \Delta_{ab}(x, L_M, L_R) \otimes f_a(x, L_R), f_b(x, L_R). \tag{6.6}$$

In the standard evaluations of cross sections it is however common to use different expression,

$$\tilde{\sigma} \sim \Delta_{ab}(x, L_M, L_R) \otimes f_a(x, 0), f_b(x, 0). \tag{6.7}$$

This in other words means, that one keeps $\mu_f \neq \mu_r$ in the coefficient functions but not in the PDFs. This as a result produces a non-zero value for a quantity $R_\sigma$ defined as follows

$$R_\sigma = \frac{\tilde{\sigma} - \sigma}{\sigma}. \tag{6.8}$$

Figures 6.13, 6.15, 6.16, 6.17 and 6.14 show the results of a particular case where $\mu_r = 2\mu_f$. In general, the stronger is the dependence of a cross section on the unphysical scales the more affected by the different treatments will the cross section be. The largest effect is therefore visible on the leading order cross sections. The value of $R_\sigma$ for the Drell-Yan and DIS is up to 10% at NNLO. In the case of Higgs boson production the difference can reach up to 40%. i

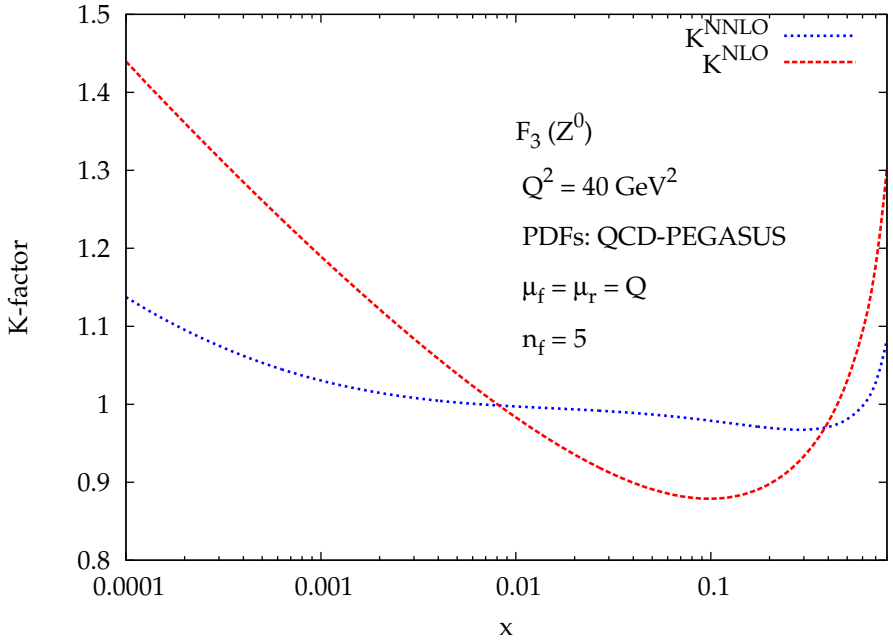


Figure 6.5.: The $K$-factors for DIS structure function $F_3$ at NLO and NNLO.

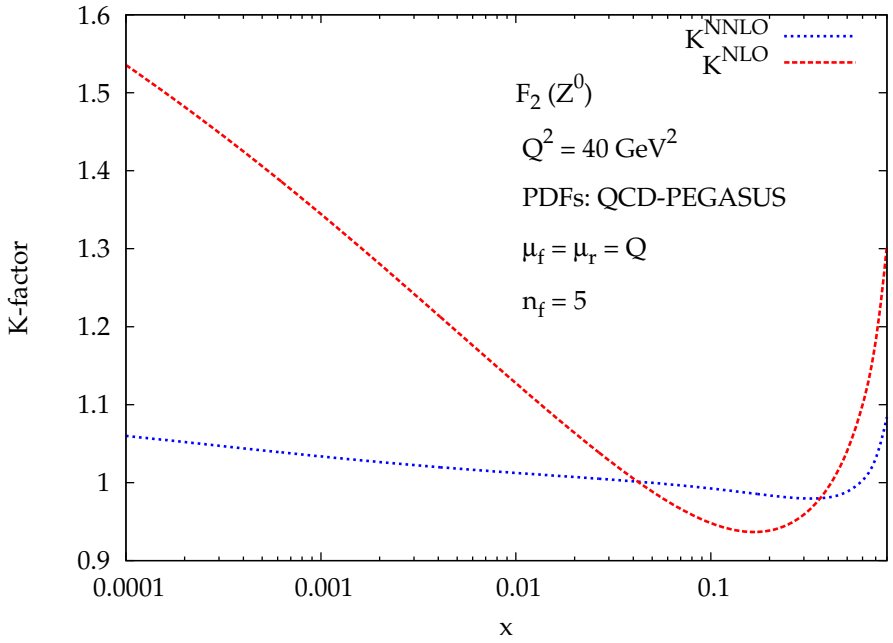


Figure 6.6.: The $K$-factors for DIS structure function $F_2$ at NLO and NNLO.

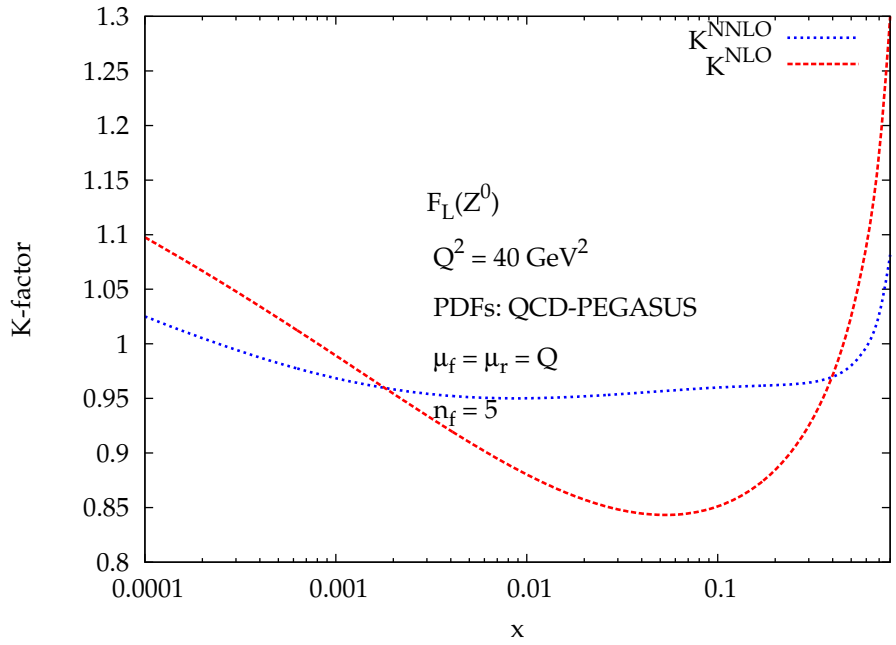


Figure 6.7.: The $K$-factors for DIS structure function $F_L$ at NLO and NNLO.

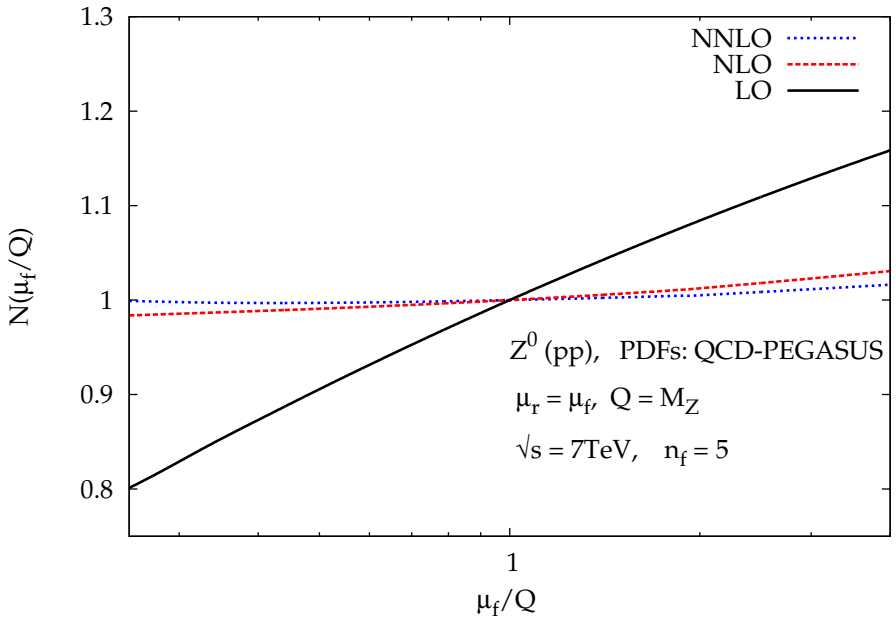


Figure 6.8.: The ratio of cross sections evaluated at scales $\mu_f$ and $Q$, defined in eq. (6.4) for Drell-Yan production at proton-proton collider using realistic PDFs.

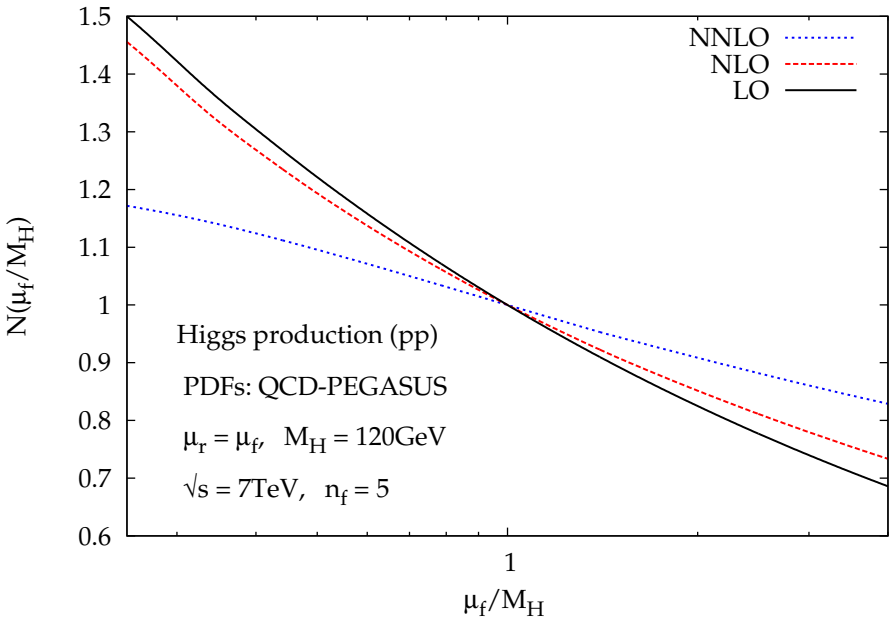


Figure 6.9.: The ratio of cross sections evaluated at scales $\mu_f$ and $M_H$, defined in eq. (6.4) for Higgs production at proton-proton collider using realistic PDFs.

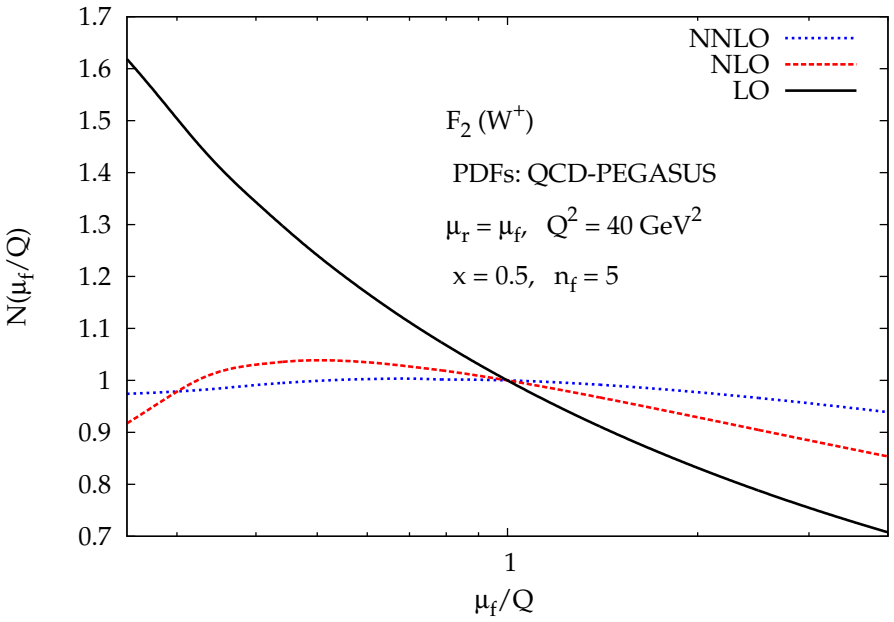


Figure 6.10.: The ratio of cross sections evaluated at scales $\mu_f$ and $Q$, defined in eq. (6.4) for DIS structure function $F_2$ using realistic PDFs.

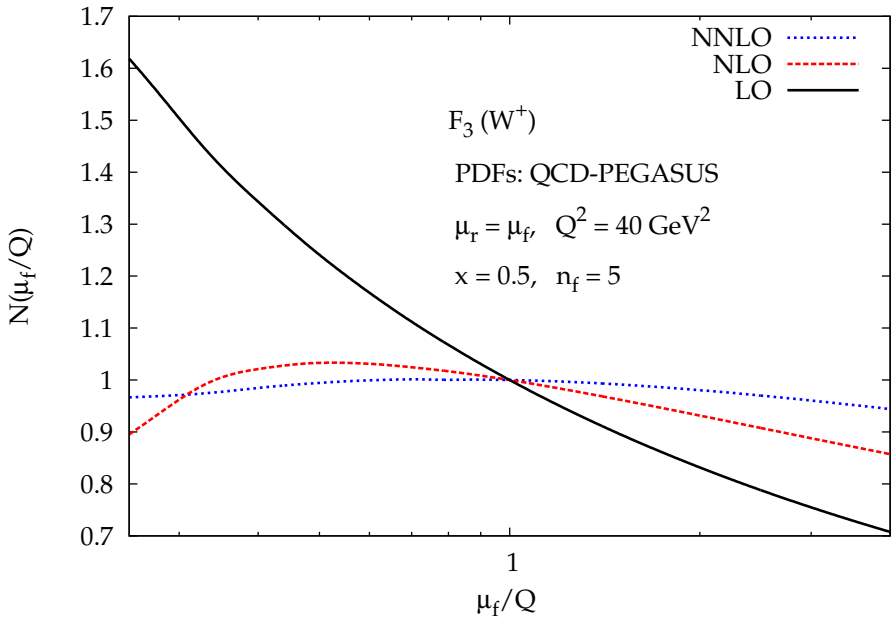


Figure 6.11.: The ratio of cross sections evaluated at scales $\mu_f$ and $Q$, defined in eq. (6.4) for DIS structure function $F_3$ using realistic PDFs.

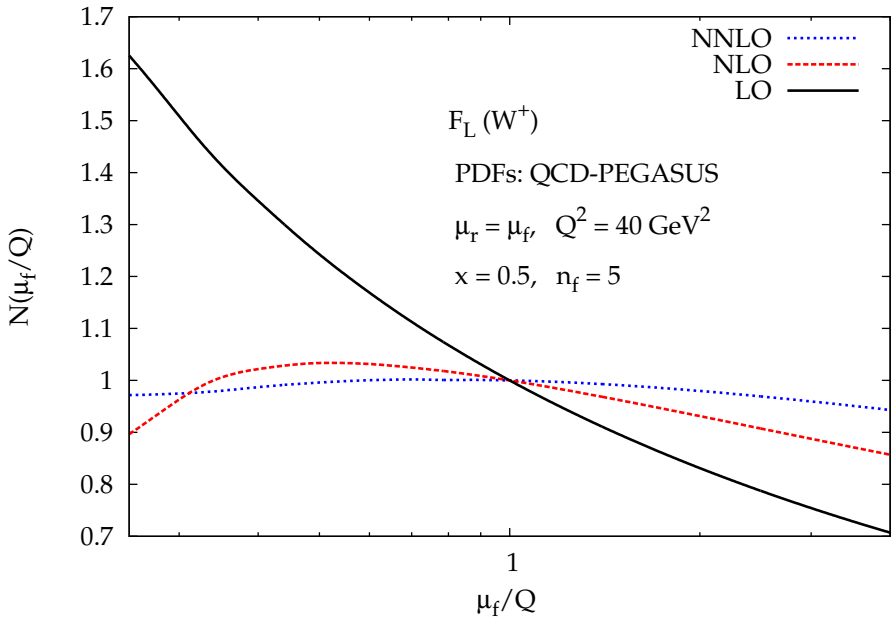


Figure 6.12.: The ratio of cross sections evaluated at scales $\mu_f$ and $Q$, defined in eq. (6.4) for DIS structure function $F_L$ using realistic PDFs.

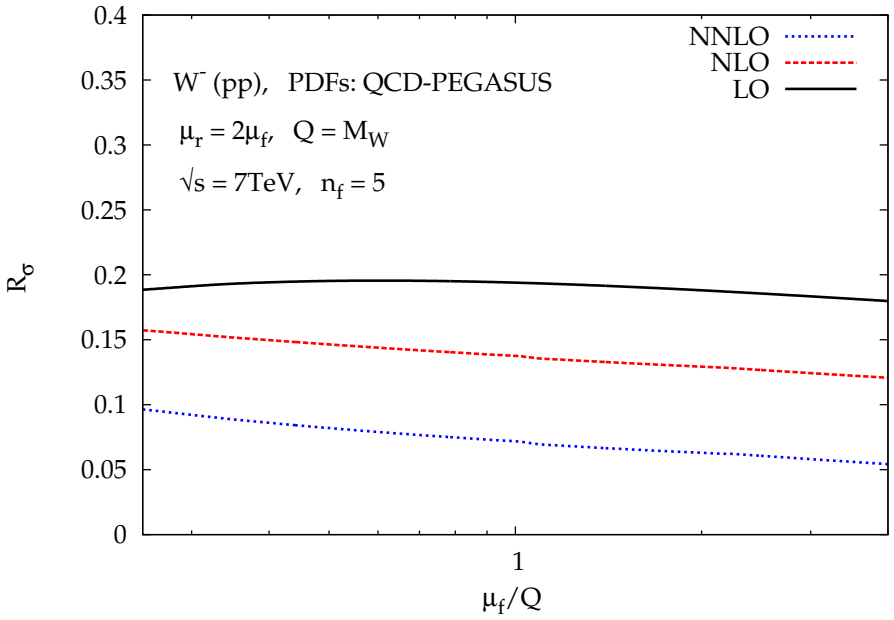


Figure 6.13.: The error of inconsistent treatment of factorisation and renormalisation scales with respect to the consistent one. $R_\sigma$ is defined in eq. (6.8).

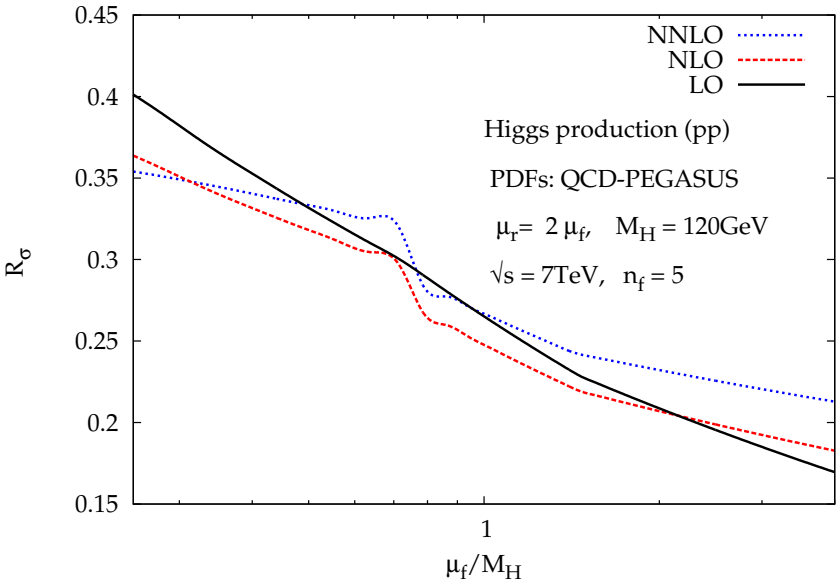


Figure 6.14.: The error of inconsistent treatment of factorisation and renormalisation scales with respect to the consistent one. $R_\sigma$ is defined in eq. (6.8).

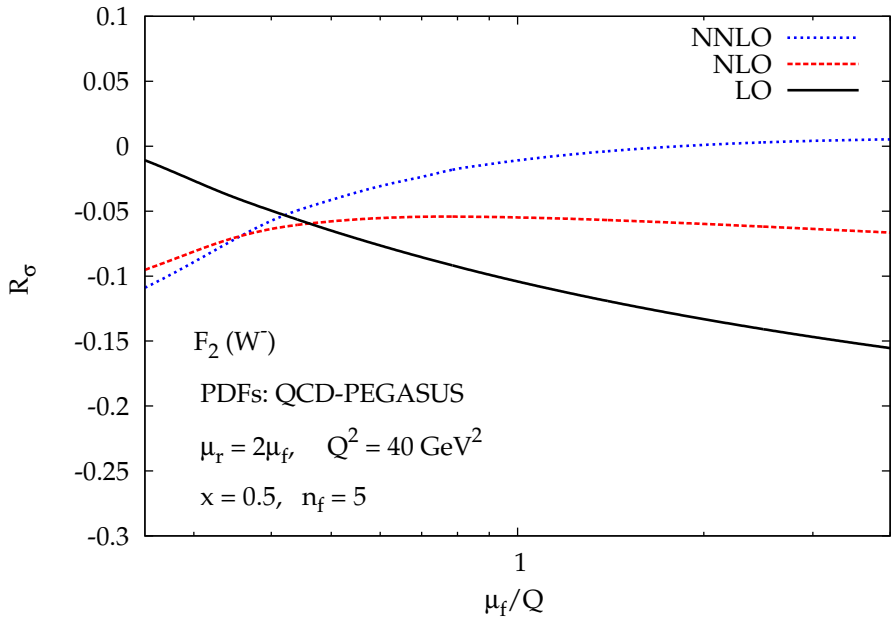


Figure 6.15.: The error of inconsistent treatment of factorisation and renormalisation scales with respect to the consistent one. $R_\sigma$ is defined in eq. (6.8).

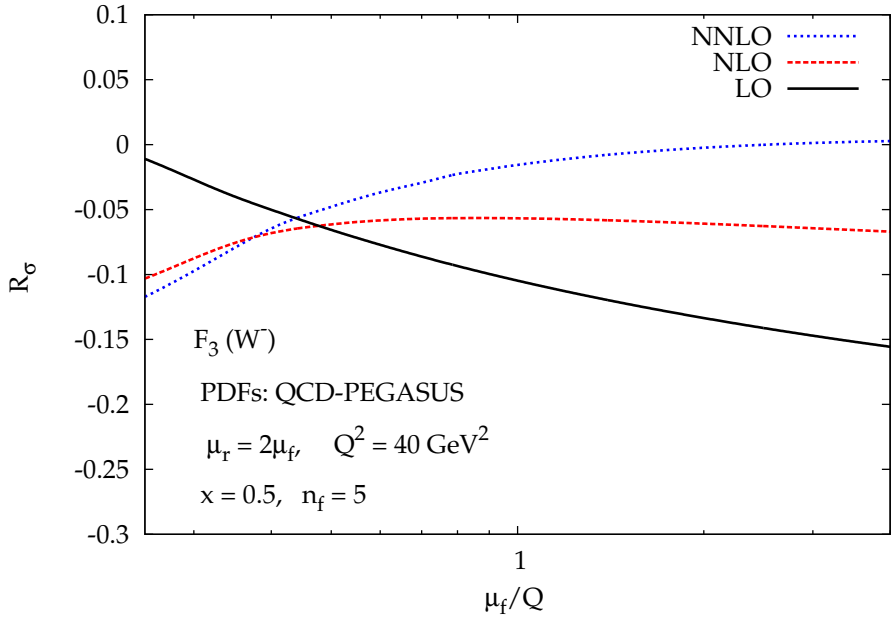


Figure 6.16.: The error of inconsistent treatment of factorisation and renormalisation scales with respect to the consistent one. $R_\sigma$ is defined in eq. (6.8).

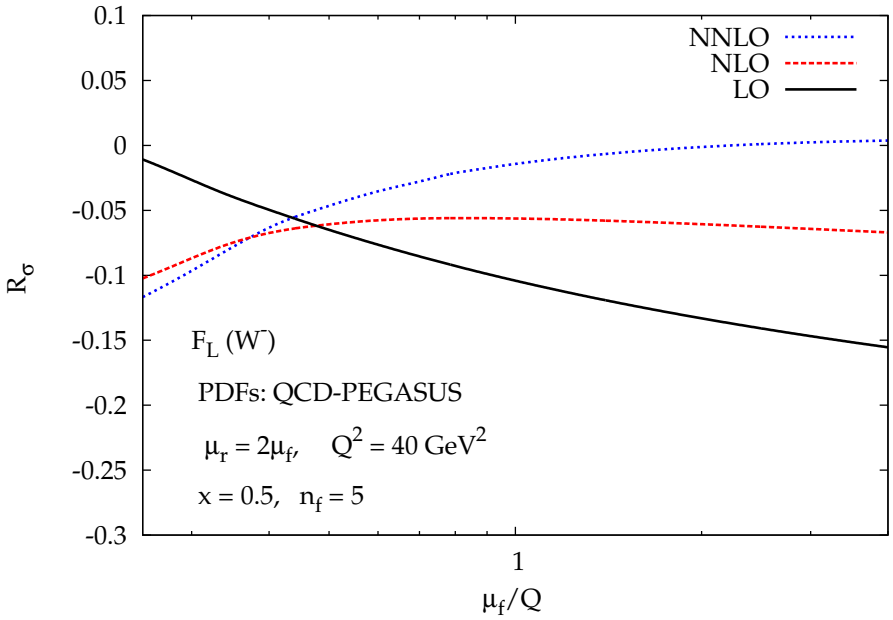


Figure 6.17.: The error of inconsistent treatment of factorisation and renormalisation scales with respect to the consistent one.

# 7. Conclusions

In this thesis we have studied precision predictions for standard model processes of prime importance at the LHC. We focused on full cross section for three processes with one or two hadrons in the initial state for which the QCD perturbative corrections are known analytically up to the next-to-next-to-leading order. We developed a computer code for a fast and accurate evaluation of total cross sections based on a Mellin space approach. A flexible `c++` implementation is publicly available from `http://www-zeuthen.desy.de/~kpetra/sbp/`.

In Chapter 2 we introduced some of the basic concepts for perturbative cross section computations in QCD. The Mellin transform of the convolution of the hard cross section with the parton distribution functions was shown to reduce the integrations into ordinary products. The method provides fast cross section evaluations which is particularly important for phenomenological studies that require repeated evaluation of cross sections.

In Chapter 3 we outlined the application of the Mellin space approach to hadron-hadron initiated processes. Two phenomenologically relevant processes were considered: the production of $W^{\pm}$ and $Z^0$ electroweak gauge bosons via the Drell-Yan mechanism and production of the Standard Model Higgs boson via gluon-gluon fusion. We discussed the validity of the narrow width approximation for the electroweak boson production and the heavy top mass limit taken in the case of Higgs boson production. The formalism applies equally well to deep inelastic lepton-hadron scattering the details of which have been introduced in Chapter 4.

We implemented this method into a `c++` package named `sbp`. The package was presented in Chapter 5. The $N$ space input for the coefficient functions has been obtained by using the `FORM` [25] package `harmpol` [26] in order to perform the Mellin transforms of $x$ space NNLO results [16–24]. The Mellin space output of coefficient functions is expressed in terms of harmonic sums [149, 150]. We followed the method of [154] in order to get an accurate implementation of those harmonic sums occurring in the result which do not have direct Mellin transforms.

An external `FORTRAN` code `QCD-PEGASUS` [27] can be linked to provide realistic parameterisation of the parton distribution functions. As a default option, we provide also model parton distribution functions, which can be useful for various cross-checks.

We performed a number of cross-checks on the implementation against some of the previously available $x$-space codes. The accuracy comparisons of Drell-Yan and Higgs cross sections at NNLO with programmes `ZWPROD` [16, 17] and `higgs.f` [23] were presented in Chapter 6. The evaluation of cross section was shown to be much faster than the $x$-space implementations, at only few seconds per full cross section at NNLO as discussed at the end of Chapter 6.

The major benefit of the NNLO corrections is the increased precision of the prediction. In Chapter 6 we looked at the dependence of the cross section on both factorisation and renormalisation scales. The significantly reduced dependence at NNLO is a test of the convergence of the perturbative series and the reliability of the fixed order predictions. In the case of Higgs boson production the large K-factors may indicate that the resummation of large logarithms lead to non-negligible contributions.

Due to its flexible interface, the package represents a framework which is open for extensions to other processes and modifications. It can be easily extended for the results of various resummations, which are naturally evaluated in $N$ space, see c.f. [157]. Other extensions to include heavy quark or jet production at NNLO would be feasible as soon as the coefficient functions become available. It also provides a possibility for a direct interface to LHAPDF grids, which would increase the range of phenomenological applications.

With the large amounts of data now collected by the LHC experiments it is likely that the Drell-Yan process may by used to impose stronger constraints on the known forms for the PDFs. It would be an interesting future direction to consider an extension to the method employed in this thesis to the fully differential cross sections required for such studies. Together with generalisations to the inclusion of a wider class of PDF parameterisation, this would open up a broad spectrum of future applications in high energy physics.

# A. Appendix

## A.1 Special functions

### A.1.1 Euler Gamma function

The Euler Gamma function is analytic on complex plane except for simple poles at $0, -1, -2, \ldots$. For integer argument $n = 0, 1, 2, \ldots$ is the Gamma function related to the factorial by

$$\Gamma(n) = (n-1)!. \tag{A.1}$$

At least three different, convenient definitions of the Gamma function are in common use: definition by infinite limit, definite integral and infinite product [155, Chapter 10],[158, Chapter 7]. The infinite limit by Euler reads

$$\Gamma(z) \equiv \lim_{n\to\infty} \frac{n! n^z}{z(z+1)(z+2)(z+3)\cdots(z+n)}, \qquad z \neq 0, -1, -2, -3, \ldots. \tag{A.2}$$

Second definition, also frequently called the Euler integral is

$$\Gamma(z) \equiv \int_0^\infty e^{-t} t^{z-1} \mathrm{d}t, \qquad \mathrm{Re}(z) > 0. \tag{A.3}$$

The third, called Weierstrass definition reads,

$$\frac{1}{\Gamma(z)} \equiv z e^{\gamma z} \prod_{n=1}^{\infty} \Big(1 + \frac{z}{n}\Big) e^{-z/n}, \tag{A.4}$$

where $\gamma$ is the Euler-Mascheroni constant. The reflection identity reads

$$\Gamma(z)\Gamma(1-z) = \frac{\pi}{\sin(z\pi)} \tag{A.5}$$

and the functional equation is

$$\Gamma(z+1) = z\Gamma(z) \qquad z \neq 0, -1, -2, \ldots. \tag{A.6}$$

The residues of $\Gamma(z)$ at $z = -m$ is

$$\mathrm{Res}[\Gamma(z)]_{z=-m} = \frac{(-1)^m}{m!} \quad \text{for} \quad m = 0, 1, 2, \ldots \tag{A.7}$$

### A.1.2 Digamma and polygamma functions

The digamma $\psi$ function is defined as a derivative of a natural logarithm of a Gamma function,

$$\psi(z) = \frac{\mathrm{d}}{\mathrm{d}z} \ln[\Gamma(z)] \equiv \psi^{(0)}(z). \tag{A.8}$$

Repeated differentiation gives rise to the polygamma function

$$\psi^{(k)}(z) = \frac{\mathrm{d}^{k+1}}{\mathrm{d}^{k+1}z} \ln[\Gamma(z)] = \frac{\mathrm{d}^k}{\mathrm{d}^k z}\psi^{(0)}(z), \qquad k = 1, 2, 3, \ldots. \tag{A.9}$$

### A.1.3 Euler Beta function

The primary definition of Euler Beta function is in terms of Gamma functions

$$B(\alpha, \beta) = \frac{\Gamma(\alpha)\Gamma(\beta)}{\Gamma(\alpha + \beta + 1)}. \tag{A.10}$$

The integral representation reads,

$$B(\alpha, \beta) = \int_0^1 x^{\alpha-1}(1-x)^{\beta-1}\mathrm{d}x \qquad \mathrm{Re}(\alpha) > 0 \quad \wedge \quad \mathrm{Re}(\beta) > 0. \tag{A.11}$$

### A.1.4 The plus distribution

In the evaluation of higher order contributions to hard scattering processes using dimensional regularisation we often encounter following types of functions

$$g(x) = (1-x)^{-1-2\epsilon}, \tag{A.12}$$

where $\epsilon = (4-d)/2$. The expansion in $\epsilon$ gives.

$$g(x) = \frac{1}{1-x}[1 - 2\epsilon \ln(1-x)] + \mathcal{O}(\epsilon^2) \tag{A.13}$$

The above expression diverges as $x \to 1$. The usual procedure is to make those divergences explicit and define $g(x)$ in terms of plus distributions – singular functions which are defined by their integral with a smooth function.[1] For a plus distribution $h_+(x)$ and a smooth function $f(x)$

$$\int_0^1 f(x)h_+(x)\mathrm{d}x = \int_0^1 h(x)(f(x) - f(1)). \tag{A.14}$$

[1] This is a perfectly reasonable assumption since the hadronic cross section represents an integral of the partonic one with a parton distribution function which is always smooth

The function $g(x)$ in terms of plus distributions is derived as follows. For an $\epsilon < 0$ [159] we can write [160]

$$\begin{aligned}\int_0^1 \mathrm{d}x\, g(x)f(x) &= \int_0^1 \mathrm{d}x\,(1-x)^{-1-2\epsilon}[f(x)-f(1)+f(1)] \\ &= \int_0^1 \mathrm{d}x\,\frac{1}{1-x}[1-2\epsilon\ln(1-x)][f(x)-f(1)] \\ &+ f(1)\Big[\frac{(1-x)^{-2\epsilon}}{(-2\epsilon)}\Big]_0^1 + \mathcal{O}(\epsilon^2) \\ &= \int_0^1 \mathrm{d}x\,\Big\{\frac{1}{(1-x)_+} - 2\epsilon\Big[\frac{\ln(1-x)}{1-x}\Big]_+\Big\} - f(1)\frac{\delta(1-x)}{2\epsilon} \\ &+ \mathcal{O}(\epsilon^2) \end{aligned} \tag{A.15}$$

and hence eq. (A.12) reads

$$(1-x)^{-1-2\epsilon} = -\delta(1-x)\frac{1}{2\epsilon} + \frac{1}{(1-x)_+} - 2\epsilon\Big[\frac{\ln(1-x)}{1-x}\Big]_+ + \mathcal{O}(\epsilon^2). \tag{A.16}$$

### A.1.5 Dirac delta function

$$\delta[f(x)] = \sum_i \frac{\delta(x-x_i)}{|f'(x)|_{x=x_i}} \tag{A.17}$$

## A.2 The phase space integral for lepton tensor

We give details on how to evaluate the following phase space integral

$$\int \mathrm{d}^d p_3 \int \mathrm{d}^d p_4 \delta^+(p_3^2)\delta^+(p_4^2)\delta^{(d)}(q-p_3-p_4) g^{\mu\nu}\langle \tilde{B}_\mu \tilde{B}_\nu^\dagger\rangle \tag{A.18}$$

with

$$\langle \tilde{B}_\mu \tilde{B}_\nu^\dagger\rangle = 2(p_{3\mu}p_{4\nu} + p_{4\mu}p_{3\nu} - g_{\mu\nu}p_3.p_4). \tag{A.19}$$

Multiplication by the metric tensor gives

$$g^{\mu\nu}\langle \tilde{B}_\mu \tilde{B}_\nu^\dagger\rangle = 2(2-d)(p_3.p_4). \tag{A.20}$$

The integration over $p_4$ sets $p_4 = q - p_3$ and we get

$$2(2-d)\int \mathrm{d}^d p_3 \delta^+(p_3^2)\delta^+\{(q-p_3)^2\}\{p_3.(q-p_3)\}. \tag{A.21}$$

We rewrite the integral over $p_3$,

$$\int \mathrm{d}^d p_3 \delta^+(p_3^2) = \int \frac{\mathrm{d}^{d-1}|p_3|}{2p_{3,0}} = \int \frac{|p_3|^{d-2}\mathrm{d}|p_3|}{2p_{3,0}} \mathrm{d}\Omega_{d-2}\sin^{d-3}\theta \mathrm{d}\theta \tag{A.22}$$

and since there is no the angular dependence of the integrand the $d-2$ dimensional angular integral can be evaluated directly and gives a factor $8\pi$ using relationships

$$\int \mathrm{d}\Omega_{d-2} = \frac{2\pi^{\frac{d-2}{2}}}{\Gamma(\frac{d-2}{2})} \tag{A.23}$$

and

$$\int_0^\pi \sin^{d-3}\theta \mathrm{d}\theta = \frac{4\{1+(-1)^{d/2}\}}{d-2}. \tag{A.24}$$

Choosing the CM system of the two leptons

$$q = (Q, 0, \ldots, 0, 0). \tag{A.25}$$

and using the properties of delta function, eq. (A.17) and $\delta^+(p^2) = \delta(p^2)\theta(p_0)$ the left-hand side of eq. (3.34) leads to

$$\begin{aligned} &\int \mathrm{d}^d p_3 \int \mathrm{d}^d p_4 \delta^+(p_3^2)\delta^+(p_4^2)\delta^{(d)}(q-p_3-p_4) g_{\mu\nu}\langle \tilde{B}_\mu \tilde{B}_\nu^\dagger\rangle \\ &\overset{d=4}{=} -32\pi \int \frac{E_3^2 \mathrm{d}E_3}{2E_3}\delta(E_3 - Q/2)\frac{E_3 Q}{2Q} = -2\pi Q^2. \end{aligned} \tag{A.26}$$

In the second step we also set $\varepsilon \to 0$ as there are no divergences.

## A.3 The Feynman rules etc.

### A.3.1 Colour algebra

The commutation relations for the colour matrices in the fundamental representation of the $SU(N)$ gauge group read,

$$[t^A, t^B] = i f^{ABC} t^C, \tag{A.27}$$

where $f^{ABC}$ are the totally antisymmetric structure constants of the $SU(N)$ group. For completeness, the adjoint representation obeys the same commutation relations and the matrix elements in adjoint representation are defined in terms of the structure constants

$$[T^A, T^B] = i f^{ABC} T^C \qquad (T^A)_{BC} - i f^{ABC}. \tag{A.28}$$

The representation of the generators $t^A$ is provided by the eight hermitian and traceless Gell-Mann matrices $\lambda^A$

$$t^A = \frac{1}{2}\lambda^A \tag{A.29}$$

The exact form of Gell-Mann matrices can be found for example in [33, Chapter 1]. The normalisation of matrices $t^A$ is chosen such that

$$\mathrm{Tr}(t^A t^B) = T_F \delta^{AB}, \tag{A.30}$$

where by convention $T_F = 1/2$ (sometimes also denoted as $T_R$). The colour algebra of Feynman diagrams can be done using the Fierz identity

$$(t^A)_{ab}(t^A)_{cd} = \frac{1}{2}\Big(\delta_{ad}\delta_{bc} - \frac{1}{N}\delta_{ab}\delta_{cd}\Big) \tag{A.31}$$

which together with understanding that $\delta_{aa} = N$ is equivalent to a trace of unit matrix leads to the following useful identities

$$t^A_{ab}t^A_{bc} = C_F\delta_{ac} \tag{A.32}$$

and

$$f^{ABC}f^{ABD} = C_A\delta^{CD}, \tag{A.33}$$

where the summation over repeated indices is assumed, and

$$C_F \equiv \frac{N^2-1}{2N}, \qquad C_A \equiv N, \tag{A.34}$$

where $N$ stands for the number of colours. Also,

$$\delta_{AB}\delta^{AB} = N^2 - 1 \qquad f^{ABC} = -2i\mathrm{Tr}([t^A, t^B]t^C). \tag{A.35}$$

## A.4 The file `example.cpp`

The mandatory content of a program is demonstrated on the file `example.cpp`. The file starts with declarations or declarations and assignments of objects of the class `Parameter`, see section 5.1.3. These lines shall not be removed. It is possible to directly modify the the objects of the class `Parameter`: `contour, phi, z[17], s1, ...s4 and pt2pdf`. The `main()` routine then contains declaration of input parameters, initialisations, call of functions calculating cross sections and printing statements.

```
1  #include <iostream>
2  #include "parameter.h"
3  #include "cross.h"
4  using namespace std;
5
6  // All objects of class Parameter need to be declared before
     ↪main()
7  //
8  // Parameters for cross sections
9  double Parameter::nf, Parameter::Q, Parameter::mh,
     ↪Parameter::muf, Parameter::mur,Parameter::alphas;
10 int Parameter::boson,Parameter::collider, Parameter::order;
11
12 // Pegasus parameters.
```

```
13 int Parameter::ipstd, Parameter::ipol, Parameter::evolpar,
     ↪Parameter::inppar;
14
15 // Parameters for contour integration.
16 double Parameter::contour = 1.5;
17 double Parameter::phi = 3.0/4.0*Constant::pi;
18 double Parameter::z[19] = {0.0, 0.05, 0.20, 0.40, 0.80, 1.00,
     ↪1.5, 2.0, 5.0, 8.0, 11.0, 14.0, 19.0, 24.0, 32.0, 44.0,
     ↪56.0, 68.0, 80.0};
19 int Parameter::s1 = 8, Parameter::s2 = 11, Parameter::s3 =
     ↪14, Parameter::s4 = 19;
20
21 // pointer to pdf funcion
22 Parameter::FPTR Parameter::pt2pdf =&toypdf; //  toy pdfs.
23 // the following line can be used when Pegasus is linked, see
     ↪makefile
24 // Parameter::FPTR Parameter::pt2pdf =&pegasuspdf; // pegasus.
25 // ============================================================
26
27 int main(){ // main program
28 //  common initial values
29 int order = 2;          // 0 = LO, 1 = NLO, 2 = NNLO
30 double nf = 5.0;
31 double alphas = 0.1;
32
33 //  process specific initial values
34 int boson = 3;          // 0 = photon (DIS only), 1 = Z, 2 =
     ↪W+, 3 = W- . DIS and DY only
35 int collider=-1;        // -1 = ppbar, 1 = pp scattering, DY
     ↪and Higgs only
36 double mh = 120.0;      // Higgs mass, Higgs only
37 double Q = 100.0;       // DIS interaction scale, DIS only
38
39 // input values for cross sections and structure function
     ↪tables
40 double sqs[10] = {150.0, 200.0, 400.0, 800.0, 1200.0, 2000.0,
     ↪4000.0, 7000.0,  10000.0,  14000.0};
41 double x[10]       = {0.00001, 0.0001, 0.0005, 0.001,  0.005,
     ↪ 0.01,  0.05,  0.1,  0.5,  0.9};
42 double s,result,r2,r3,rL;
43
44
45 init_dy(nf,alphas,order,boson,collider); // initialise
     ↪Drell-Yan
46 printparameters(); // optional, to see what the
     ↪initialisation routine set
47 // some printing
```

⋮

```
50 for ( int k = 0; k < 10; k++ ){ // loop over the array of cm
     ↪energies
51   s =   sqs[k]*sqs[k];
52   result = sigma(s); // evaluate the cross section
```

⋮

```
56 // continue with Higgs and DIS
57 init_higgs(nf, mh, alphas, order,collider); // Higgs
     ↪initialisation.
```

### A.4.1 The benchmark tables

The output of executable `example.exe` provides benchmark values for cross sections at NNLO with the toy parton distributions preceded with values of initialisation parameters and it is written in the file `example.log`:

```
info:    Drell-Yan initialized.
info:     printparameters()
------------------------------------------------------------
         number of flavours              5.000000
         Q                               80.399000
         mh (higgs only)                 120.000000
         muf                             80.399000
         mur                             80.399000
         order                           2
         boson                           3
         collider (hadron-hadron only)   -1
         alphas                          0.100000
------------------------------------------------------------

         cm energy [GeV^2]       | cross section  [nb]
         ------------------------|--------------------
             2.2e+04             |  1.7162106243e-01
             4.0e+04             |  8.3980454207e-01
             1.6e+05             |  3.9493760307e+00
             6.4e+05             |  6.4206088741e+00
             1.4e+06             |  7.4915904024e+00
             4.0e+06             |  8.9163993514e+00
             1.6e+07             |  1.1439668002e+01
             4.9e+07             |  1.4157460384e+01
             1.0e+08             |  1.6242121647e+01
             2.0e+08             |  1.8477140203e+01
         ------------------------|--------------------

info:    Higgs initialized.
info:     printparameters()
------------------------------------------------------------
```

```
         number of flavours              5.000000
         Q                               120.000000
         mh (higgs only)                 120.000000
         muf                             120.000000
         mur                             120.000000
         order                           2
         boson                           4
         collider (hadron-hadron only)   -1
         alphas                          0.100000
-------------------------------------------------------------

         cm energy [GeV^2]       | cross section  [pb]
         ------------------------|--------------------
             2.2e+04             |  1.2300383111e-08
             4.0e+04             |  2.4130191079e-05
             1.6e+05             |  1.2126075274e-02
             6.4e+05             |  1.3498171840e-01
             1.4e+06             |  3.1118472777e-01
             4.0e+06             |  6.7906689943e-01
             1.6e+07             |  1.5070321724e+00
             4.9e+07             |  2.5502660214e+00
             1.0e+08             |  3.4610808256e+00
             2.0e+08             |  4.5519431090e+00
         ------------------------|--------------------

info:    DIS Initialized.
info:     printparameters()
-------------------------------------------------------------
         number of flavours              5.000000
         Q                               100.000000
         mh (higgs only)                 120.000000
         muf                             100.000000
         mur                             100.000000
         order                           2
         boson                           3
         collider (hadron-hadron only)   1
         alphas                          0.100000
-------------------------------------------------------------

               x                 |          F_2
         ------------------------|--------------------
            1.0e-05              |  2.9400967192e+00
            1.0e-04              |  2.3386888688e+00
            5.0e-04              |  2.0040289405e+00
            1.0e-03              |  1.8828822504e+00
            5.0e-03              |  1.6730856500e+00
            1.0e-02              |  1.6283184197e+00
            5.0e-02              |  1.6707494275e+00
            1.0e-01              |  1.7293526360e+00
```

| | |
|---|---|
| 5.0e-01 | 7.7367088451e-01 |
| 9.0e-01 | 1.3527875359e-02 |

| x | F_3 |
|---|---|
| 1.0e-05 | -4.7208189106e+04 |
| 1.0e-04 | -3.6823338905e+03 |
| 5.0e-04 | -5.8683976287e+02 |
| 1.0e-03 | -2.5366727510e+02 |
| 5.0e-03 | -2.0470328969e+01 |
| 1.0e-02 | 2.0543328436e+00 |
| 5.0e-02 | 1.1765485335e+01 |
| 1.0e-01 | 9.8403801285e+00 |
| 5.0e-01 | 1.4944729248e+00 |
| 9.0e-01 | 1.5009640285e-02 |

| x | F_L |
|---|---|
| 1.0e-05 | 1.4276537103e+05 |
| 1.0e-04 | 1.1351375915e+04 |
| 5.0e-04 | 1.9446811445e+03 |
| 1.0e-03 | 9.1339790450e+02 |
| 5.0e-03 | 1.6226866023e+02 |
| 1.0e-02 | 7.8970164496e+01 |
| 5.0e-02 | 1.6244967379e+01 |
| 1.0e-01 | 8.4343059843e+00 |
| 5.0e-01 | 7.6657974051e-01 |
| 9.0e-01 | 7.5058184545e-03 |

# Bibliography


[1] S.L. Glashow. Partial Symmetries of Weak Interactions. *Nucl.Phys.*, 22:579–588, 1961.

[2] A. Salam. In Elementary Particle Theory, 1968. N. Svartholm, Almquist and Forlag, Stockholm (1968).

[3] Steven Weinberg. A Model of Leptons. *Phys.Rev.Lett.*, 19:1264–1266, 1967.

[4] David J. Gross. Twenty five years of asymptotic freedom. *Nucl.Phys.Proc.Suppl.*, 74:426–446, 1999.

[5] Gerard 't Hooft. When was asymptotic freedom discovered? or the rehabilitation of quantum field theory. *Nucl.Phys.Proc.Suppl.*, 74:413–425, 1999.

[6] John C. Collins, Davison E. Soper, and George F. Sterman. Factorization for Short Distance Hadron - Hadron Scattering. *Nucl.Phys.*, B261:104, 1985.

[7] John C. Collins, Davison E. Soper, and George F. Sterman. Soft Gluons and Factorization. *Nucl.Phys.*, B308:833, 1988.

[8] Geoffrey T. Bodwin. Factorization of the Drell-Yan Cross-Section in Perturbation Theory. *Phys.Rev.*, D31:2616, 1985. Revised version.

[9] Dru B. Renner. Status of Average-x from Lattice QCD. *AIP Conf.Proc.*, 1369: 29–36, 2011.

[10] L.N. Lipatov. The parton model and perturbation theory. *Sov.J.Nucl.Phys.*, 20: 94–102, 1975.

[11] V.N. Gribov and L.N. Lipatov. Deep inelastic e p scattering in perturbation theory. *Sov.J.Nucl.Phys.*, 15:438–450, 1972.

[12] Guido Altarelli and G. Parisi. Asymptotic Freedom in Parton Language. *Nucl.Phys.*, B126:298, 1977.

[13] Yuri L. Dokshitzer. Calculation of the Structure Functions for Deep Inelastic Scattering and e+ e- Annihilation by Perturbation Theory in Quantum Chromodynamics. *Sov.Phys.JETP*, 46:641–653, 1977.

[14] Matteo Cacciari and Nicolas Houdeau. Meaningful characterisation of perturbative theoretical uncertainties. *JHEP*, 1109:039, 2011.

[15] J.R. Andersen et al. The SM and NLO Multileg Working Group: Summary report. pages 21–189, 2010.

[16] R. Hamberg, W.L. van Neerven, and T. Matsuura. A Complete calculation of the order $\alpha_s^2$ correction to the Drell-Yan K factor. *Nucl.Phys.*, B359:343–405, 1991.

[17] R. Hamberg, W. L. van Neerven, and T. Matsuura. Erratum to: A complete calculation of the order $\alpha_s^2$ correction to the Drell-Yan K-factor: [Nucl. Phys. B 359 (1991) 343]. `http://www.sciencedirect.com/science/ARTICLE/B6TVC-46SP07H-3/2/1fda7e6dccc93b4d47dbe4755ced532c`, 2002. ISSN 0550-3213.

[18] J.A.M. Vermaseren, A. Vogt, and S. Moch. The Third-order QCD corrections to deep-inelastic scattering by photon exchange. *Nucl.Phys.*, B724:3–182, 2005.

[19] S. Moch, J.A.M. Vermaseren, and A. Vogt. Third-order QCD corrections to the charged-current structure function F(3). *Nucl.Phys.*, B813:220–258, 2009.

[20] W.L. van Neerven and E.B. Zijlstra. Order $\alpha_s^2$ contributions to the deep inelastic Wilson coefficient. *Phys.Lett.*, B272:127–133, 1991.

[21] S. Moch, M. Rogal, and A. Vogt. Differences between charged-current coefficient functions. *Nucl.Phys.*, B790:317–335, 2008.

[22] E.B. Zijlstra and W.L. van Neerven. Order $\alpha_s^2$ correction to the structure function F3 $(x, Q^2)$ in deep inelastic neutrino - hadron scattering. *Phys.Lett.*, B297:377–384, 1992.

[23] V. Ravindran, J. Smith, and W. L. van Neerven. NNLO corrections to the total cross-section for Higgs boson production in hadron hadron collisions. *Nucl.Phys.*, B665:325–366, 2003.

[24] V. Ravindran, J. Smith, and W.L. van Neerven. Two-loop corrections to Higgs boson production. *Nucl.Phys.*, B704:332–348, 2005.

[25] J.A.M. Vermaseren. New features of FORM. arXiv:math-ph/0010025, 2000.

[26] E. Remiddi and J.A.M. Vermaseren. Harmonic polylogarithms. *Int.J.Mod.Phys.*, A15:725–754, 2000.

[27] A. Vogt. Efficient evolution of unpolarized and polarized parton distributions with QCD-PEGASUS. *Comput.Phys.Commun.*, 170:65–92, 2005.

[28] Stefano Catani and Massimiliano Grazzini. An NNLO subtraction formalism in hadron collisions and its application to Higgs boson production at the LHC. *Phys.Rev.Lett.*, 98:222002, 2007.

[29] Stefano Catani, Leandro Cieri, Giancarlo Ferrera, Daniel de Florian, and Massimiliano Grazzini. Vector boson production at hadron colliders: A Fully exclusive QCD calculation at NNLO. *Phys.Rev.Lett.*, 103:082001, 2009.

[30] Ryan Gavin, Ye Li, Frank Petriello, and Seth Quackenbush. W physics at the LHC with FEWZ 2.1. arXiv:hep-ph/1201.5896, 2012.

[31] Charalampos Anastasiou, Stephan Buehler, Franz Herzog, and Achilleas Lazopoulos. Total cross-section for Higgs boson hadroproduction with anomalous Standard Model interactions. *JHEP*, 1112:058, 2011. doi: 10.1007/JHEP12(2011)058.

[32] Charalampos Anastasiou, Kirill Melnikov, and Frank Petriello. Fully differential Higgs boson production and the di-photon signal through next-to-next-to-leading order. *Nucl.Phys.*, B724:197–246, 2005.

[33] R. K. Ellis, W. J. Stirling, and B. R. Webber. *QCD and Collider Physics*. Cambridge University Press, 2003. ISBN 0 521 54589 7.

[34] Michael E. Peskin and Daniel V Schroeder. *An Introduction to Quantum Field Theory*. Westview Press, 1995. ISBN 978-0-201-50397-5.

[35] Michelangelo L Mangano. Introduction to qcd. oai:cds.cern.ch:454171, 1999.

[36] Michelangelo L. Mangano. QCD and the physics of hadronic collisions. *Phys.Usp.*, 53:109–132, 2010.

[37] Stefano Forte. Parton distributions at the dawn of the LHC. *Acta Phys.Polon.*, B41:2859–2920, 2010.

[38] Abdelhak Djouadi. The Anatomy of electro-weak symmetry breaking. I: The Higgs boson in the standard model. *Phys.Rept.*, 457:1–216, 2008.

[39] Abdelhak Djouadi. The Anatomy of electro-weak symmetry breaking. II. The Higgs bosons in the minimal supersymmetric model. *Phys.Rept.*, 459:1–241, 2008.

[40] S. Dittmaier et al. Handbook of LHC Higgs Cross Sections: 1. Inclusive Observables. arXiv:hep-ph/1101.0593, 2011.

[41] Siegfried Bethke. The 2009 World Average of $\alpha_s$. *Eur.Phys.J.*, C64:689–703, 2009.

[42] Graeme Watt. Parton Distributions: HERA-Tevatron-LHC. *PoS*, HCP2009:014, 2009.

[43] John M. Campbell, J.W. Huston, and W.J. Stirling. Hard Interactions of Quarks and Gluons: A Primer for LHC Physics. *Rept.Prog.Phys.*, 70:89, 2007.

[44] Guido Altarelli. A QCD primer. arXiv:hep-ph/0204179, 2002.

[45] H.David Politzer. Reliable Perturbative Results for Strong Interactions? *Phys.Rev.Lett.*, 30:1346–1349, 1973.

[46] D.J. Gross and Frank Wilczek. Ultraviolet Behavior of Nonabelian Gauge Theories. *Phys.Rev.Lett.*, 30:1343–1346, 1973.

[47] William E. Caswell. Asymptotic Behavior of Nonabelian Gauge Theories to Two Loop Order. *Phys.Rev.Lett.*, 33:244, 1974.

[48] O.V. Tarasov, A.A. Vladimirov, and A.Yu. Zharkov. The Gell-Mann-Low Function of QCD in the Three Loop Approximation. *Phys.Lett.*, B93:429–432, 1980.

[49] S.A. Larin and J.A.M. Vermaseren. The Three loop QCD Beta function and anomalous dimensions. *Phys.Lett.*, B303:334–336, 1993.

[50] T. van Ritbergen, J.A.M. Vermaseren, and S.A. Larin. The Four loop beta function in quantum chromodynamics. *Phys.Lett.*, B400:379–384, 1997.

[51] M. Czakon. The Four-loop QCD beta-function and anomalous dimensions. *Nucl.Phys.*, B710:485–498, 2005.

[52] K. Nakamura et al. Review of Particle Physics. *J. Phys.*, G37, 2010.

[53] S. Alekhin, J. Blümlein, P. Jimenez-Delgado, S. Moch, and E. Reya. NNLO Benchmarks for Gauge and Higgs Boson Production at TeV Hadron Colliders. *Phys.Lett.*, B697:127–135, 2011.

[54] G. Curci, W. Furmanski, and R. Petronzio. Evolution of Parton Densities Beyond Leading Order: The Nonsinglet Case. *Nucl.Phys.*, B175:27, 1980.

[55] W. Furmanski and R. Petronzio. Singlet Parton Densities Beyond Leading Order. *Phys.Lett.*, B97:437, 1980.

[56] E.G. Floratos, D.A. Ross, and Christopher T. Sachrajda. Higher Order Effects in Asymptotically Free Gauge Theories: The Anomalous Dimensions of Wilson Operators. *Nucl.Phys.*, B129:66–88, 1977.

[57] Erratum. *Nuclear Physics B*, 139(4):545 – 546, 1978. ISSN 0550-3213. URL `http://www.sciencedirect.com/science/article/pii/055032137890367X`.

[58] E. G. Floratos, D. A. Ross, and C. T. Sachrajda. Erratum. *Nuclear Physics B*, 152 (3-4):493 – 520, 1979. ISSN 0550-3213. URL `http://www.sciencedirect.com/science/article/pii/0550321379900944`.

[59] Antonio Gonzalez-Arroyo, C. Lopez, and F.J. Yndurain. Second Order Contributions to the Structure Functions in Deep Inelastic Scattering. 1. Theoretical Calculations. *Nucl.Phys.*, B153:161–186, 1979.

[60] E.G. Floratos, C. Kounnas, and R. Lacaze. Higher Order QCD Effects in Inclusive Annihilation and Deep Inelastic Scattering. *Nucl.Phys.*, B192:417, 1981.

[61] S. Moch, J.A.M. Vermaseren, and A. Vogt. The Three loop splitting functions in QCD: The Nonsinglet case. *Nucl.Phys.*, B688:101–134, 2004.

[62] A. Vogt, S. Moch, and J.A.M. Vermaseren. The Three-loop splitting functions in QCD: The Singlet case. *Nucl.Phys.*, B691:129–181, 2004.

[63] S. Alekhin, J. Blümlein, S. Klein, and S. Moch. 3-, 4-, and 5-flavor next-to-next-to-leading order parton distribution functions from deep-inelastic-scattering data and at hadron colliders. *Phys. Rev. D*, 81(1):014032, Jan 2010.

[64] The Durham HepData Project. Hepdata parton distribution server. `http://hepdata.cedar.ac.uk/pdfs`.

[65] S. Alekhin, J. Blumlein, and S. Moch. Parton distribution functions and benchmark cross sections at NNLO. arXiv:hep-ph/1202.2281, 2012.

[66] A.D. Martin, W.J. Stirling, R.S. Thorne, and G. Watt. Parton distributions for the LHC. *Eur.Phys.J.*, C63:189–285, 2009.

[67] Hung-Liang Lai, Marco Guzzi, Joey Huston, Zhao Li, Pavel M. Nadolsky, et al. New parton distributions for collider physics. *Phys.Rev.*, D82:074024, 2010. doi: 10.1103/PhysRevD.82.074024.

[68] P. Jimenez-Delgado and E. Reya. Dynamical NNLO parton distributions. *Phys.Rev.*, D79:074023, 2009. doi: 10.1103/PhysRevD.79.074023.

[69] Richard D. Ball et al. Unbiased global determination of parton distributions and their uncertainties at NNLO and at LO. *Nucl.Phys.*, B855:153–221, 2012. doi: 10.1016/j.nuclphysb.2011.09.024.

[70] Sergey Alekhin, Simone Alioli, Richard D. Ball, Valerio Bertone, Johannes Blumlein, et al. The PDF4LHC Working Group Interim Report. arXiv:hep-ph/1101.0536, 2011.

[71] Peter W. Higgs. Broken symmetries, massless particles and gauge fields. *Phys.Lett.*, 12:132–133, 1964.

[72] Peter W. Higgs. Spontaneous symmetry breakdown without massless bosons. *Phys. Rev.*, 145:1156–1163, May 1966. URL `http://link.aps.org/doi/10.1103/PhysRev.145.1156`.

[73] F. Englert and R. Brout. Broken Symmetry and the Mass of Gauge Vector Mesons. *Phys.Rev.Lett.*, 13:321–322, 1964.

[74] G.S. Guralnik, C.R. Hagen, and T.W.B. Kibble. Global Conservation Laws and Massless Particles. *Phys.Rev.Lett.*, 13:585–587, 1964.

[75] T.W.B. Kibble. Symmetry breaking in nonAbelian gauge theories. *Phys.Rev.*, 155:1554–1561, 1967.

[76] S. D. Drell and Tung-Mow Yan. Massive lepton pair production in hadron-hadron collisions at high-energies. *Phys. Rev. Lett.*, 25:316–320, 1970.

[77] Guido Altarelli, R.Keith Ellis, and G. Martinelli. Large Perturbative Corrections to the Drell-Yan Process in QCD. *Nucl.Phys.*, B157:461, 1979.

[78] Guido Altarelli, R.Keith Ellis, and G. Martinelli. Leptoproduction and Drell-Yan Processes Beyond the Leading Approximation in Chromodynamics. *Nucl.Phys.*, B143:521, 1978.

[79] Erratum. *Nuclear Physics B*, 146(2):544 – 544, 1978. ISSN 0550-3213. URL `http://www.sciencedirect.com/science/article/pii/0550321378900858`.

[80] J. Abad and B. Humpert. PERTURBATIVE QCD CORRECTIONS IN e p SCATTERING. *Phys.Lett.*, B77:105, 1978.

[81] J. Abad and B. Humpert. LARGE CONSTANT TERMS FROM SOFT GLUONS. *Phys.Lett.*, B78:627, 1978.

[82] Erratum. *Physics Letters B*, 80(4-5):433 – 433, 1979. ISSN 0370-2693. URL `http://www.sciencedirect.com/science/article/pii/0370269379912103`.

[83] J. Abad and B. Humpert. PERTURBATIVE VERSUS AF CORRECTIONS IN e p SCATTERING. *Phys.Lett.*, B80:115, 1978.

[84] J. Abad and B. Humpert. PERTURBATIVE QCD CORRECTIONS IN DRELL-YAN PROCESSES. *Phys.Lett.*, B80:286, 1979. Revised Version.

[85] J. Kubar-Andre and Frank E. Paige. Gluon Corrections to the Drell-Yan Model. *Phys.Rev.*, D19:221, 1979.

[86] K. Harada, T. Kaneko, and N. Sakai. Hadronic Lepton Pair Production Beyond the Leading Order in Perturbative QCD. *Nucl.Phys.*, B155:169, 1979.

[87] Erratum. *Nuclear Physics B*, 165(3):545 – 545, 1980. ISSN 0550-3213. URL `http://www.sciencedirect.com/science/article/pii/0550321380900486`.

[88] B. Humpert and W.L. Van Neerven. AMBIGUITIES IN THE INFRARED REGULARIZATION OF QCD. *Phys.Lett.*, B84:327, 1979.

[89] Erratum. *Physics Letters B*, 85(4):471 – 471, 1979. ISSN 0370-2693. URL `http://www.sciencedirect.com/science/article/pii/0370269379912991`.

[90] B. Humpert and W.L. van Neerven. HOW TO REGULARIZE THE INFRARED AND MASS SINGULARITIES IN QCD. *Phys.Lett.*, B89:69, 1979.

[91] B. Humpert and W.L. van Neerven. INFRARED AND MASS REGULARIZATION IN AF FIELD THEORIES 2. QCD. *Nucl.Phys.*, B184:225, 1981.

[92] J. Kubar, M. Le Bellac, J.L. Meunier, and G. Plaut. QCD Corrections to the Drell-Yan Mechanism and the Pion Structure Function. *Nucl.Phys.*, B175:251, 1980.

[93] W. Furmanski and R. Petronzio. Lepton - Hadron Processes Beyond Leading Order in Quantum Chromodynamics. *Z.Phys.*, C11:293, 1982. and references therein.

[94] C. Albajar et al. Intermediate Vector Boson Cross-Sections at the CERN Super Proton Synchrotron Collider and the Number of Neutrino Types. *Phys.Lett.*, B198: 271, 1987.

[95] J. Alitti et al. A Measurement of the $W$ and $Z$ production cross-sections and a determination of Gamma ($W$) at the CERN $\bar{p}p$ collider. *Phys.Lett.*, B276:365–374, 1992.

[96] Sergey Alekhin, Kirill Melnikov, and Frank Petriello. Fixed target Drell-Yan data and NNLO QCD fits of parton distribution functions. *Phys.Rev.*, D74:054033, 2006.

[97] U. Baur, S. Keller, and W.K. Sakumoto. QED radiative corrections to $Z$ boson production and the forward backward asymmetry at hadron colliders. *Phys.Rev.*, D57:199–215, 1998.

[98] U. Baur, S. Keller, and D. Wackeroth. Electroweak radiative corrections to $W$ boson production in hadronic collisions. *Phys.Rev.*, D59:013002, 1999.

[99] U. Baur, O. Brein, W. Hollik, C. Schappacher, and D. Wackeroth. Electroweak radiative corrections to neutral current Drell-Yan processes at hadron colliders. *Phys.Rev.*, D65:033007, 2002.

[100] Stefan Dittmaier and 1 Kramer, Michael. Electroweak radiative corrections to W boson production at hadron colliders. *Phys.Rev.*, D65:073007, 2002.

[101] William B. Kilgore and Christian Sturm. Two-Loop Virtual Corrections to Drell-Yan Production at order $\alpha_s\alpha^3$. arXiv:hep-ph/1107.4798, 2011.

[102] Charalampos Anastasiou, Lance J. Dixon, Kirill Melnikov, and Frank Petriello. High precision QCD at hadron colliders: Electroweak gauge boson rapidity distributions at NNLO. *Phys.Rev.*, D69:094008, 2004.

[103] Richard P. Feynman. Very high-energy collisions of hadrons. *Phys.Rev.Lett.*, 23: 1415–1417, 1969.

[104] V. Ravindran. Unpublished.

[105] Robert V. Harlander and William B. Kilgore. Next-to-next-to-leading order Higgs production at hadron colliders. *Phys.Rev.Lett.*, 88:201801, 2002.

[106] Johannes Blümlein and Vajravelu Ravindran. Mellin moments of the next-to-next-to leading order coefficient functions for the Drell-Yan process and hadronic Higgs-boson production. *Nucl.Phys.*, B716:128–172, 2005.

[107] Tsuyoshi Matsuura. *HIGHER ORDER CORRECTIONS TO THE DRELL-YAN PROCESS*. PhD thesis, Rijksuniversiteit te Leiden, 1989.

[108] G. Passarino and M.J.G. Veltman. One Loop Corrections for e+ e- Annihilation Into mu+ mu- in the Weinberg Model. *Nucl.Phys.*, B160:151, 1979.

[109] Michael Spira. QCD effects in Higgs physics. *Fortsch.Phys.*, 46:203–284, 1998.

[110] H.M. Georgi, S.L. Glashow, M.E. Machacek, and Dimitri V. Nanopoulos. Higgs Bosons from Two Gluon Annihilation in Proton Proton Collisions. *Phys.Rev.Lett.*, 40:692, 1978.

[111] D. Graudenz, M. Spira, and P.M. Zerwas. QCD corrections to Higgs boson production at proton proton colliders. *Phys.Rev.Lett.*, 70:1372–1375, 1993.

[112] M. Spira, A. Djouadi, D. Graudenz, and P.M. Zerwas. Higgs boson production at the LHC. *Nucl.Phys.*, B453:17–82, 1995.

[113] Michael Kramer, Eric Laenen, and Michael Spira. Soft gluon radiation in Higgs boson production at the LHC. *Nucl.Phys.*, B511:523–549, 1998.

[114] S. Dawson. Radiative corrections to Higgs boson production. *Nucl.Phys.*, B359: 283–300, 1991.

[115] A. Djouadi, M. Spira, and P.M. Zerwas. Production of Higgs bosons in proton colliders: QCD corrections. *Phys.Lett.*, B264:440–446, 1991.

[116] Robert V. Harlander. Virtual corrections to g g —> H to two loops in the heavy top limit. *Phys.Lett.*, B492:74–80, 2000.

[117] Stefano Catani, Daniel de Florian, and Massimiliano Grazzini. Higgs production in hadron collisions: Soft and virtual QCD corrections at NNLO. *JHEP*, 0105: 025, 2001.

[118] Robert V. Harlander and William B. Kilgore. Soft and virtual corrections to proton proton —> H + x at NNLO. *Phys.Rev.*, D64:013015, 2001.

[119] Charalampos Anastasiou and Kirill Melnikov. Higgs boson production at hadron colliders in NNLO QCD. *Nucl.Phys.*, B646:220–256, 2002.

[120] Stefano Catani, Daniel de Florian, Massimiliano Grazzini, and Paolo Nason. Soft gluon resummation for Higgs boson production at hadron colliders. *JHEP*, 0307: 028, 2003.

[121] S. Moch and A. Vogt. Higher-order soft corrections to lepton pair and Higgs boson production. *Phys.Lett.*, B631:48–57, 2005.

[122] Eric Laenen and Lorenzo Magnea. Threshold resummation for electroweak annihilation from DIS data. *Phys.Lett.*, B632:270–276, 2006.

[123] Ahmad Idilbi, Xiang-dong Ji, Jian-Ping Ma, and Feng Yuan. Threshold resummation for Higgs production in effective field theory. *Phys.Rev.*, D73:077501, 2006.

[124] R.Keith Ellis, I. Hinchliffe, M. Soldate, and J.J. van der Bij. Higgs Decay to tau+ tau-: A Possible Signature of Intermediate Mass Higgs Bosons at the SSC. *Nucl.Phys.*, B297:221, 1988.

[125] U. Baur and E.W.Nigel Glover. Higgs Boson Production at Large Transverse Momentum in Hadronic Collisions. *Nucl.Phys.*, B339:38–66, 1990.

[126] V. Del Duca, W. Kilgore, C. Oleari, C. Schmidt, and D. Zeppenfeld. Higgs + 2 jets via gluon fusion. *Phys.Rev.Lett.*, 87:122001, 2001.

[127] V. Del Duca, W. Kilgore, C. Oleari, C. Schmidt, and D. Zeppenfeld. Gluon fusion contributions to H + 2 jet production. *Nucl.Phys.*, B616:367–399, 2001.

[128] Carl R. Schmidt. H —> g g g (g q anti-q) at two loops in the large M(t) limit. *Phys.Lett.*, B413:391–395, 1997.

[129] D. de Florian, M. Grazzini, and Z. Kunszt. Higgs production with large transverse momentum in hadronic collisions at next-to-leading order. *Phys.Rev.Lett.*, 82: 5209–5212, 1999.

[130] V. Ravindran, J. Smith, and W.L. Van Neerven. Next-to-leading order QCD corrections to differential distributions of Higgs boson production in hadron hadron collisions. *Nucl.Phys.*, B634:247–290, 2002.

[131] Russel P. Kauffman, Satish V. Desai, and Dipesh Risal. Production of a Higgs boson plus two jets in hadronic collisions. *Phys.Rev.*, D55:4005–4015, 1997.

[132] Russel P. Kauffman, Satish V. Desai, and Dipesh Risal. Erratum. *Phys. Rev. D*, 58(11):119901, Oct 1998.

[133] K.G. Chetyrkin, Bernd A. Kniehl, and M. Steinhauser. Hadronic Higgs decay to order $\alpha_s^4$. *Phys.Rev.Lett.*, 79:353–356, 1997.

[134] Richard Phillips Feynman. *Photon-HadronInteractions*. W. A. Bejnamin, Inc., 1972. ISBN 0-805-32511-5.

[135] G. Miller, E. D. Bloom, G. Buschhorn, D. H. Coward, H. DeStaebler, J. Drees, C. L. Jordan, L. W. Mo, R. E. Taylor, J. I. Friedman, G. C. Hartmann, H. W. Kendall, and R. Verdier. Inelastic electron-proton scattering at large momentum transfers and the inelastic structure functions of the proton. *Phys. Rev. D*, 5: 528–544, Feb 1972. URL `http://link.aps.org/doi/10.1103/PhysRevD.5.528`.

[136] J.D. Bjorken. Asymptotic Sum Rules at Infinite Momentum. *Phys.Rev.*, 179: 1547–1553, 1969.

[137] G.P. Zeller et al. A Precise determination of electroweak parameters in neutrino nucleon scattering. *Phys.Rev.Lett.*, 88:091802, 2002. `http://www.fnal.gov/pub/presspass/press_releases/NuTeV.html`.

[138] G. P. Zeller, K. S. McFarland, T. Adams, A. Alton, S. Avvakumov, L. de Barbaro, P. de Barbaro, B. H. Bernstein, A. Bodek, T. Bolton, J. Brau, D. Buccholz, H. Budd, L. Bugel, J. Conrad, R. B. Drucker, B. T. Fleming, R. Frey, J. A. Formaggio, J. Goldman, M. Goncharov, D. A. Harris, R. A. Johnson, J. H. Kim, S. Koutsoliotas, M. J. Lamm, W. Marsh, D. Mason, J. McDonald, C. McNulty, D. Naples, P. Nienaber, A. Romosan, W. K. Sakumoto, H. Schellman, M. H. Shaevitz, P. Spentzouris, E. G. Stern, N. Suwonjandee, M. Tzanov, M. Vakili, A. Vaitaitis, U. K. Yang, J. Yu, and E. D. Zimmerman. Erratum: Precise determination of electroweak parameters in neutrino-nucleon scattering [phys. rev. lett. 88, 091802 (2002)]. *Phys. Rev. Lett.*, 90:239902, Jun 2003. URL `http://link.aps.org/doi/10.1103/PhysRevLett.90.239902`.

[139] A. Aktas et al. A Determination of electroweak parameters at HERA. *Phys.Lett.*, B632:35–42, 2006.

[140] S. Moch, J.A.M. Vermaseren, and A. Vogt. The Longitudinal structure function at the third order. *Phys.Lett.*, B606:123–129, 2005.

[141] Andreas Vogt, Sven Moch, and Jos Vermaseren. Third-order QCD results on form factors and coefficient functions. *Nucl.Phys.Proc.Suppl.*, 160:44–50, 2006.

[142] Jr. Callan, Curtis G. and David J. Gross. High-energy electroproduction and the constitution of the electric current. *Phys.Rev.Lett.*, 22:156–159, 1969.

[143] M. Klein and T. Riemann. ELECTROWEAK INTERACTIONS PROBING THE NUCLEON STRUCTURE. *Z.Phys.*, C24:151, 1984.

[144] Paolo Bolzoni, Fabio Maltoni, Sven-Olaf Moch, and Marco Zaro. Vector boson fusion at NNLO in QCD: SM Higgs and beyond. *Phys. Rev. D 85,*, 035002, 2012. doi: 10.1103/PhysRevD.85.035002.

[145] W.L. van Neerven and A. Vogt. NNLO evolution of deep inelastic structure functions: The Singlet case. *Nucl.Phys.*, B588:345–373, 2000.

[146] S. Moch and J.A.M. Vermaseren. Deep inelastic structure functions at two loops. *Nucl.Phys.*, B573:853–907, 2000.

[147] J. Blümlein and V. Ravindran. Dyhig 1.00. `http://www-zeuthen.desy.de/~blumlein/`.

[148] W. Giele, E.W.Nigel Glover, I. Hinchliffe, J. Huston, Eric Laenen, et al. The QCD / SM working group: Summary report. arXiv:hep-ph/0204316, 2002. section 1.3.

[149] J.A.M. Vermaseren. Harmonic sums, Mellin transforms and integrals. *Int.J.Mod.Phys.*, A14:2037–2076, 1999.

[150] Johannes Blümlein and Stefan Kurth. Harmonic sums and Mellin transforms up to two loop order. *Phys.Rev.*, D60:014018, 1999.

[151] J.A.M. Vermaseren. Harmonic sums, Mellin transforms and integrals. *Int.J.Mod.Phys.*, A14:2037–2076, 1999.

[152] T. Gehrmann and E. Remiddi. Numerical evaluation of harmonic polylogarithms. *Comput.Phys.Commun.*, 141:296–312, 2001.

[153] Eric W. Weisstein. Nielsen generalized polylogarithm. `http://mathworld.wolfram.com/NielsenGeneralizedPolylogarithm.html`. From MathWorld–A Wolfram Web Resource.

[154] Johannes Blümlein. Analytic continuation of Mellin transforms up to two loop order. *Comput.Phys.Commun.*, 133:76–104, 2000.

[155] George B. Arfken and Hans J. Weber. *Mathematical Methods For Physicists*, chapter 10, page 631. Harcourt Academic Press, 2001. ISBN 0-12-059826-4.

[156] J. Blümlein, A. Hasselhuhn, P. Kovacikova, and S. Moch. $O(\alpha_s)$ Heavy Flavor Corrections to Charged Current Deep-Inelastic Scattering in Mellin Space. *Phys.Lett.*, B700:294–304, 2011.

[157] S. Moch, A. Vogt, and J. Vermaseren. Sudakov resummations at higher orders. *Nucl.Phys.Proc.Suppl.*, 157:179–186, 2006.

[158] Jerrold E. Marsden and Michael J. Hoffman. *Basic Complex Analysis*, chapter 7. W.H.Freeman and Company, 1999. ISBN 978-0-7167-2877-1.

[159] George Sterman. *An Introduction to quantum field theory*, chapter 14, pages 457 – 458. Cambridge University Press, 1993. ISBN 0-521-31132-2.

[160] Simone Alioli. Personal notes.

[161] Claude Amsler et al. Review of PARTICLE Physics. *Phys.Lett.*, B667:1–1340, 2008.

[162] M. R. Whalley, D. Bourilkov, and R. C. Group. The Les Houches Accord PDFs (LHAPDF) and Lhaglue. arXiv:hep-ph/0508110, `http://hepforge.cedar.ac.uk/lhapdf/`, 2005.

[163] S. Moch, J.A.M. Vermaseren, and A. Vogt. Higher-order corrections in threshold resummation. *Nucl.Phys.*, B726:317–335, 2005.

[164] Ryan Gavin, Ye Li, Frank Petriello, and Seth Quackenbush. FEWZ 2.0: A code for hadronic Z production at next-to-next-to-leading order. arXiv:hep-ph/1011.3540, 2010.

[165] Johannes Blümlein. Structural Relations of Harmonic Sums and Mellin Transforms up to Weight w = 5. *Comput.Phys.Commun.*, 180:2218–2249, 2009.

[166] Sky McKinley and Megan Levine. Cubic Spline Interpolation, Jan 2011. URL `http://online.redwoods.edu/instruct/darnold/laproj`.

[167] George F. Sterman. Some Basic Concepts of Perturbative QCD. *Acta Phys.Polon.*, B39:2151–2172, 2008.

[168] Frank Wilczek. Decays of Heavy Vector Mesons Into Higgs Particles. *Phys.Rev.Lett.*, 39:1304, 1977.

[169] John R. Ellis, M.K. Gaillard, Dimitri V. Nanopoulos, and Christopher T. Sachrajda. Is the Mass of the Higgs Boson About 10-GeV? *Phys.Lett.*, B83:339, 1979.

[170] Thomas G. Rizzo. GLUON FINAL STATES IN HIGGS BOSON DECAY. *Phys.Rev.*, D22:178, 1980.

[171] M. Spira, A. Djouadi, D. Graudenz, and P.M. Zerwas. SUSY Higgs production at proton colliders. *Phys.Lett.*, B318:347–353, 1993.

[172] W.L. van Neerven and A. Vogt. NNLO evolution of deep inelastic structure functions: The Nonsinglet case. *Nucl.Phys.*, B568:263–286, 2000.

[173] W.L. van Neerven and A. Vogt. Nonsinglet structure functions beyond the next-to-next-to-leading order. *Nucl.Phys.*, B603:42–68, 2001.

[174] A. C. Benvenuti et al. A High Statistics Measurement of the Proton Structure Functions F(2) $(x, Q^2)$ and R from Deep Inelastic Muon Scattering at High $Q^2$. *Phys. Lett.*, B223:485, 1989.

[175] T. Ahmed et al. A Measurement of the proton structure function f2 (x, $Q^2$). *Nucl.Phys.*, B439:471–502, 1995.

[176] M. Derrick et al. Measurement of the proton structure function F2 from the 1993 HERA data. *Z.Phys.*, C65:379–398, 1995.

[177] S. Moch and M. Rogal. Charged current deep-inelastic scattering at three loops. *Nucl.Phys.*, B782:51–78, 2007.

[178] Hugh D. Young and Freedman Roger A. *University Physics with Modern Physics.* Addison-Wesley, 11 edition, 2003. ISBN 978-805386844.

[179] Alan D. Martin. Proton structure, Partons, QCD, DGLAP and beyond. *Acta Phys.Polon.*, B39:2025–2062, 2008.

[180] Amanda M. Cooper-Sarkar, R.C.E. Devenish, and A. De Roeck. Structure functions of the nucleon and their interpretation. *Int.J.Mod.Phys.*, A13:3385–3586, 1998. doi: 10.1142/S0217751X98001670.

[181] Johannes Blumlein and Stefan Kurth. On the Mellin transform of the coefficient functions of F(L)(x,Q**2). arXiv:hep-ph/9708388, 1997.

[182] T. Hahn. CUBA: A Library for multidimensional numerical integration. *Comput.Phys.Commun.*, 168:78–95, 2005. doi: 10.1016/j.cpc.2005.01.010.

[183] Richard D. Ball, Valerio Bertone, Francesco Cerutti, Luigi Del Debbio, Stefano Forte, et al. Impact of Heavy Quark Masses on Parton Distributions and LHC Phenomenology. *Nucl.Phys.*, B849:296–363, 2011. doi: 10.1016/j.nuclphysb.2011.03.021.

# List of Figures

# List of Tables

# Selbständigkeitserklärung

Ich erkläre, dass ich die vorliegende Arbeit selbständig und nur unter Verwendung der angegebenen Literatur und Hilfsmittel angefertigt habe.

København, den August 18, 2013 Petra Kovačíková